Stony Brook University

The official electronic file of this thesis or dissertation is maintained by the University Libraries on behalf of The Graduate School at Stony Brook University.

Pancreas specific ablation of β1 integrin in mouse:
Biology of epithelial cells in a model of chronic pancreatitis.

A Dissertation presented

By

Lorenzo Bombardelli

To

The Graduate School

In Partial Fullfillment of the

Requirements

For the Degree of

Doctor of Philosophy

in

Genetics

Stony Brook University

May 2008

Stony Brook University

The Graduate School

Lorenzo Bombardelli

We, the dissertation committee for the above candidate for the

Doctor of Philosophy degree, hereby recommend

acceptance of this dissertation.

Howard Crawford, Ph.D.
Assistant Professor
Dissertation Advisor
Department of Pharmacological Sciences

Daniel Bogenhagen, M.D.
Professor
Chairperson
Department of Pharmacological Sciences

Senthil Muthuswamy, Ph.D.
Associate Professor
Cold Spring Harbor Laboratory

Kenneth Marcu, Ph.D.
Professor
Department of Biochemistry and Cell Biology

Stanley Zucker, M.D.
Professor
School of Medicine

This dissertation is accepted by the Graduate School

Lawrence Martin
Dean of the Graduate School

Abstract of the Dissertation

Pancreas specific ablation of β1 integrin in mouse:
Biology of epithelial cells in a model of chronic pancreatitis.

By

Lorenzo Bombardelli

Doctor of Philosophy

in

Genetics

Stony Brook University

2008

Integrins are a large family of transmembrane molecules that mediate cell contact with the extracellular environment, especially the extracellular matrix. Integrin-mediated contact with the basement membrane underlying glandular epithelial cells, such as pancreatic acini, determines cellular polarity required for appropriate exocrine function. Growing evidence from *in vivo* and *in vitro* studies highlights the requirement of β1 integrin function in stem cells and in three-dimensional tumor biology, where the β1 integrin modulates cellular differentiation and contributes to the malignant behavior of cancer cells.

I tested hypothesis that β1 integrin ablation in the pancreas would eliminate the ability of acinar cells to maintain contact with the basement membrane, potentially compromising their function in both normal and pathological situations.

In order to address these questions and understand the fate of acinar cells lacking BM contact, a pancreas-specific knockout of β1 integrin was developed. This allowed us to follow completely the biology of acinar cells, from development to adulthood, in normal condition and in the context of experimental pancreatitis.

In my studies, I found that β1 integrin was not required for the initial establishment of acinar cell polarity, but was necessary for the maintenance of acinar

homeostasis. I showed that β1 integrin is involved in directional secretion, and this is a critical element for the maintenance of acinar cell integrity.

Finally, I suggest the possibility that the contribution of β1 integrin might be related to its signaling function, rather than to the role of physical cell-cell and cell-BM link. Accordingly, identifying the signaling defect that lead β1 null mice to irreversible degeneration, could lead the way for the development of therapy of acute and chronic pancreatitis

Table of contents

List of figures

.

List of tables

Chapter 1:

General Introduction

Section 1
Introduction to the pancreas .

The pancreas is a mixed exocrine and endocrine gland organ. Its exocrine function is the release of salts and digestive enzymes, while its endocrine function is the hormonal regulation of blood glucose levels. More than 95% of the pancreas is composed of exocrine tissue, comprised of acinar cells and their associated ducts. Endocrine cells, which secrete insulin, glucagon and other hormones directly into a network of capillaries, are found in groups called Islets of Langerhans and are evenly distributed in the human pancreas. [1] A schematic representation is shown in Figure 1.

Pancreatic exocrine cells form clusters called acini that secrete digestive enzymes into a lumens, the delimited extracellular spaces located in the center of acini. The secreted content is drained from the lumen into the ductal system. The acinus is a structure composed of polarized cells: the nuclei of exocrine cells are positioned at the basal surface in contact with the basement membrane (BM), while an extensive Golgi complex and a large intracellular storage of zymogen granules are clustered at the apical pole. The tight junctions (zonula occludens) between neighboring acinar cells seal the lumen protecting the basolateral surface from exocytosed enzymes.

The central lumen collects the secretions of acinar cells and directs them into intralobular ducts, which merge into progressively larger ducts and finally into the main pancreatic duct. The terminal cells of interlobular ducts that reach into the lumen of the acinus are called centroacinar cells and are hypothesized to be the stem cell of the adult pancreas [2].

Pancreatic secretion, in general, is regulated by hormones made by the gastrointestinal tract (GI) and by sympathetic innervation. Pancreatic acinar cells make a large number of digestive enzymes, including proteases, amylases, lipases, phosphatases and nucleases with the function of breaking down specific components of the chyme released from the stomach into the duodenum. Many of these proteolytic enzymes are typically secreted as inactive precursors and are activated only after their release into the duodenum to prevent potential intracellular damage to pancreatic cells. The main non-proteolytic pancreatic enzymes are α-amylase, an enzyme that breaks down starch and long-chain carbohydrates to dextrins, and pancreatic lipase, which breaks down triglycerides into monoglycerides and free fatty acids. DNAses and RNAses, secreted in active forms, break down the nucleic acids into free nucleotides.
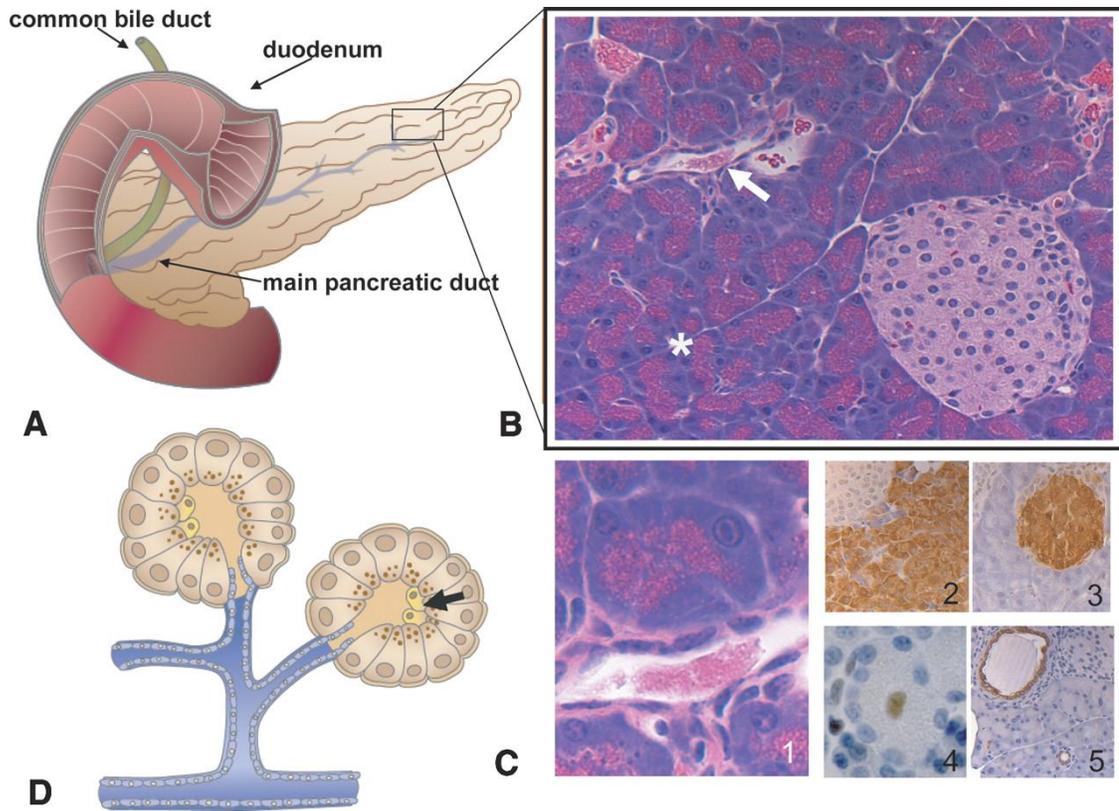
Figure 1: Anatomy of the pancreas. The pancreas is comprised of separate functional units that regulate two major physiological processes: digestion and glucose metabolism. (*A*) Gross anatomy of the pancreas demonstrating its close anatomical relationship with the duodenum and common bile duct. (*B*) The major components of the pancreatic parenchyma on a histological level. At *lower right* is an islet of Langerhans, the endocrine portion of the pancreas, which is principally involved in regulating glucose homeostasis. The asterisk is placed among acini, which are involved in secreting various digestive enzymes (zymogens) into the ducts (indicated by the solid arrow). (*C*) Photomicrographs of H&E- and immunohistochemical-stained sections of pancreatic tissue demonstrating the various cell types. (Panel *1*) An acinar unit in relationship to the duct. (Panel *2*) Acinar units visualized with an antibody to amylase are seen as brown due to Diaminobenzidine staining. (Panel *3*) Islet of Langerhans shown stained with an antibody to insulin. (Panel *4*) A centroacinar cell showing robust Hes1 staining. (Panel *5*) Ductal cells (seen here in cross-section) are stained with an antibody to cytokeratin-19. (*D*) Representation of an acinar unit showing the relationship to the pancreatic ducts. Also depicted are centroacinar cells (arrow), which sit at the junction of the ducts and acini. From: Genetics and biology of pancreatic ductal adenocarcinoma. Genes Dev. 2006 May 15;20(10):1218-49.

The main pancreatic proteases, secreted as inactive zymogens, are trypsin and chymotrypsin. The activity of trypsin is regulated in the pancreas by the concentration of trypsin inhibitor, and is converted into active trypsin by enterokinase in the intestine. Active trypsin can, in turn, activate more trypsinogen and chymotrypsinogen, both of which are also pancreatic serine protease zymogens. Further digestion of peptides is done by pancreatic carboxypeptidases which cleave the C-terminal amino acids, and elastases, serine proteases which digest elastin and collagen type IV. Pancreatic ductal epithelial cells express carbonic anhydrase, which allows for the secretion of basic bicarbonate and water into the lumen of the duct. This is required to counterbalance the acidity of the contents coming from the stomach and the small intestine, and to ensure the optimal pH for other digestive enzyme activity.

Regulation of pancreatic secretion involves both a neural and an endocrinal element. Pancreatic secretion is strongly stimulated as chyme exits the stomach and enters the small intestine. The main hormones that regulate enzyme secretion are secreted by the small intestine. Cholecystokinin (CCK), a hormone which binds to pancreatic acinar cell receptors to trigger enzyme secretion, is synthesized and released into the bloodstream by endocrine G-cells in the duodenum. Gastrin is another hormone produced by duodenal G-cells that induces pancreatic secretion of digestive enzymes. Secretin, triggered by the presence of acid in the duodenum, stimulates duct cells to secrete water and bicarbonate.

Section 2.

Pancreatic diseases.

Pancreatitis, the inflammation of the pancreas, is a complex disease that has been known for decades. At the S*ymposium of Marseilles* in 1963 [3, 4] it was agreed that pancreatitis was : a) acute, b) relapsing acute, c) chronic and d) chronic with acute exacerbations. Alcoholism was the first described risk factor of pancreatitis [5], because 80-90% of pancreatitis patients are alcoholics. Other recognized causes included the obstruction of the main pancreatic duct (or bile tract diseases), viral infections, postoperative trauma, and drug abuse.

Today, thanks to technological advancements, we have a better knowledge of the spectrum of genetic lesions or molecular disorders that represent risk factors for pancreatitis; however, there is no model so far that can explain its occurrence. For example, despite the obvious link between alcoholism and acute pancreatitis, it is known that only 10% of chronic alcohol abusers will develop pancreatitis in the course of a lifetime.

The current state of the art is represented by the "Toxic–metabolic, Idiopathic, Genetic, Autoimmune, Recurrent and severe acute pancreatitis–associated chronic

pancreatitis, and Obstructive chronic pancreatitis" (TIGAR-O) risk factor classification system, developed recently by the Midwest Multicenter Pancreatic Study Group [6, 7]. Rather than etiologies, it proposes a list of risk modifiers, each of which proceed through a distinct molecular mechanism [8] that can determine the unique nature and the outcome of the pancreatic disease of any one patient.

Pathophysiology of pancreatitis.

The first hypotheses about the pathophysiology of pancreatitis were built around the concept that active components of the pancreatic secretion, if not properly directed into the duodenum, could cause severe damage and result in an acute or a chronic condition. This general model, widely accepted today, explained the observation of fat tissue necrosis in patients who died of pancreatitis as a consequence of pancreatic lipase secreted in active form [9]. The detection of activated proteases and phospholipases [10, 11] in the parenchyma of pancreatitis patients further supported the model of an injury due to leak of active enzymes into the parenchyma. Finally, experimental models showed that the injection of pancreatic juice into the pancreas, especially in combination with bile acids, results in pancreatitis [12].

A better molecular understanding of the mechanisms responsible for initiating pancreatitis did not surface until last the decade when the available genetic and molecular tools allowed a fine analysis of isolated acini in experimental models of pancreatitis. In fact, most of the evidence for the central role of acinar cells in the onset of pancreatitis comes from experimental models rather than from clinical studies, mainly for two reasons. First, the pancreas in humans is quite inaccessible because of its retroperitoneal location and any collection of biological samples requires invasive techniques; second, in patients admitted to a hospital the disease in general has already progressed to a state when it is difficult to distinguish causes from effects. Furthermore, the patients that incur in the life-threatening severe form of pancreatitis and would mostly benefit of clinical trials for therapeutic agents, are only a small percentage of all AP cases, making it difficult to design clinical trials for multiple drugs.

Experimental models of pancreatitis.

Given the problematic access to the pancreas in humans and the lack of models for early and advanced stages of pancreatitis, significant effort was consequently directed towards the characterization of experimental animal models of pancreatitis. These models, most notably in rodents, helped to establish a controlled system to define the sequence of events that initiate pancreatitis.

For example, the enzymatic dissociation of the pancreas into isolated acini *in vitro* allows for the minimization of systemic effects, like inflammation, and permits the study of multiple experimental conditions, including the use of different agonists and concentrations simultaneously. In fact, stimulation of isolated acini with secretagouges has been the major source of information about the molecular events within acinar cells that lead to the onset of pancreatitis [13].

In vivo, one of the most used and well-established systems, is the supramaximal stimulation with a secretagogue, like cholecystokinin (CCK) or its octapeptide analogue, cerulein, at a concentration of 2 or more orders of magnitude higher than the physiological levels (supramaximal). This technique was shown to induce a mild, reversible form of edematous pancreatitis in rat, mouse and dog models [14, 15] and best recapitulates the non-severe form of human disease, while repeated cerulein administration can induce a chronic disease. Other *in vivo* models [16] are the surgical ligation of the pancreatic duct, which mimics gallstone obstructive pancreatitis and causes CP, or necrotizing-hemorrhagic pancreatitis, (choline-deficient, ethionine-supplemented, short term diet, CDE) [17] which induces a severe form of AP and is used mainly to study the systemic consequences of massive tissue damage.

The molecular mechanism that links supramaximal secretagogues stimulation to pancreatitis in rodent, however, is unknown. It is also unlikely that human pancreatitis proceeds through the same mechanism, because human acinar cells express very low levels of CCK and lack a functional response to CCK [18]. Supramaximal secretagogue stimulation is used because it ultimately triggers acinar cell damage and inappropriate enzyme activity, which is the outcome of the human disease.

Therefore, it requires particular caution to translate mouse research readouts to human pancreatitis. Animal models of pancreatitis, in combination with genetic background manipulation, are however a great tool to elucidate the role a particular gene or a pathway in pancreatic cell injury.

Intracellular origin of pancreatitis .

Acinar cells contain a large number of "zymogen granules", secretory vesicles which contain the inactive precursors of active enzymes, most notably precursors of proteases. The regulation of proteolytic activity is tightly regulated and inhibited in the pancreas by several mechanisms. Regulation of trypsin activity, for example, is a good model of how acinar cells are protected from proteolytic activity.

Trypsin is one of the main pancreatic products and is an activator of other zymogens, such as proelastase, procarboxypeptidase, or prophospholipase A_2. Trypsin is synthesized by acinar cells as an inactive precursor, trypsinogen, and packaged in secretory vesicles with its own inhibitor (trypsin inhibitor, TI) at a low intravesicular pH, preventing an intracellular cascade of proteolytic activation. When trypsin and other enzymes are secreted into the ducts, the pH is balanced by the ductal secretion of bicarbonate and dilution of trypsin inhibitor, leading to full conversion of trypsinogen into trypsin and activation of other zymogens only in the duodenum.There is also evidence for a "failsafe mechanism" that proteolytically degrades excess active trypsin within the zymogen granules. [19] Any perturbance of this complex system would lead to an inappropriate activation of trypsin and other proteases, ultimately causing cell damage.

Premature zymogen activation within the acinar cells is the current model for the initiating molecular event in AP [20]. Figure 2 shows a schematic of the effects of premature activation of trypsinogen and the immediate consequences, although the order of occurrence is not clear, but the outcome is a disruption of the apical actin cytoskeleton and fusion of zymogen granules with each other and with lysosomes, which contain cathepsin B, a trypsinogen-activating protease [21]. Basolateral discharge and loss of adherence junctions further expose the protected surface of acinar cells to the potentially harmful content of secretory vesicles. In addition to this, large amounts of calcium stored in zymogen granules can cause further cell damage by activating calcium-dependent proteases, such as calpains. [22]

Genetic and experimental evidence.

The central role of trypsin in the onset of pancreatitis is supported by a breakthrough discovery in 1996 that hereditary pancreatitis, an autosomal dominant condition with 80% penetrance, is related to mutations in the cationic trypsinogen gene (PRSS1). [19] The finding suggested the hypothesis that the R122H mutation eliminates a critical hydrolysis site that was first believed to make trypsinogen more resistant to degradation by other proteases (the "failsafe" mechanism) and precipitate pancreatitis.

More detailed structural and functional analysis of other mutations discovered in the PRSS1 gene demonstrated, however, hereditary pancreatitis is not simply the result of a mutant trypsinogen capable of enhanced autoactivation (N29I mutation). Instead, the recent discovery of the A16V mutation leading to a less active trypsinogen, suggest that any imbalance in the intracellular trypsinogen/trypsin balance is also a possible cause of pancreatitis, [23] although the precise mechanism is unknown.
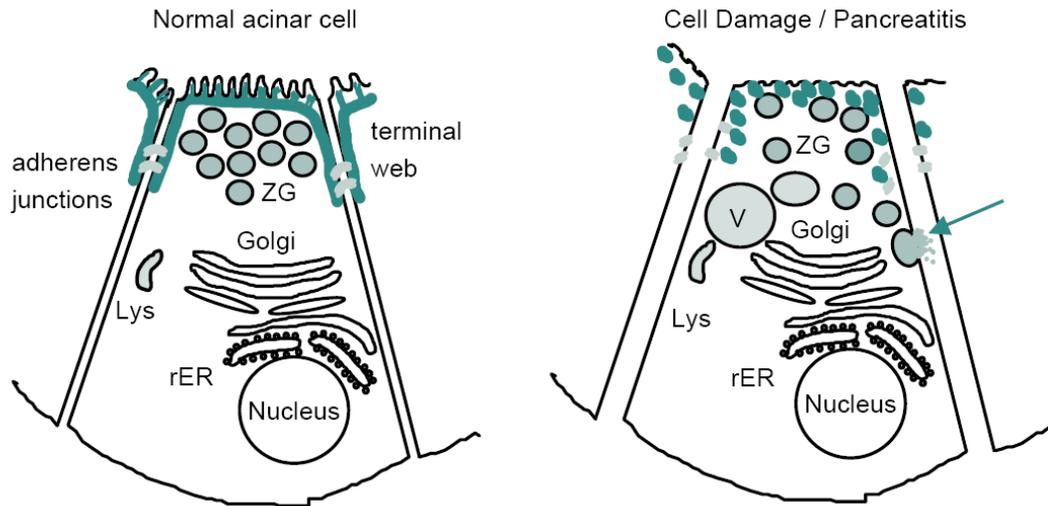
Figure 2. Initiation of acute pancreatitis within acinar cells. Left: normal acinar cell with intact terminal web at the top of the cells and adherens junctions between neighboring acinar cells. Right: following damage the terminal web and adherens junctions are dissolved, zymogen granules (ZG) no longer fuse to the apical plasma membrane but come in close contact with the basolateral plasma membrane (arrow) and intracellular vacuoles appear. From: Has the biology and treatment of pancreatic diseases evolved? Best Pract Res Clin Gastroenterol. 2004;18 Suppl:83-90.

Finally, transgenic mice bearing the R122H mutation in the PRSS1 gene, reported independently by two groups in 2006, showed a mild pancreatitis-like phenotype that was strongly enhanced and yielded a chronic condition only after repeated supramaximal cerulein stimulation. [24, 25] To this date, many mutations have been discovered and characterized in the cationic (PRSS1) and anionic (PRSS2) trypsinogen genes, the serine protease inhibitor Kazal type 1(SPINK1) gene, and the cystic fibrosis (CFTR) genes. Hereditary pancreatitis is now considered a complex genetic disease. An updated list of risk factors is maintained at: http://www.uni-leipzig.de/pancreasmutation/db.html

The central role of zymogen activation is further confirmed by other experimental evidence, including the appearance of the trypsin activation peptide (TAP) in the plasma during early acute pancreatitis, and the reduction of injury in experimental models by serine protease inhibitors. [26] Taken together, these observations suggest that the direct effect of active trypsin itself might be rather small, but trypsin may be a starting point and a regulatory element in a larger cascade of events that ultimately leads to the activation of pro-enzymes and proteases that can severely compromise cellular integrity and result in a chronic condition.

Section 3

Integrins.

Integrins comprise one of the largest and most well characterized families of ubiquitous cellular receptors for extracellular matrix (ECM) components and adhesion molecules. Together with their ligands, they are key elements of development, immune responses, cancer, genetic and autoimmune responses; they are also considered a promising class of therapeutic targets, because, for example, they mediate the entry of viruses and bacteria into cells. [27]

Integrins are heterodimeric adhesion receptors formed by an α and a β subunit. Each subunit is a type I transmembrane glycoprotein. The extracellular domains are 700 to 900 amino acids long and are responsible for ligand binding. Each has a single transmembrane domain and a cytoplasmic domain that consists of 20 – 60 amino acid residues, with the exception of the β4 integrin which is much larger at ~1000 amino acids. There are 18 known α and 8 β subunits that combine to form 24 different dimers, each of which seems to have a specific, non redundant function in binding ECM components and soluble protein ligands. (Figure 3)

Most evidence for integrin function is not based on studies on ligand affinities, but on the phenotypes of transgenic mice. To date, almost every subunit has been knocked-out in the mouse. The particular phenotype of each knockout, many of which are lethal, highlights the importance and the specificity of each integrin dimer. The striking diversity among integrin knockout phenotypes indicates how besides mechanical attachment to the ECM, integrins are involved in many different aspects of signal transduction [28].

Cytoplasmic domains of integrins, with the exception of β4, which binds intermediate filaments, bind and modulate the sub-membrane actin cytoskeleton. The interaction with the cytoskeleton can in turn trigger directly a number of signaling events that can modulate cell proliferation, apoptosis, shape, polarity, motility, gene expression and differentiation.

Some of the signaling pathways activated by integrins resemble the pathways activated by growth factors. In fact, signaling path ways activated by EGF, PDGF, LPA and thrombin [29] require integrin-mediated attachment to a substrate. This suggests that suggesting that integrins provide epithelial cell with the combination of attachment and signaling required for survival and proliferation.

Integrins also provides an important survival signal to many epithelial cells by preventing them from undergoing *anoikis*, a form of apoptosis induced by the loss of contact with the ECM [30, 31]. In normal cells integrins prevent apoptosis by signaling via PI3K and AKT, while in transformed cells the survival/ substrate adhesion signal is provided by oncogenes instead [32].
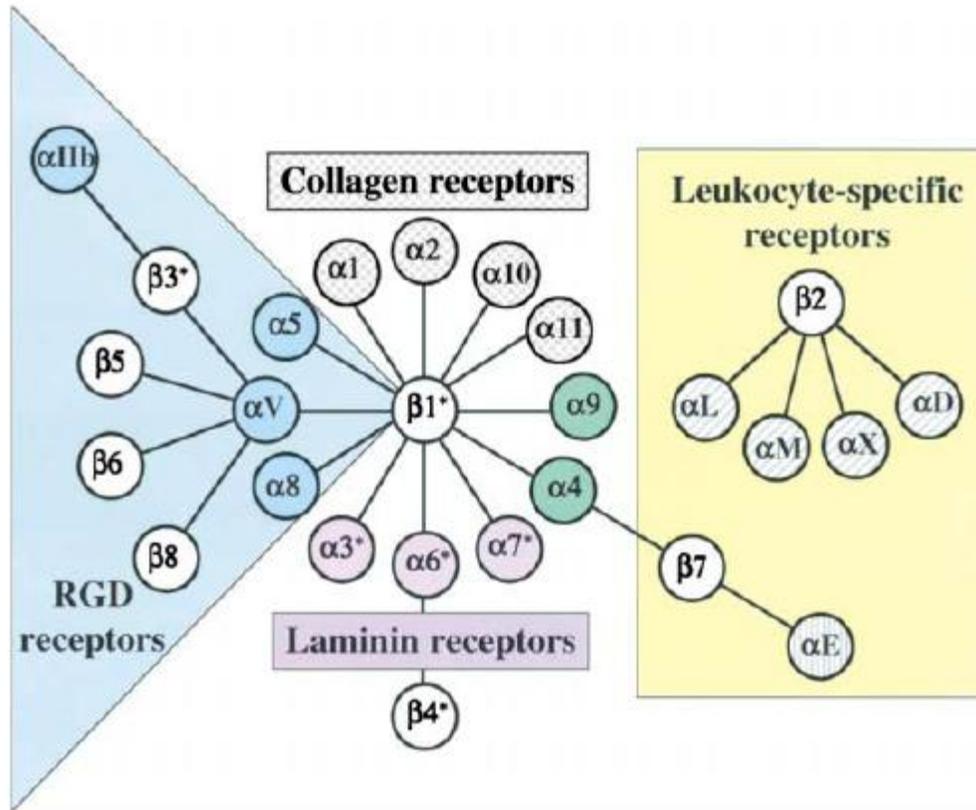
Figure 3. The Integrin Receptor Family Integrins are α β heterodimers; each subunit crosses the membrane once, with most of each polypeptide (1600 amino acids in total) the extracellular space and two short cytoplasmic domains (20–50 amino acids). The figure depicts the mammalian subunits and their α β associations; 8 β subunits can assort with 18 α subunits to form 24 distinct integrins. These can be considered in several subfamilies based on evolutionary relationships (coloring of α subunits), ligand specificity and, in the case of β 2 and β 7 integrins, restricted expression on white blood cells. α subunits with gray hatching or stippling have inserted I/A domains (see text). Such α subunits are restricted to chordates, as are α 4 and α 9 (green) and subunits β 2- β 8. In contrast, α subunits with specificity for laminins (purple) or RGD (blue) are found throughout the metazoa and are clearly ancient (see text). Asterisks denote alternatively spliced cytoplasmic domains. A few extracellular domains are also alternatively spliced (not shown). Further information on integrin subunit structures and details of ligand specificity are given in several extensive reviews (Hemler, 1999; Plow et al., 2000; van der Flier and Sonnenberg, 2001). From : Hynes, R.O., *Integrins: bidirectional, allosteric signaling machines.* Cell, 2002. 110(6): p. 673-87.

Activation of integrins.

Integrin function and structure are closely linked. Integrins depend on a conformational change from an inactive "OFF" state to an active, ligand binding "ON" state. Most structural studies suggest that the separation between the transmembrane domains or the cytoplasmic tails between α and β subunits is the basic switch from ON to OFF, but it is not completely clear.

The best supported model, the "switchblade" model, suggests that upon ligand binding, integrins switch from the bent, inactive conformation to a straight, active one, where the cytoplasmic tails are separated and free to interact with the actin cytoskeleton. This is also known as "outside-in" signaling because it is mediated by the extracellular proteins binding the integrin dimer and triggering an intracellular signaling cascade. There is also an "inside-out" process, where integrin activation is mediated by intracellular proteins binding the cytoplasmic tail through conserved motifs (GFFKR) and changing the conformation of the whole dimer and thus modulating its substrate affinity. [33]

A paradigm of integrin activation is represented by the $\beta 2$ subunit expressed by leukocytes [34]. Resting cells express $\beta 2$ integrin in an inactive state; upon rapid activation, at the onset of an inflammatory response, integrins switch to the active, ICAM-binding state and allow leukocytes to adhere to endothelial cells. In addition, activated integrin allows leukocytes to bind other cells and thus engaging phagocytosis or cytotoxic killing. This property of integrins makes them promising therapeutic targets for a wide spectrum of inflammatory diseases.

Integrin cytoplasmic domains are very important determinants of integrin function. Not only do they control the activation state of the dimer but they serve as a mechanical ECM-cytoskeleton link to bridge extracellular stimuli with intracellular signaling. This link regulates integrin activation by directly binding a plethora of intracellular signaling molecules through conserved domains and recognition sequences. Extensive mutational analysis disrupting this binding suggests that the cytoplasmic integrin tails are crucial regulators of both "outside-in" and "inside-out" signaling as well as the ability to lock integrins in an active or inactive conformational state.

To date at least 21 proteins are known to bind to one or more integrin cytoplasmic tails and most of them bind the β subunit rather than the α subunit. Classes of binding partners include actin-binding proteins, signal adaptor proteins, as well as a few enzymes and transcriptional co-activators [28].

Integrin signaling.

Upon interaction with ECM components, integrins bind and activate numerous signaling molecules, such as Rho GTPases, focal adhesion kinase (FAK), extracellular signal regulated–kinase (Erk), tyrosine phosphatases, cyclic AMP (cAMP)-dependent protein kinase, protein kinase C (PKC) as well as the production of phosphatidylinositol (4,5) bisphosphate (PIP_2). These signaling molecules have been studied for decades and there is solid evidence describing their roles in differentiation, survival, shape and migration of diverse cell types. However, how the signaling cascades initiated by integrins and propagated through specific pathways are often cell type specific, very complex and difficult to delineate.

The activation of FAK is an early event in integrin signaling and serves as paradigm (Figure 4) to explain the complexity and the potential of integrin signaling in physiological and pathological circumstances. FAK recently has been proposed to mediate cell migration and survival by recruiting Src family kinases by acting as an integrin-regulated scaffold. [35] In addition, integrin-FAK signaling can promote anoikis [31], a type of apoptosis due to loss of ECM adhesion, in pancreatic cancer cell lines as well as suppression of metastasis in nude mice. [36-38]

C-Src, another downstream effector of β1 integrin and FAK, is commonly upregulated in tumors derived from the colon, liver, lung, breast, and pancreas. [39] In this respect, a major focus has been to understand the mechanisms of c-Src activation in human cancer.

Therefore, the knowledge of how β1 integrin affects, directly or indirectly Src and FAK mediated signaling can provide relevant insight on the fate of pancreatic cells, for example in the context of pancreatitis or PDAC onset or progression. Furthermore, the combination of availability of integrin inhibitor peptides and the knowledge of the downstream pathways, leads the way to design clever, pathway-specific therapeutic strategies.
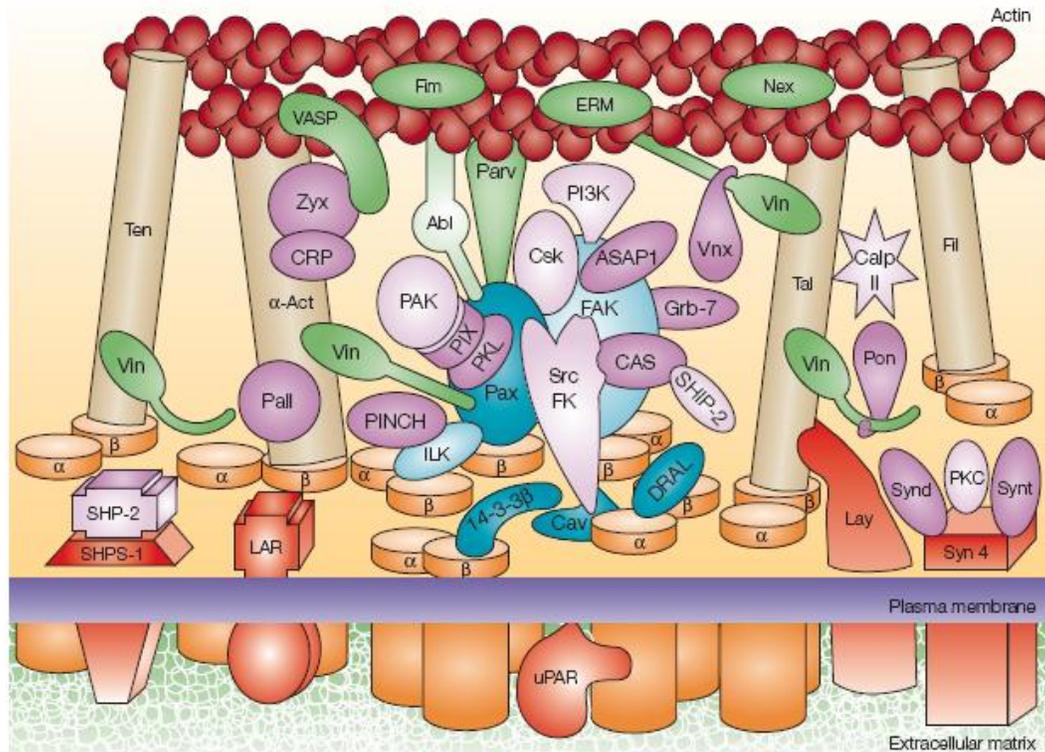
Figure 4 The primary adhesion receptors are heterodimeric (α and β) integrins, represented by orange cylinders. Additional membrane-associated molecules enriched in these adhesions (red) include syndecan-4 (Syn4), layilin (Lay), the phosphatase leukocyte common antigen-related receptor (LAR), SHP-2 substrate-1 (SHPS-1) and the urokinase plasminogen activator receptor (uPAR). Proteins that interact with both integrin and actin, and which function as structural scaffolds of focal adhesions, include α-actinin (α-Act), talin (Tal), tensin (Ten) and filamin (Fil), shown as golden rods. Integrin-associated molecules in blue include: focal adhesion kinase (FAK), paxillin (Pax), integrin-linked kinase (ILK), down-regulated in rhabdomyosarcoma LIM-protein (DRAL), 14-3-3β and caveolin (Cav). Actin-associated proteins (green) include vasodilator-stimulated phosphoprotein (VASP), fimbrin (Fim), ezrin–radixin–moesin proteins (ERM), Abl kinase, nexillin (Nex), parvin/actopaxin (Parv) and vinculin (Vin). Other proteins, many of which might serve as adaptor proteins, are coloured purple and include zyxin (Zyx), cysteine-rich protein (CRP), palladin (Pall), PINCH, paxillin kinase linker (PKL), PAK-interacting exchange factor (PIX), vinexin (Vnx), ponsin (Pon), Grb-7, ASAP1, syntenin (Synt), and syndesmos (Synd). Among these are several enzymes, such as SH2-containing phosphatase-2 (SHP-2), SH2- containing inositol 5-phosphotase-2 (SHIP-2), p21-activated kinase (PAK), phosphatidyl inositol 3-kinase (PI3K), Src-family kinases (Src FK), carboxy-terminal src kinase (Csk), the protease calpain II (Calp II) and protein kinase C (PKC). Enzymes are indicated by lighter shades. From: Geiger, B., et al., *Transmembrane crosstalk between the extracellular matrix--cytoskeleton crosstalk.* Nat Rev Mol Cell Biol, 2001. **2**(11): p. 793-805.

14

Section 4.

Pancreatic ablation of β1 integrin :project description and rationale.

The initiating molecular events of AP has been shown to be the activation of proteolytic enzymes within acinar cells, followed by the loss of acinar cell integrity, uncontrolled release of secretory and cytoplasmic content onto the parenchyma, resulting in necrotic cell death and widespread tissue damage.

Because acinar cells synthesize, store and secrete large amounts of digestive enzymes that can initiate AP, the mechanism regulating their homeostasis are the subject of active study. A critical aspect of the viability and the regeneration of acinar cells is their interaction with the basement membrane (BM), a specialized type of extracellular matrix (ECM) that encapsulates the basal surface of epithelial cells and represents a structural scaffold that guides cells adhesion, polarity and accessibility to growth factors. The importance of the BM in maintaining the functionality of the pancreas and driving the regenerative process was recognized decades ago; in a model of necrotizing pancreatitis, chemical destruction of 90 % of the exocrine cells, but sparing the BM framework still allows a complete regeneration of the organ, while partial pancreatectomy only results in hyperplasia and compensatory enlargement [40, 41].

In epithelial cells, the most common ECM components are bound primarily by integrins based on the β1 integrin subunit and consequently have been the focus of intense research in a number of different models; not surprisingly, germline ablation of β1 integrin is embryonic lethal. As with most epithelial cells, acinar cells contact the surrounding BM mainly through integrins. To date, β1 integrin function has been associated with cell differentiation, survival, shape and migration in different organ systems, both *in vivo* and *in vitro*, but an exocrine pancreas-specific knockout has not yet been characterized. Interestingly, in pancreatic acinar cells, which do not express β4 [42], β1 is the only type of β subunit capable of binding collagen (Figure 3) and laminins, the most abundant component of the BM. Consequently, I hypothesized that β1 integrin plays a critical role in acinar cell-BM contact.

I hypothesized that β1 integrin ablation in the pancreas would eliminate the ability of acinar cells to maintain contact with the basement membrane, potentially compromising their function in both normal and pathological situations. β1 integrin has been shown to be a marker of stem cells [43] and a requirement for their maintenance in several tissues [44], but it is unknown if and how it can affect acinar cells during tissue regeneration.

In order to address these questions and understand the fate of acinar cells lacking BM contact, we developed a pancreas-specific knockout of β1 integrin. This allowed us

15

to follow completely the biology of acinar cells, from development to adulthood, in normal condition and in the context of experimental pancreatitis.

Chapter 2:

Experimental procedures

Pancreas specific ablation of the β1 integrin subunit.

Pancreas specific ablation of the β1 integrin subunit was obtained by crossing β1 integrin conditional knockout mice (referred as β1 integrin $^{flox/flox}$ and described elsewhere [45]) with C57BL/6J Ptf1a-cre *mice* [46]*,* which express *Cre* recombinase in all progenitor cells of the pancreatic lineage. All β1 integrin $^{flox/flox}$ animals (obtained from Dr. JE Pessin, Pharmacology dept., Stony Brook University) were backcrossed at least for 10 generations in the C57BL/6J background. All mice were bred and maintained at the maximum isolation facility in the Department of Laboratory Animal Resources at Stony Brook University, in cages under controlled temperature and humidity and a twelve hours light cycle, fed a regular chow diet with unlimited access to water. All protocols were approved by the Institutional Animal Care and Use Committee at Stony Brook University.

Genotyping and detection of *floxed* alleles recombination.

Genotyping of the β1 integrin $^{flox/flox}$ alleles was performed on phenol-chloroform extracted tail DNA. *Cre*-mediated recombination in the pancreas-extracted DNA was detected using primers upstream and downstream of the floxed alleles that yield an 800 bp PCR product only upon excision of the large floxed genomic region. PCR conditions for both routine genotyping and detection of recombination were the same: 1 cycle of 94 °C for 5 min, 35 cycles of (94 °C for 30 sec., 55 °C for 40sec, 72 °C for 50 sec), 1 cycle of 72°C for 10 min. The genotyping primers, described in the results section as P1 and P2 were 5'GCCGCCACAGCTTTCTGCTGTAGG3' and 5'CTGATCAATCCAATCCAGGAAACC3', respectively. Recombination was assayed with P1 as upstream and P3, 5'TGCCGCTCATCCGCCACA3' as downstream primer.

Acinar cell preparation.

Primary acinar cell cultures were prepared by modifying a previously published protocol. [47] Pancreata were aseptically removed and minced into 1-0.5 mm pieces using sterile scissors. After centrifugation (250 g for 1 min), the supernatant was removed and the acinar cells were digested in 0.2 mg/ml collagenase P (Roche, Nutley, NJ) in Hanks balanced salt solution (HBSS) at 37 °C for 20-30 min. Acini were washed once in cold HBSS supplemented with 5% fetal bovine serum (FBS) and 3 times in cold Krebs-Ringer Solution (KRS) consisting of: 104 mM NaCl, 5 mM KCl, 1 mM KH_2PO_4, 1.2 mM $MgCl_2$, 2 mM $CaCl_2$, 0.2 % (w/v) BSA, 0.01 % (w/v) soybean trypsin inhibitor (Sigma-Aldrich), 10 mM glucose, 25 mM HEPES/NaOH, pH 7.4, supplemented with minimal essential and non-essential amino acid solution and glutamine). All collagenase P-digested pancreatic tissues were filtered twice through 500 μm polypropylene mesh Spectrum Laboratories, Laguna, CA), and subsequently passed through a 105μm mesh for *wild type* animals and through a 201 μm mesh for β1 integrin $^{flox/flox}$ Ptf1a-cre mice only. The filtrate was washed three times in cold KRS and plated onto Matrigel (BD Biosciences, Franklin Lakes, NJ) coated coverslides plates (Matek corp., Ashland, MA)

for living cell imaging or incubated in 1.5 ml centrifuge tubes in KRS for amylase secretion assays. Acini on Matrigel-coated supports were incubated in KRS at 37 °C for 30 min before assay and viability was determined by Trypan blue exclusion.

Experimental Pancreatitis and tissue processing.

Control (saline injected or untreated) and experimental (cerulein injected) mice groups consisted of age matched (average age 10 weeks) and randomly assigned animals.

Acute pancreatitis was induced by 7 hourly intraperitoneal injections of 50 µg cerulein (Sigma-Aldrich, St. Louis, MO-Aldrich, St. Louis, MO) per kg body weight followed by 1 hour, 24 hours or a week of recovery. Mice were anesthetized by isofluorane/oxygen sacrificed by cervical dislocation; blood was immediately collected by cardiac puncture and spun for 5 min at 4000 rpm for plasma collection; plasma was stored at -80 °C. Pancreata were removed, trimmed of fat deposits and weighed. Part of the tissue was then fixed overnight in 10 % buffered formalin, dehydrated by sequential 1 hour -steps in 70 %, 80 %, 90 %, 100 % ethanol, Histoclear (National Diagnostics, Atlanta, GA) and embedded in paraffin. 5 µm-paraffin sections were stained with Hematoxylin and eosin (H&E), or trichrome staining kit (Sigma-Aldrich, St. Louis, MO kit) for histological assessment of the phenotype. Pancreatic tissue samples for immunofluorescence were briefly washed with cold PBS after excision, immediately placed in OCT resin (Sakura Finetek, Torrance, CA) and stored at -80°C.

Immunohistochemistry, Immunofluorescence and LacZ staining.

Formalin-fixed paraffin-embedded pancreatic tissue sections (5 µm) were rehydrated in sequential 5 minutes-steps of Histoclear, 100 %, 90 %, 80 %, 70 %, 50% ethanol, distilled water, TBS (Tris-buffered solution, 150 mM NaCl, 50 mM Tris pH 7.4). Antigens on sections were unmasked by microwave treatment in 10 mM sodium citrate pH 6.0; slides were then incubated with 3 % Hydrogen peroxide in TBS for 15 min, washed 5 min in TBS and placed for 1 hour in blocking solution (10 mM $MgCl_2$, 1 % BSA, 5 % serum of the animal the secondary antibody was raised in, 0.05 % Tween-20, in TBS). Sections were then incubated overnight at 4 °C with the indicated primary antibody in blocking solution, washed 3 times for 15 min in TBS–Tween-20, incubated 1 hour with the appropriate biotinylated secondary goat antibody (Vector labs, Burlingame, CA) at 1 µg/ml final concentration, washed 3 times for 15min in TBS – Tween-20, incubated 30 min with the ABC reagent mix (Vector labs, Burlingame, CA), washed 3 times for 15 min in TBS – Tween20 and the colored substrate reaction was developed in TBS containing 0.01% Hydrogen peroxide and 0.3 mg/ml 3,3'-diaminobenzidine (DAB). Slides were then counterstained for 1 min in hematoxylin, dehydrated, washed in water, mounted and photographed on an Olympus BX41 light microscope.

Immunofluorescence was performed on 8μm cryosections from OCT embedded tissue samples. Sections air-dried, briefly washed in phosphate buffered saline (PBS), fixed 10 min in 4% cold paraformaldehyde or 10 min in ice-cold 100% methanol, washed 3 times for 5 min in PBS, blocked 1 hour in 3% BSA in PBS, then incubated with the indicated primary antibodies at a concentration of 0.5 ng/ml (1:200) in 3% BSA for 1.5 hours at room temperature, washed 3 times for 15 min in TBS–Tween-20, incubated with the appropriate Alexafluor488 or Alexafluor594 –conjugated secondary antibody (Vector labs, Burlingame, CA), washed 3 times for 15 min in PBS and mounted in aqueous mounting medium containing 4',6-diamidino-2-phenylindole (DAPI) at 50ug/ml (Vector labs, Burlingame, CA). Fluorescence and phase-contrast images were acquired on a Zeiss 510LS Meta confocal microscope.

LacZ activity was detected on 8 μm frozen tissue sections. Sections were briefly washed in PBS, fixed in 1 % formalin for 1 min, washed in PBS and incubated 12-16 hours at 37 °C in 40mM phosphate/citrate buffer (pH 7.5), 2 mM $MgCl_2$, 5 mM potassium ferrocyanide, 5 mM potassium ferricyanide, X-gal (5-bromo-4-chloro-3-indolyl-β-D-galactoside) to a final concentration of 1 mg/ml. After staining, tissue sections were washed in PBS and mounted without counterstaining.

Immunofluorescence on isolated acini.

Acini were isolated as described above, resuspended in Waymouth's medium supplemented with 1 % FBS and mixed with an equal volume of collagen gel (83.7% rat tail type I collagen, 10% 10x Waymouth's medium, 6.6% 0.34 N NaOH). 500 μl/well of the gel/cell suspension mix were plated in a 24-well plate and allowed to polymerize for 15 minutes at 37 °C. The solid collagen matrix was overlaid with 500 μl of Waymouth medium supplemented with 50 ng/ml TGF-α. And inciubated for 0, 24, 48 and 36 hours. At the indicated time points , collagen discs were removed from the wells, rinsed in PBS and fixed for 30 min in 4% PFA. Collagen discs were rinsed 3x for 15 min in 100 mM glycine in PBS, blocked for 1 hour at room temperature in blocking buffer (PBS, 0.1% BSA; 0.2% Triton X-100; 0.05% Tween-20, 10% goat serum) and incubated overnight at 4 °C with the primary antibodies at the indicated concentrations (table 1) diluted in blocking buffer. Collagen discs were then washed three times for 20 min with IF buffer (PBS, 0.1% BSA; 0.2% Triton X-100; 0.05% Tween-20) at room temperature with gentle rocking and incubated with the appropriate fluorescent secondary antibodies at the indicated concentrations (table 1) in blocking buffer for 1 hour at room temperature. Collagen discs were washed 3 times for 20 min in IF buffer, incubated for 15 min with 50ug/ml DAPI in PBS, washed in PBS for 5 minutes and mounted.

Amylase activity assay and protein quantitiation.

Amylase levels in plasma and pancreatic tissue lysates were determined by a colorimetric method, using the Liquid Amylase Reagent (Pointe Scientific, Canton MI) based on the 2-chloro-p-nitrophenyl-ı-D-maltotrioside chromogenic substrate. Plasma was diluted 1:800 in 200 μl of amylase reagent and tissue lysates 1:4000 to 1:25000. Amylase content was determined by the kinetic of substrate hydrolysis according to the manufacturer's instructions.

Protein lysates were prepare by brief sonication on ice of ~100 mg pancreatic tissue in 50 mM Tris, 0.5 % NP-40, 150 mM NaCl in the presence of a protease inhibitor cocktail solution (Roche, Nutley, NJ). Protein concentration was measured by a bichinonic acid-based assay, BCA kit. (Pierce, Rockford, IL)

Live cell imaging.

Acini were prepared as described above, resuspended in 1 mL of KRS and placed on coverslip plates covered by a thin layer of Matrigel (BD biosciences, Franklin Lakes, NJ) of approximately $3\mu l/cm^2$. Matrigel was applied to the glass bottom of the plates at 4 °C by pipetting and immediately aspirated, and then the coat was allowed to polymerize 15 min at 37 °C. Cells were loaded with 2 μM FM1-43 (Invitrogen, Carlsbad, CA) and imaged on Zeiss LSM 510 confocal microscope equipped with a heated stage and objective. After obtaining stable fluorescent signal, cerulein was added to the acini to a final concentration of 1 nM. Fluorescent and bright field images were acquired at regular intervals of 20 seconds.

MMP-7 RNAi silencing vector construction.

Knockdown of MMP-7 was achieved by delivering a double-stranded interfering RNA hairpin expressed by the vector pSuper-Retro-puro (Oligoengine, Seattle, WA). Two silencing constructs targeting two different sequences in the MMP-7 gene were generated. A non-silencing construct was designed using the scrambled 19 bp sequence TAGACACAGTGACTCGGAG. The silencing sequences used were referred to as "n.1" (AAGCCAAACTCAAGGAGAT) and "n.4" (AAGCACTGTTCTTCCACTC). An 80% confluent 10 cm plate of the packaging cell line 293-phoenix amphi was transfected with 10 μg of the construct DNA. 6 ml of the culture medium, Dulbecco's modified Early medium (DMEM) supplemented with 10% FBS containing viral particles were harvested after 12-16 hours and incubated with S2-013 and CFPAC-1 cells for 12-16 hours at 37 C. Infected cells were selected with puromycin (1 μg/ml for CFPAC-1 cells, 5 μg/ml for S2-013) for 2 weeks.

Proliferation assays.

CFPAC-1 and S2-013 Cells were plated in 24wells plates at semi-confluent (50%-80) or confluent density (corresponding approximately to $5x10^5$ cells), supplemented with high (1 ml) or low (250 μL) DMEM medium, in the presence or absence of 10% fetal bovine serum (FBS). Media conditioning was achieved by culturing cells in 250 μL DMEM medium (medium were not replaced; only 50 μL/day of fresh medium was added to prevent drying of the wells). A well was trypsinized at 1 or 2 days intervals for 6 days; cells were resuspended and counted by hemacytometer excluding Trypan Blue-stained cells; the number of surviving cells was computed and plotted as average of at least 3 counts.

Methionine starvation.

S2-013 cell pools were cultured in 1 ml DMEM +10% FBS lacking cysteine and methionine, changed every 48 hours. Cells were counted by Trypan Blue exclusion every 1-2 days and the number of cells per well was computed and plotted as average of 3 counts.

Migration assays.

CFPAC-1 and S2-103 cells were resuspended in 250 μl of serum free DMEM medium, $1.5x10^4$ cells were placed in the upper chamber of a BD Biosciences cell Culture Inserts containing an 8 μm pore-size PET membrane. The insert with the cell suspension was immediately placed in 24 well plates containing 0.5ml serum free media; the bottom of the wells were coated with 150 μL of a chemoattractant gel, composed of 75% rat tail type I polymerized collagen and 25% FBS. The control experiment did not include any chemoattractant gel.

Cells were allowed to migrate toward the chemoattractant for 6 to18 hours; the optimal time point was experimentally determined to be 6-8 hours for both cell lines. Non adherent cells and media were removed from the inner insert chamber by aspiration. Membranes were washed 3x with PBS in order to remove loosely attached cells. Membranes were then fixed in 4% paraformaldehyde in PBS, washed gently and hematoxylin stained for 5 minutes and mounted onto a microscope slide. The number of stained cells per 10x microscope field was counted. The average of 15 random fields, corresponding to approximately 50% of the membrane area, was analyzed and the counts were plotted as percentage cells relative to the control.

Invasion assays.

CFPAC-1 and S2-103 cells were resuspended in 250 μl of serum free DMEM medium, counted and $1.5x10^4$ cells were placed in the upper chamber of a BD Biosciences cell

Culture Inserts containing an 8 μm pore-size nylon membrane. The membrane was coated with a layer of liquid growth factor reduced-Matrigel at 4 °C for 5 minutes; excess Matrigel was removed at 4 °C by pipetting and polymerization was allow in a humidified tissue culture incubator at 37C for 15 minutes. The cell suspension was then added to the insert and immediately placed in wells containing 0.5 ml serum free media; the bottom of the plate's wells were coated with 150 μL of a chemoattractant gel, composed of 75% rat tail type I polymerized collagen and 25% FBS. The control experiment did not include any chemoattractant gel.

Cells were allowed to migrate through the Matrigel layer towards the chemoattractant for 10-12 hours. Non adherent cells and media were removed from the inner insert chamber by aspiration, the Matrigel layer was removed by a cotton swab; membranes were washed 3x with PBS in order to remove Matrigel residues. Membranes were then fixed in 4% paraformaldehyde in PBS, washed gently and hematoxylin stained for 5 minutes and mounted onto a microscope slide. The number of stained cells per 10x microscope field was counted. The average of 15 random fields, corresponding to approximately 50% of the membrane area, was analyzed and the counts were plotted as percentage cells relative to the control.

Tumorigenesis in athymic nude mice.

Two tumorigenic cell lines were used (CFPAC-1 and S2-013); after puromycin selection cell were infected with a GFP-expressing viral vector (pSuper PGK-GFP, gift of Dr. Ken Marcu) and FACS sorted. The sorted pools were re-tested for MMP-7 expression (Figure 10) and showed similar levels of MMP-7 compared to the original GFP negative cell pools. 700.000 GFP positive cells of each pool were resuspended in 150 μL of PBS and injected subcutaneously for a total of two injections per animal; each animal received two injections of the same pool MMP-7 RNAi or non silencing RNAi.

The progression of tumor formation was monitored by fluorescent *in vivo* imaging; tumor volume, approximated to an ellipsoid shape, was computed on the acquired images, measuring the width and the length of each fluorescent mass. . Optimal image acquisition was obtained by positioning tumor protrusion in axis with the objective lenses.

The tumor burden per animal was computed by adding the volumes of each tumor mass on each animal. The average GFP signal intensity was used as an indicator of the local density of GFP-positive cells in tumours.

Pancreatic tumorigenesis and progression in wild type and MMP-7$^{-/-}$ backgrounds.

LSL-Kras^{G12D} mice and p48-Cre mice were first crossed with MMP-7$^{-/-}$ mice, all three of which were maintained in the C57Bl/6J genetic background, to generate LSL-Kras^{G12D};MMP7$^{-/-}$ and Ptf1a-cre;MMP7$^{-/-}$ animals. LSL-Kras^{G12D};Ptf1a-cre;MMP-7$^{-/-}$ were generated by crossing these animals with each other. Separately, C57Bl/6J LSL-

Kras and Ptf1a-cre animals were mated to generate wild type control versions of the LSL-Kras^{G12D};Ptf1a-cre model system. In these mice, the K-Ras^{G12D} mutant allele is expressed in exocrine, endocrine and centroacinar cells after a Ptf1a promoter-driven, recombinase-mediated removal of the lox-stop-lox (LSL) element early in development. Mice were sacrificed at the time points indicated in table 3 and mouse weight and pancreatic wet weight were determined. Males and females mice were equally distributed in the *wild type* and MMP-7$^{-/-}$ groups. Pancreata were fixed, dehydrated, paraffin embedded and sectioned for histological analysis.

A total of 40 consecutive sections were prepared from each paraffin embedded sample. In order to obtain representative samples for morphological analysis, twenty consecutive sections were cut at approximately 1/3 of depth into the paraffin block embedding the tissue and twenty more at 2/3 of the total block depth. Every quantitative analysis was considered valid only if consistent between sections taken at different spots in the embedded sample. Two sections were placed on each slide such that the second section was approximately 200 μm from the first section. Thus, each stained slide represented data progressively from regions 200 μm apart in the pancreatic tissue.

Mouse and pancreatic mass were determined upon sacrifice and the following parameters were obtained by light microscopy or from scanned digital images of histological sections:

Number of tumor foci/area analyzed; Dimensions (approximated to an elliptical shape, length and width were measured) of every tumor lesion; used to estimate volume; Histological features of lesions (presence of ductal or undifferentiated component); Properties of every tumor lesion (number of ducts, cells per duct, proliferative/apoptotic cells per duct); Proliferation was determined by anti-BrdU immunostain (IP injected twice 2 and 20 hrs before sacrifice, 50mg/kg body weight).

Statistical Analysis.

Data relative to acinar size, organ/body mass ratios and amylase levels are presented as means +/- SEM unless otherwise stated and are calculated on triplicate measurements obtained from at least 3 mice per group/genotype. Histological and immunofluorescence pictures are representative fields of at least 3 mice per group/genotype and 3 repeats of the same experiment. Quantitiation of immunostaining is presented as the mean +/- SEM of the counts of positive stained cells on 10 or more random microscopic fields at 40x magnification of at least 3 different experiments/mice/genotypes. Minitab software (Minitab, State College, PA) was used for statistical analysis. Group means were compared by unpaired, 2 tailed, Student's T test. A value of *P <0.05* was considered statistically significant.

Antigen	Application and working concentration	Species	Vendor
Laminin α2	IF on frozen tissue sections. 1 hour incubation at 20 μg/ml	rat	Sigma
ZO-1	IF on frozen tissue sections. 1 hour incubation at 1 μg/ml	rabbit	Zymed
α-amylase	IF on isolated acini. 1 hour incubation of 1:500 stock dilution	rabbit	Sigma
HMGB-1	IHC on paraffin-embedded sections. 16-24 hours incubation at 0.5 μg/ml	mouse	Abcam
E-cadherin	IF on frozen tissue sections. 1 hour at 0.7 μg/ml	mouse	BD Biosciences
α-dystroglycan	IF on frozen tissue sections. 1 hour at 1:100 stock dilution	mouse	Upstate USA
β1-integrin	IF on frozen tissue sections. 1 hour at 10 μg/ml	rabbit	Chemicon Millipore
Alexafluor488 and Alexafluor 594-conjugated fluorescent secondary antibodies (anti-rat, rabbit and mouse)	IF on frozen tissue sections and IF on isolated acini. 1 hour incubation at 2 μg/ml for both applications	goat	Vector Labs

Table 1. List of the used antibodies and working concentrations

Chapter 3:

Pancreatic ablation of β1 integrin : results

Cre-mediated recombination and pancreatic ablation of β1 integrin

To study the role of β1 integrin in the pancreas I crossed Ptf1a-*cre* mice [46] to conditional β1 integrin knockout mice [45], which carry functional copies of the β1 integrin gene, with exons 2-7 flanked by LoxP sites. Upon recombination, the LacZ reporter gene is driven by the endogenous β1 integrin promoter. In Ptf1a-*cre* mice, the *Cre* recombinase transgene is knocked into the Ptf1-a locus and expressed in early development by the vast majority of pancreatic progenitor cells. Consequently, in β1 integrin $^{flox/flox}$;Ptf1a-*cre* mice, most exocrine and endocrine cells in the adult lack β1 integrin.

After establishing a colony of β1 integrin $^{flox/flox}$;Ptf1a-cre mice, I confirmed allele-specific recombination by PCR (Figure 5A). The 800 bp PCR amplification product is detectable exclusively in the pancreas-extracted (lane 2), but not in tail-extracted DNA of the same β1 integrin $^{flox/flox}$;Ptf1a-cre mouse (lane 1). Consistent with the published characterization of Ptf1a-cre animals [46], I detected LacZ activity in β1 integrin$^{flox/flox}$;Ptf1a-cre mice by X-gal staining in the vast majority (>95%) of acinar, ductal, insular and centroacinar (Figure 5B).

I also confirmed the tissue specific loss of β1integrin protein by immunofluorescence (Figure 5C and 5D). The loss of β1 integrin in the exocrine cells appeared to be near complete, while surrounding cells continued to express robust levels of the protein.
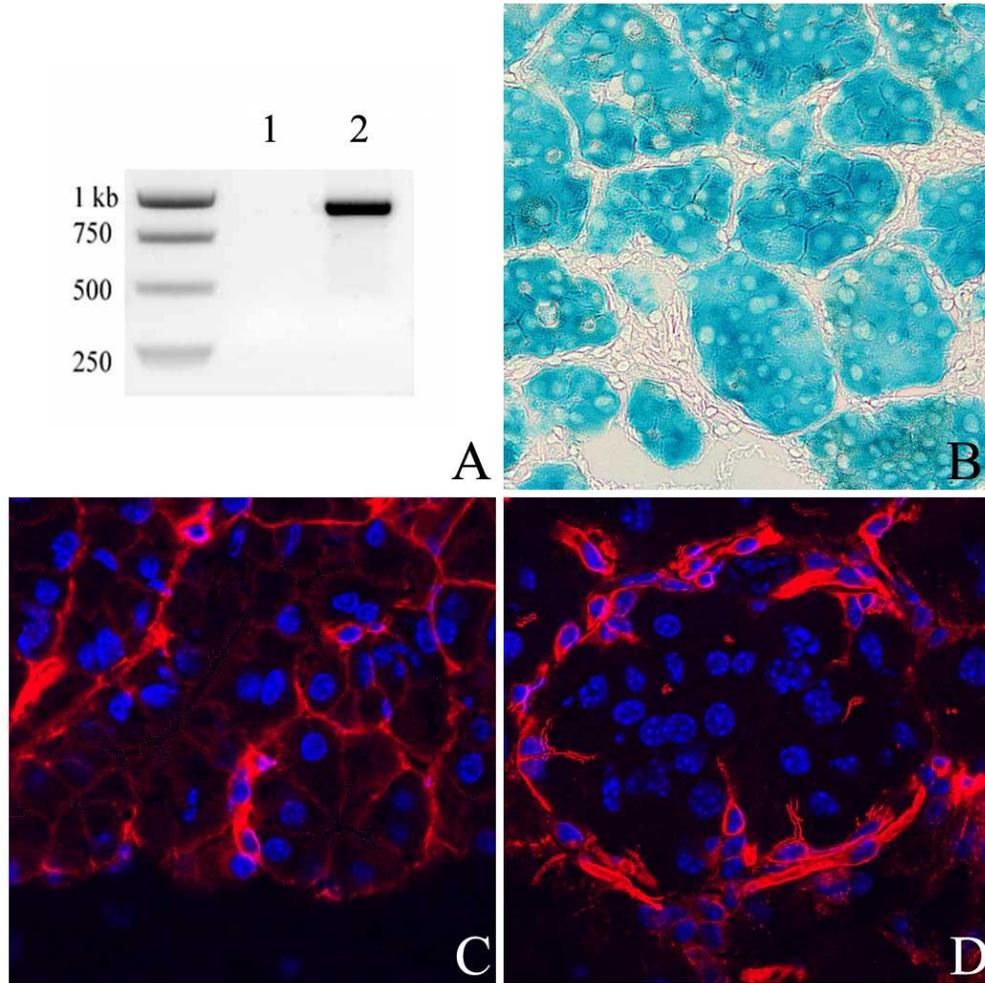
Figure 5. β1 integrin (in red) is expressed at the basolateral surface of acinar cells. Positive immunofluorescence staining for β1 integrin was detected in β1 integrin [flox/flox] (**A**) but not in β1 integrin [flox/flox];Ptf1a-cre (**B**) tissue sections β1 integrin-proficient cells surrounding pancreatic acini showed always intense immunoreactivity. (63x magnification) Nuclei (in blue) were stained with DAPI. (**C**) Recombination of the floxed alleles in β1 integrin [flox/flox];Ptf1a-cre pancreata. X-gal staining was performed to detect LacZ reporter activity. Intense blue staining was detected in the vast majority (>95%) of acinar cells by phase-contrast light microscopy (20x magnification), indicating recombination of the floxed alleles. No staining was detected in interstitial, non-recombined cells or in wild type controls (data not shown). (**D**) PCR detection of floxed alleles recombination. Primers P1 and P3, complementary to sequences upstream and downstream of the floxed allele, yielded an 800 bp PCR amplification exclusively in the pancreas-extracted (lane 2), but not in tail-extracted DNA of the same β1 integrin [flox/flox];Ptf1a-cre mouse (lane 1).

28

Loss of β1 integrin results in pancreatic degeneration.

β1 integrin $^{flox/flox}$;Ptf1a-cre mice were born at the expected Mendelian frequency, had a normal lifespan, were fertile and grossly indistinguishable from β1 integrin $^{flox/flox}$ littermates. Heterozygous β1 integrin $^{flox/wild\ type}$;Ptf1a-cre mice did not reveal any phenotypic difference compared to wild type animals up to 1.3 years of age, the termination point of this study.

At a gross organ level, I observed age-dependent, phenotypic changes in the β1 integrin $^{flox/flox}$;Ptf1a-cre animals, most notably a progressive reduction in the pancreatic mass. (Figure 6A) As a first level of assessment, I compared the pancreas/body mass ratio of wild type and β1 integrin null mice. In the three age groups considered (3weeks, 7-14 weeks, >9 months old mice; N ≥ 4/group) this ratio was consistently on the order of 1.1% in the wild type background.

In the β1 integrin null background relative mass was ~0.8% up to 7-14 weeks and progressively decreased to 0.25% (P<0.05%) at 1 year of age. (Figure 6 B) In order to rule out the possibility that the weight of the animals was affected by the pancreatic phenotype, I normalized pancreatic mass to femur length of adult wild type and β1 integrin $^{flox/flox}$;Ptf1a-cre, but found no significant differences with the method of normalization. (Data not shown)

Histological examination of H&E stained sections of revealed that up day P7-10, both *wild type* and β1 integrin $^{flox/flox}$;Ptf1a-cre mice developed a histologically normal pancreas. In fact, all β1 integrin-proficient acinar cells, independent of age, always had the expected structural symmetry with nuclei appropriately oriented to the basal surface (Figure 7 A). In contrast, β1 integrin $^{flox/flox}$;Ptf1a-cre pancreata after day P21 were characterized by the presence of abnormal, larger acini, containing cells with little cytoplasm and located in the center of the acinar structure (Figure 7 C, D) and apparent loss of distinct basolateral polarity.

After the 3 weeks of age the percentage of these large β1 integrin-null acini compared to total acini progressively increased from 1-2% to approximately 50% at 3 months of age and became the predominant type by one year of age. This process was accompanied by an accumulation of cells in the stromal compartment, (Figure 7 E, F) characterized by the accumulation of inflammatory cells in the interstitial spaces and reminiscent of a mild form of AP. Wild-type controls did not display any significant stromal reaction, regardless of age.

Taken together, these observations reveal that the lack of β1 integrin *in vivo* was not required for the initial formation of polarized acini, but affected the maintenance of this architecture of the organ in adult mice.
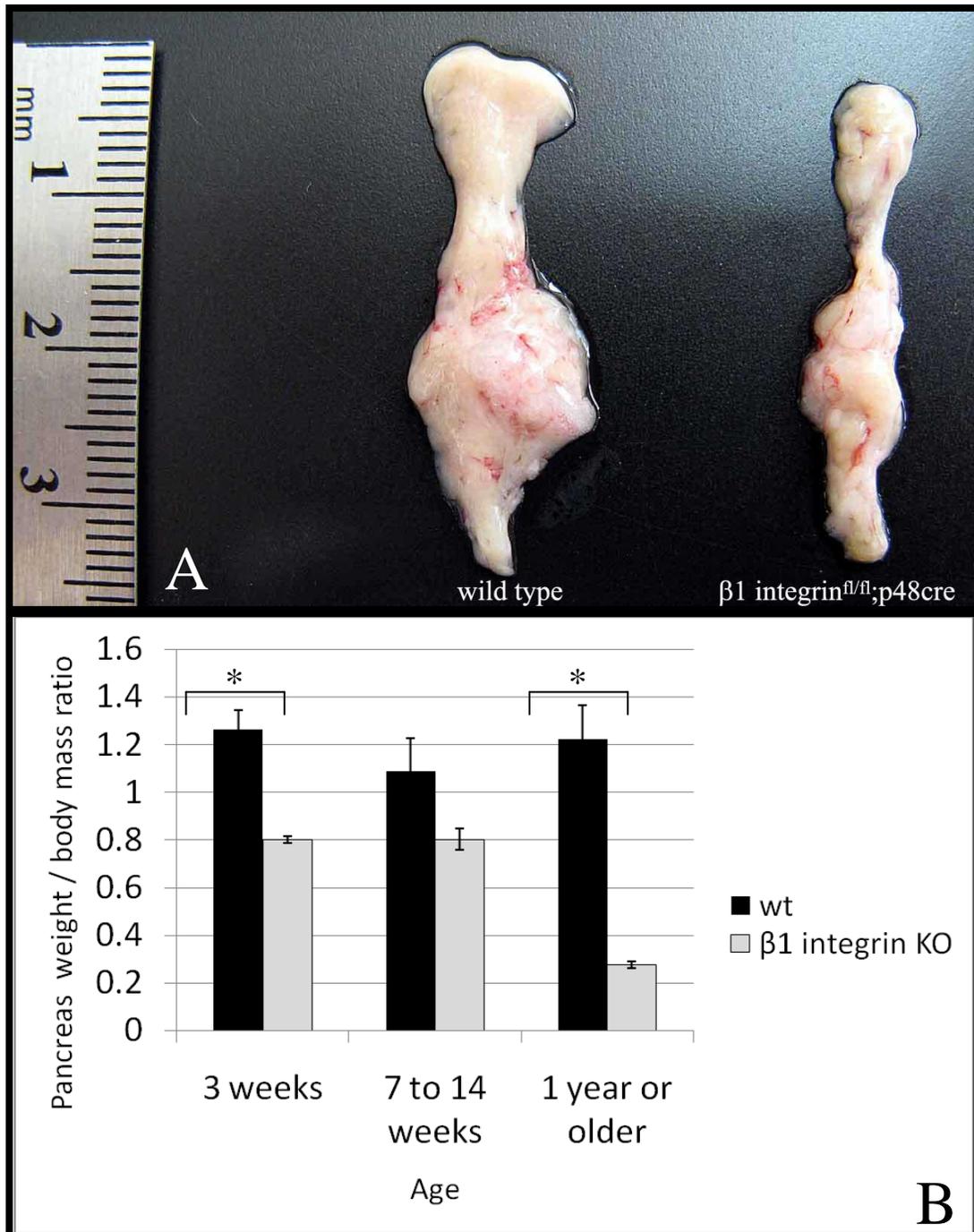
Figure 6. (**A**) Pancreata of 1 year-old *wild type* (left) and in β1 integrin $^{flox/flox}$;Ptf1a-cre mice (right) (**B**) Pancreas weight/body mass ratio in β1 integrin $^{flox/flox}$;Ptf1a-cre and *wild type* animals. Beginning at 7-14 weeks, the pancreas weight/body mass ratio progressively decreased only in β1 integrin $^{flox/flox}$;Ptf1a-cre mice (grey) and dropped to about 25 % of a normal *wild type* control (black) at 1 year of age (P<0.05).
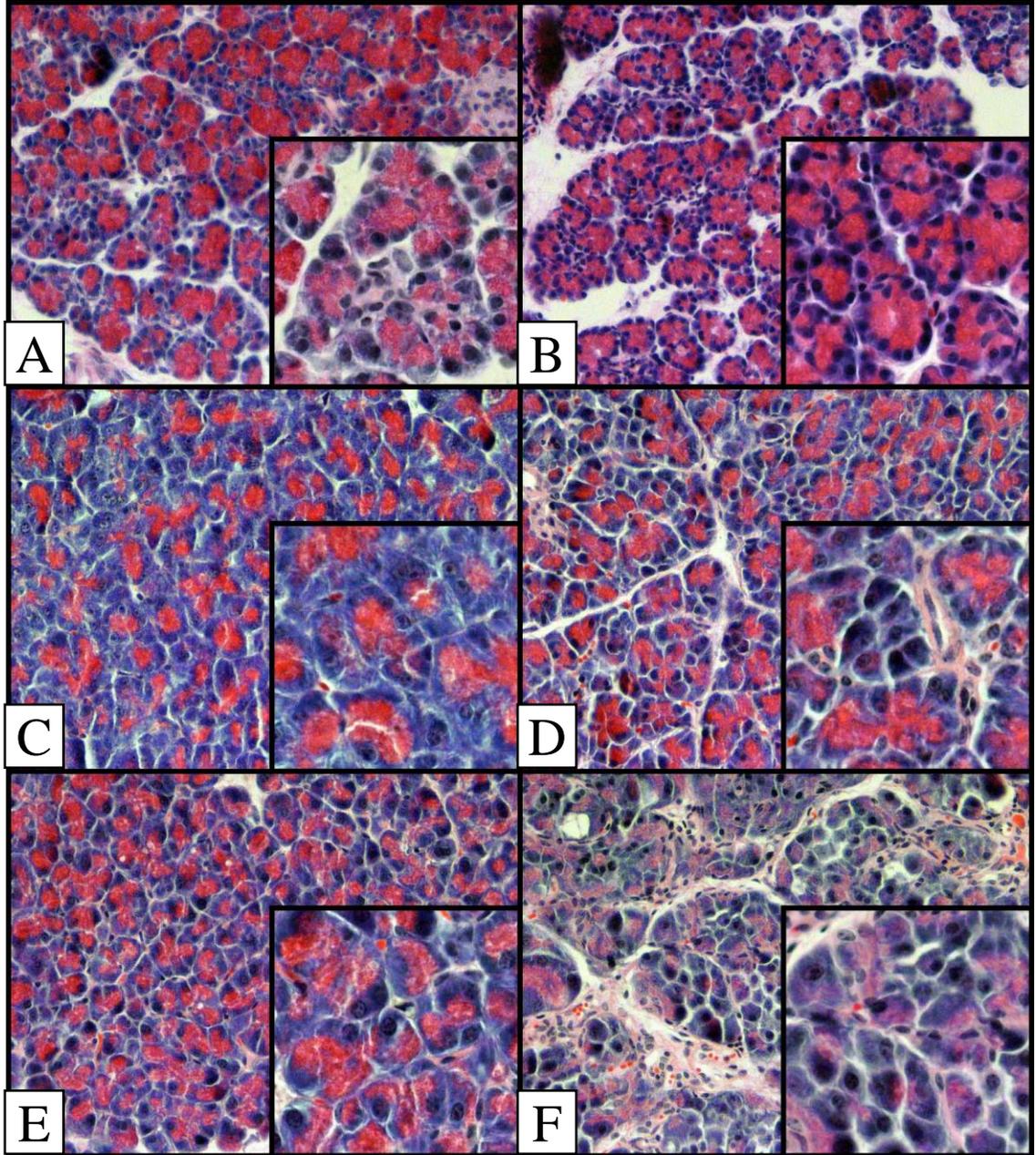
**Figure 7.** Progressive pancreatic degeneration in β1 integrin [flox/flox];Ptf1a-cre pancreata. Shown are representative pictures of H&E stained sections of *wild type* (**A,C,E**) and β1 integrin [flox/flox];Ptf1a-cre (**B,D,F**) at 1 week of age (**A,B**), 3 weeks(**C,D**) and 1.2 years of age (**E,F**). (20x magnification, 40x inset)
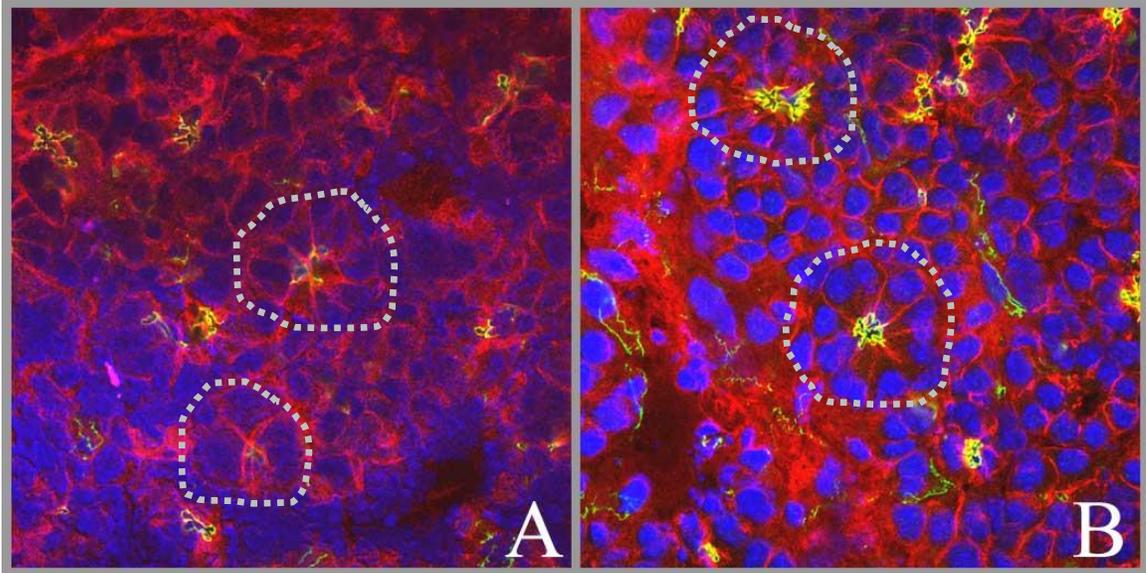
Figure 8. Cell-cell adhesion molecule E-cadherin is expressed in 1 week old *wild type* and β1 integrin $^{flox/flox}$;Ptf1a-cre acini. Strong immunofluorescence staining for E-cadherin (in red) was detected in *wild type* (**A**) and β1 integrin $^{flox/flox}$;Ptf1a-cre (**B**) acini (highlighted by the dashed line; 63x magnification. Apical marker ZO-1 in green; merge: yellow.) Nuclei (blue) were stained with DAPI.

Morphology of β1 integrin $^{flox/flox}$;Ptf1a-cre isolated acini.

I further characterized β1 null acini, using co-immunofluorescence for laminin α2 chain to define the basement membrane surrounding each acinus and ZO-1, tight junctions marker, to define the acinar apical surface.

Measurements of laminin-encompassed acini indicated that in β1 integrin $^{flox/flox}$;Ptf1a-cre mice at the age of 8 weeks already had a significantly larger diameter compared to age matched controls (data not shown) and this difference is maintained in aging animals (Figure 11, $P<0.05\%$), confirming qualitative observations on H&E stained slides.
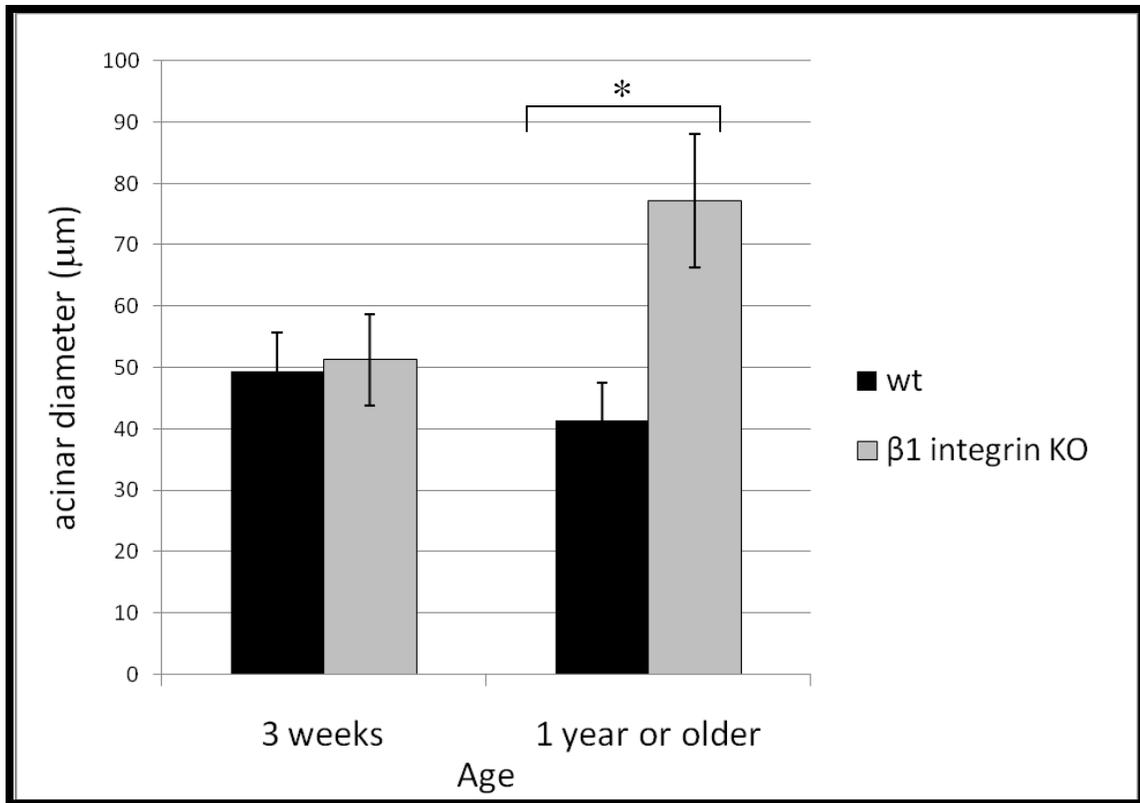
Figure 9. β1integrin-null acini of 1 year old mice have a larger average diameter (P<0.05). Immunofluorescence staining on tissue sections for the BM protein laminin α2 was used to define the acinar perimeter. The major axis of >50 randomly chosen acini/mouse of the indicated age was taken as acinar diameter. Shown are averages of 3 *wild type* (black) and 3 β1 integrin [flox/flox];Ptf1a-cre pancreata (grey) (averages in μm; error bars ± SEM).
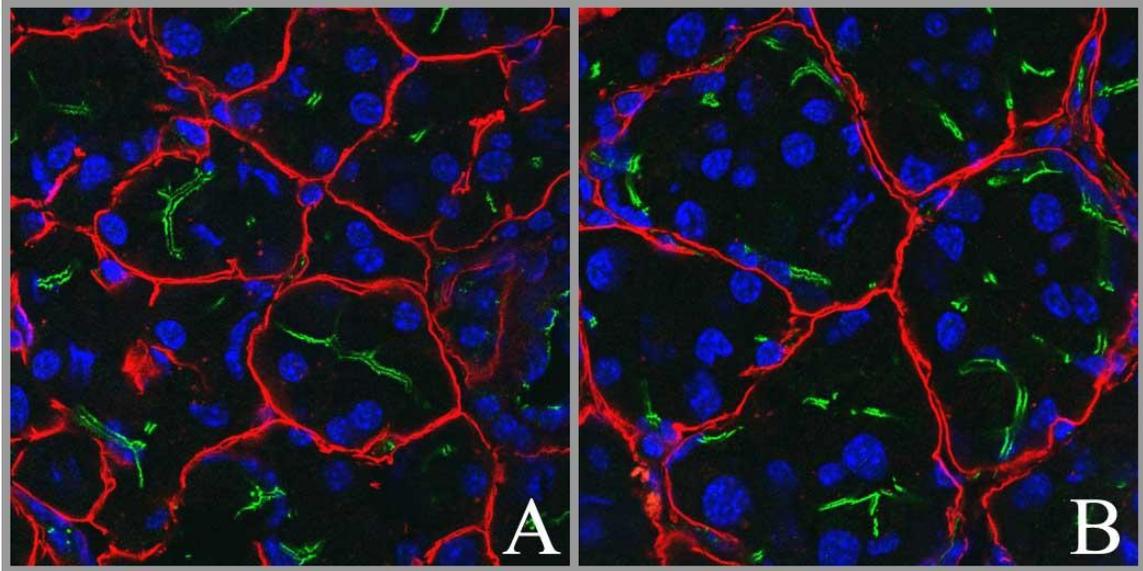
Figure 10. Lumens are centrally localized in *wild type* acini but mislocalized in β1 integrin null acini. Tissue sections of *wild type* (**A**) and β1 integrin^{flox/flox};Ptf1a-cre (**B**) pancreata were stained for laminin α2 chain (red) to define the BM and apical marker ZO-1 (green) to highlight the lumen. Representative pictures at 63x magnification are shown.
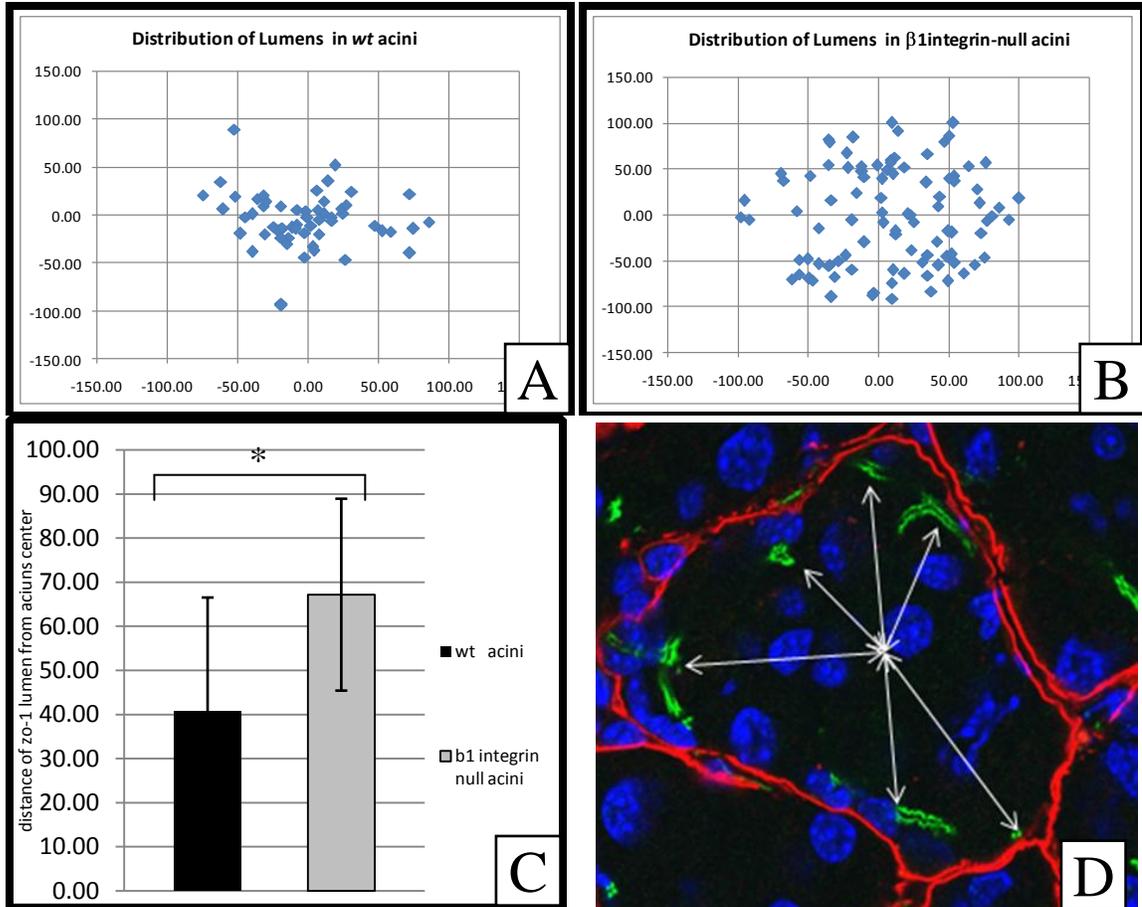
**Figure 11**: The average distance of the lumen from BM is greater (P <0.05) in β1 integrin [flox/flox];Ptf1a-cre compared to *wild type* controls. Scatterplots showing the average relative distance of the ZO-1 positive apical regions from the center of the acinus in *wild type* (**A**) and β1 integrin [flox/flox];Ptf1a-cre (**B**). Scale: "0" represents the geometrical center of acinus, "100" the position of the basement membrane. Average distances of the lumens from the BM (**C**) in *wild type* (**black bar**) and β1 integrin [flox/flox];Ptf1a-cre (**grey bar**). Example of the measured lumen-BM distances (**D**, white arrows). Shown are the averages in μm of >50 acini/mouse ; 3 or more mice/group; error bars ± SD.

I assessed the loss of acinar cell polarity more precisely by examining the localization of ZO-1, a protein found in the tight junctions at the apical surface of polarized epithelia. In a section of a normal *wild type* pancreas, ZO-1 immunostaining highlights the apical regions of acinar cells, which together delimit the lumen, an extracellular space located in the center of the wild type acinus.   ZO-1 immunofluorescence on β1 integrin [flox/flox];Ptf1a-cre sections revealed scattered ZO-1 - positive regions located on average further away (P<0.05) from the geometric center of the acini, regardless of the size of their size. (Figure 11)

I first hypothesized that the loss of β1 integrin caused changes in acinar structure leading to misregulated secretion of digestive enzymes and as a result, a slow, progressive death of acinar cells, either apoptotic or necrotic, that was not compensated by a regenerative response. In order to address how that the changes in acinar structure might be linked to the degenerative phenotype, I tested if the amylase-positive cells in the center of the acinus and detached from the laminin-rich BM were undergoing anoikis.

I stained for the apoptotic marker cleaved caspase-3, but I found no indication of apoptosis in the wild type or β1 integrin [flox/flox];Ptf1a-cre pancreata, neither in 1 year-old or 8 weeks old mice. While unexpected, apoptosis is not the only form of cell death that the tissue could be susceptible to; necrosis, for example, is a form of cell death commonly found in AP.

I tested for necrosis by HMGB-1 immunohistochemistry.   In normal cells, HMGB-1 is found in the nucleus tightly associated with chromatin; in cells undergoing necrosis, however, it is transported out of the nucleus and is expelled into the extracellular space, where it acts as an inflammatory cytokine [48]. I detected a higher number of necrotic acinar cells in β1 integrin [flox/flox];Ptf1a-cre mice compared to *wild type* acinar cells. (Figure 12 A, B)

Besides the focal necrotic areas, I did not detect other types of cell death that could account for the pancreatic degeneration, probably because of the slow course of the phenotype development or fast clearance by phagocytes. A recent work on a model of endocrine pancreatic cancer [49] showed that the lack of β1 integrin can induce senescence in transformed β cells. In our system, however, due to the LacZ reporter expression in β1 integrin [flox/flox];Ptf1a-cre mice staining for senescence associated β-galactosidase gave questionable results due to the activity of the bacterial form the endogenous β-galactosidase. [50]

β1 Integrin ^{flox/flox};Ptf1a-cre mice have increased susceptibility to cerulein-induced pancreatitis and have a delayed recovery.

My observations that β1 integrin ^{flox/flox};Ptf1a-cre pancreata progressively degenerate was consistent with the hypothesis that these mice were exposed to a constant level of a tissue damage caused by the continuous escape of digestive enzymes possibly resulting from luminal mislocalization.

I thus hypothesized that β1 integrin ^{flox/flox};Ptf1a-cre mice would be more susceptible to an induced supramaximal secretory stimulus. I chose the well-established model of secretagogue-induced pancreatitis [14] to test whether both the extent of tissue injury and subsequent regeneration were affected by the loss of β1 integrin. The employed protocol, consisting of a single cycle of 7 hour ly cerulein injections, is designed to induce a condition of mild acute pancreatitis in *wild type* animals. Mice of 7-8 weeks of age were sacrificed at 1 hour, 24 hours or 1 week after the last injection. These studies revealed dramatic differences between *wild type* and β1integrin^{flox/flox};Ptf1a-cre animals with respect to both the response and the recovery from the drug induced damage.

One hour after injection, β1 integrin null acinar cells showed extensive vacuolization and discharge of membrane-containing bodies and broad loss of acinar structure, while wild type pancreata showed, in general, the expected mild phenotype. (Figure 13 A, B) Plasma amylase activity, a marker of transient pancreatic injury, [51] was, as expected, elevated after cerulein injections, but significantly higher in β1integrin^{flox/flox};Ptf1a-cre mice (P<0.05) compared to *wild type* controls, correlating to a greater degree of tissue damage at this time point. (Figure 14)

Wild type mice were phenotypically normal when allowed 24 hours of recovery, while β1 integrin ^{flox/flox};Ptf1a-cre mice showed only partial regeneration of the acinar tissue and a marked persistence of inflammatory cells. (Figures 13 C, D)

In order to assess the extent of tissue damage after cerulein-induced pancreatitis, I measured the specific activity of amylase in tissue lysates as an indicator of functional exocrine tissue. Untreated *wild type* controls had a 3-fold higher amylase activity per mg of lysate (P<0.05%) compared to age-matched β1 integrin^{flox/flox};Ptf1a-cre mice. (Figure 15A) This is possibly due to a higher number of cells per tissue volume in *wild type* acini, or the result of a lower amount of cytoplasmic amylase in β1 integrin-null cells. The amylase activity levels of *wild type* or saline injected mice were comparable at any time point after the single cycle of cerulein injections.
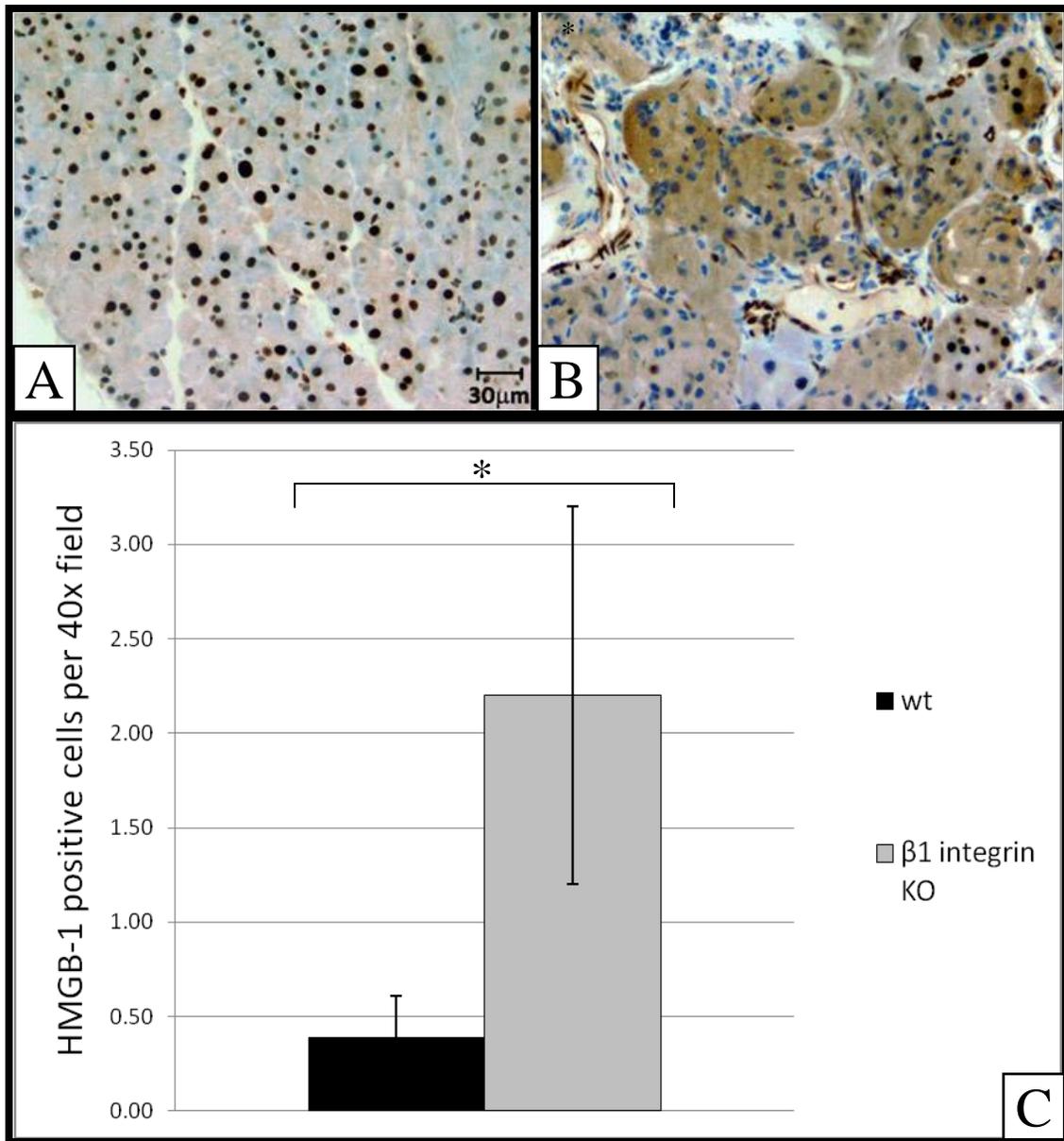
Figure 12: β1 integrin ^{flox/flox};Ptf1a-cre mice acinar cells displayed a consistent loss of nuclear HMGB-1 accompanied by a gain of cytoplasmic staining compared to controls. Immunostaining for the necrosis marker HMGB-1on paraffin-embedded tissue sections showed nuclear reactivity in the vast majority of *wild type* acinar cells (**A**) and cytoplasmic reactivity (**B**) in focal necrotic areas on β1 integrin^{flox/flox};Ptf1a-cre pancreata. (20x magnification; scale bar 30 μm) Quantitation of acinar cells displaying cytoplasmic immunoreactivity (**C**) indicated a significantly higher number of necrotic cells in β1 integrin ^{flox/flox};Ptf1a-cre (P<0.05) (Averages of 3 or more mice shown; error bars ± SEM).

Taken together with the histological analysis, these results indicated that besides the acute effect seen 1 hour after cerulein injection (Figure 13 A), *wild type* acini retained cell integrity and recovered rapidly from mild induction of pancreatitis. β1 integrin [flox/flox];Ptf1a-cre lysates, however, showed a significantly reduced amylase activity ($P<0.05\%$) 1 and 24 hours after cerulein injections (Figure 15 A), suggesting extensive tissue damage occurred 1 hour after injection and a poor regeneration of acinar tissue after 24 hours (Figures 13 B, D). One week after cerulein injections amylase activity and exocrine tissue histology was indistinguishable from untreated controls, in both wild type and β1 integrin [flox/flox];Ptf1a-cre mice, indicating an adequate supply of progenitor cells capable of repopulating the severely damaged tissue. (Figure 15 A)

I measured the extent of BrdU incorporation to test if the delayed recovery seen in β1 integrin [flox/flox];Ptf1a-cre (Figure 15 B) was due to an intrinsic proliferation defect of acinar cells, which is needed for the regenerative process [52]. BrdU incorporation in wild type acinar cells was significantly elevated 24 hours after injections and returned to normal levels after 1 week. The incorporation in β1 integrin null cells never went significantly above the level of untreated or saline injected mice. (Figure 15 B) These data, together with the histological analysis and the amylase activity in tissue lysates, suggests that the proliferative response in β1 integrin[flox/flox];Ptf1a-cre acinar cells is either delayed or it is proceeding slower compared to *wild type* controls.

Amylase secretion of β1 integrin [flox/flox];Ptf1a-cre isolated acini.

While I saw that acinar lumen was mislocalized, the TEM ultrastructure of the cells appeared largely normal, with properly localized tight junctions between acinar cells. (Figure 16) One possible explanation of the readout of the cerulein injections experiments in β1 integrin [flox/flox];Ptf1a-cre mice was that the mislocalized lumen of β1 integrin null acini was misdirecting secretory products into the parenchyma consequently causing a direct damage to the whole tissue. However, based on my previous studies, it was also a formal possibility that β1 integrin null exocrine cells were over-responsive to cerulein stimulation.

In order to test the latter hypothesis, I analyzed the secretion of amylase *in vitro* by exposing isolated primary acini to a range of cerulein concentrations. *Wild type* acini were able to secrete between 12 and 23% of their total cellular amylase content and displayed maximal sensitivity to 0.1- 0.01 nM cerulein. (Figure 15 C, black) In β1 integrin[flox/flox];Ptf1a-cre isolated acini the relative amount of secreted amylase was significantly lower, approximately around 3 to 8% of the cell content. (Figure 15 C, grey) and the maximal secretory response was obtained with 0.1nM cerulein.
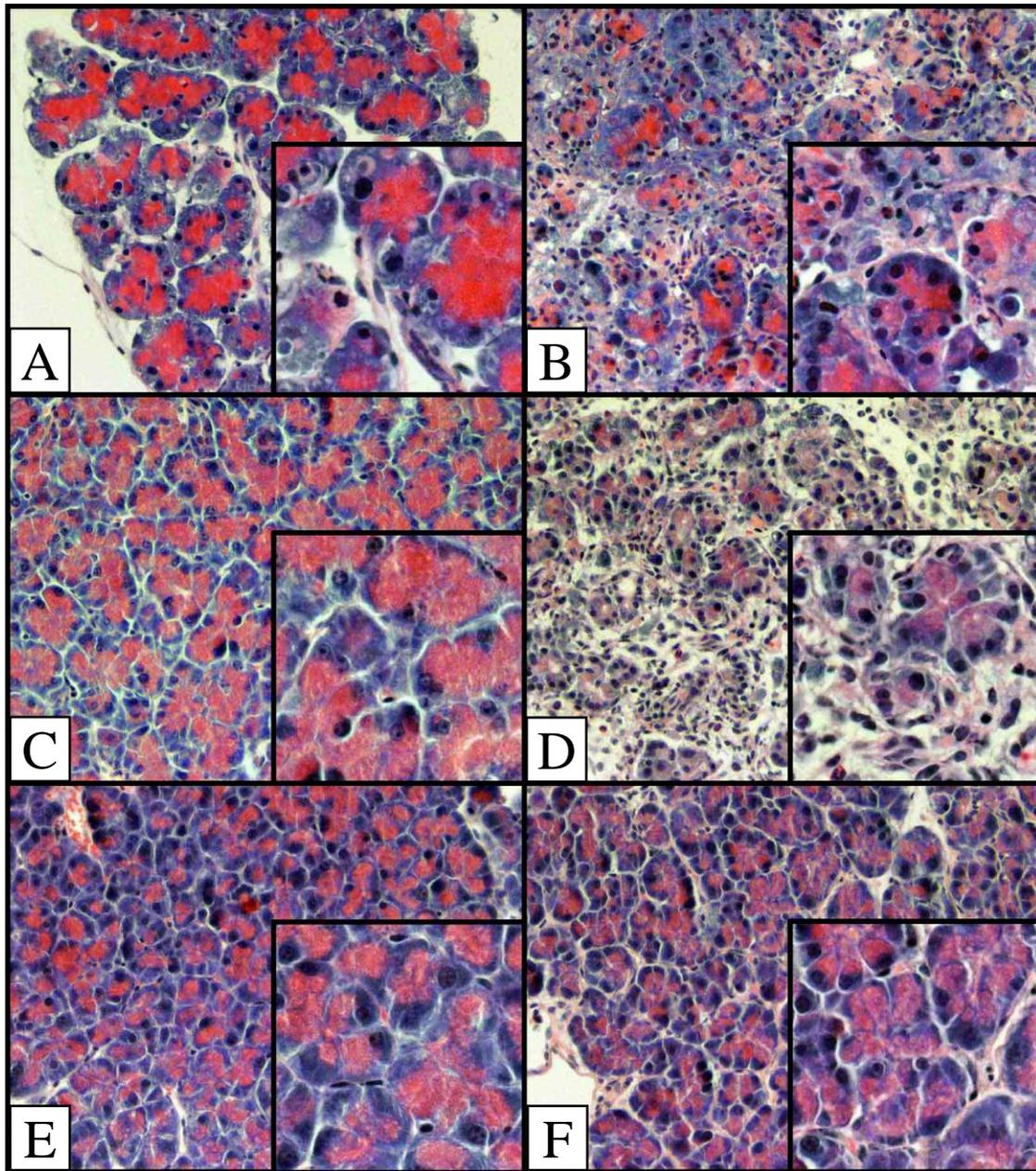
Figure 13. Recovery of *wild type* and β1 integrin [flox/flox];Ptf1a-cre mice from cerulein-induced pancreatitis . Mice were given 7 hourly injections of 50μg/kg cerulein and sacrificed after 1hour (A,B), 24 hours (C,D) and 1 week (E,F). One hour after injections H&E sections of β1 integrin [flox/flox];Ptf1a-cre pancreata (B) indicated extensive vacuolization and loss of membrane integrity compared to *wild type* (A). *Wild type* animals completely recovered after 24 hours (C), while β1 integrin [flox/flox];Ptf1a-cre pancreata showed poor tissue regeneration and persistence of inflammatory cells (D). 1 week after injection both *wild type* (E) and β1 integrin [flox/flox];Ptf1a-cre (F) pancreata appeared normal. (20x magnification, 40x inset)
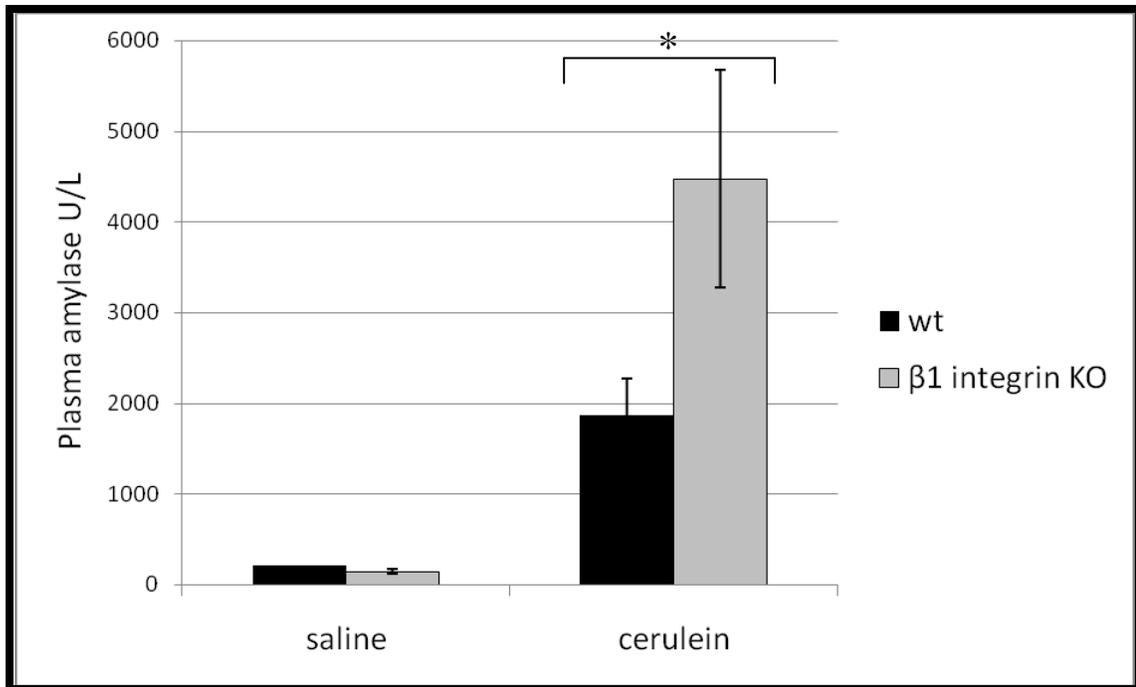
Figure 14. Plasma amylase 1 hour after cerulein injections is higher in 10-12 weeks old β1 integrin [flox/flox];Ptf1a-cre mice compared to age-matched *wild type* mice. Plasma amylase activity was increased 3-fold in β1 integrin [flox/flox];Ptf1a-cre (grey) mice compared to *wild type* (black) in response to cerulein stimulation. Control animals were saline injected. (Averages of 3 or more mice/group shown; error bars ± SEM).
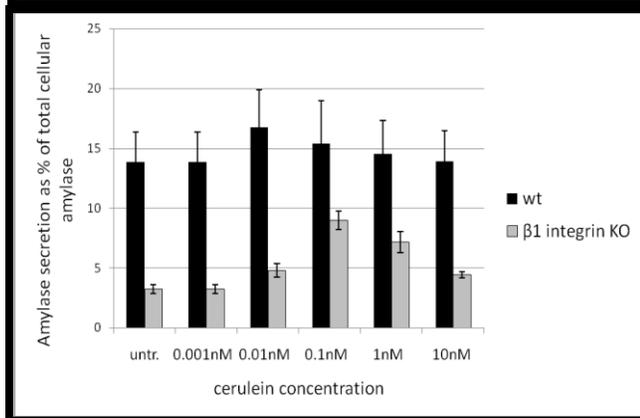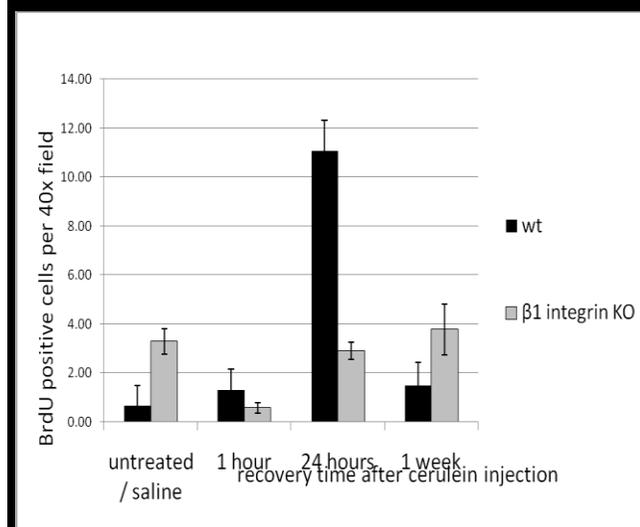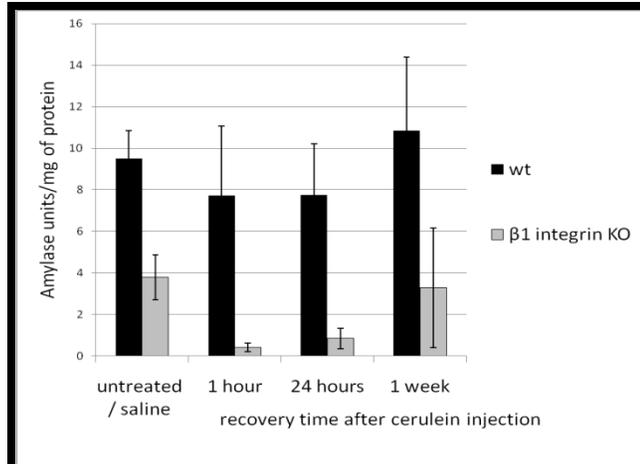
Figure 15. Delayed recovery after cerulein injection in β1 integrin -null acini. *Wild type* tissue lysates (**A**, black bars) did not display significant changes in tissue amylase activity at any time point. β1 integrin$^{flox/flox}$;Ptf1a-cre (grey bars) had significantly less of tissue amylase activity (P<0.05) at 1 and 24 hours after injections. BrdU incorporation in *wild type* acinar cells was elevated 24 hours after injections (**B,** P<0.05) and returned to normal levels after 1 week. The incorporation in β1 integrin null acinar cells never went significantly above the level of untreated or saline injected mice, indicating a slower proliferative response after cerulein injections. **(C)** β1 integrin-null isolated acini secrete less amylase and require higher cerulein concentrations to yield maximal secretion compared to *wild type*. Maximal secretion was reached by wild type acini at a concentration of 1 order of magnitude lower when compared to β1 integrin-null acini. Wild type acini secreted, proportionally to their cellular content, more amylase than β1 integrin null cells. (Values represent the secreted versus of total present amylase, shown are averages of triplicate assays for 3 or more mice; error bars ± SEM).
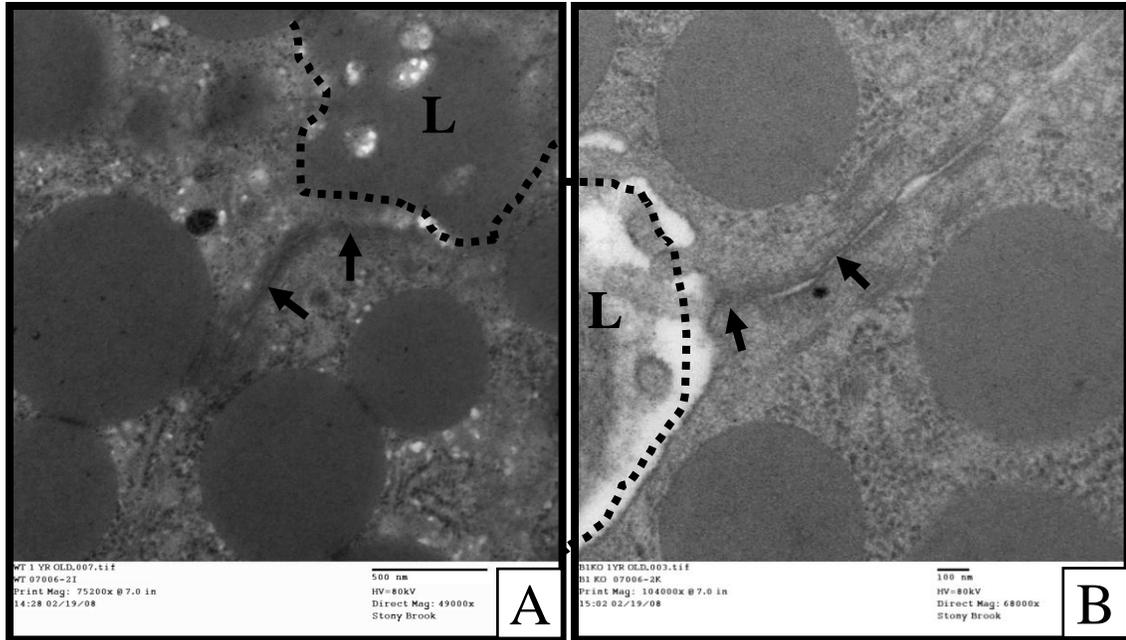
Figure 16. Tight junctions between acinar cells of *wild type* and β1integrin^flox/flox;Ptf1a-cre pancreata. Tight junctions, visualized TEM microscopy, were present at the apical portion of acinar cells is both *wild type* (**A,** 49000x magnification) and β1integrin^flox/flox;Ptf1a-cre pancreata (**B,** 68000x magnification)

This led us to the conclusion that β1 integrin ^flox/flox;Ptf1a-cre isolated acini store less intracellular amylase and actually require a higher concentration of cerulein to yield the maximal secretion (0.1 nM versus 0.01 nM of *wild type* acini, Figure 15 C), making it unlikely that the exacerbated phenotype of cerulein-injected β1 integrin^flox/flox;Ptf1a-cre mice was due to an higher sensitivity of their acini to the hormone or caused by a higher amount of missecreted enzymes.

Cerulein stimulation can also be performed on isolated pancreatic acini in order to study the directionality of secretion. This is achieved by time-course confocal imaging of living cells loaded with a styryl dye (FM1-43), which is fluorescent when bound to membranes [53]. Exocytosis, the simultaneous fusion of multiple vesicles with the plasma membrane, increases the dye-accessible surface and consequently intensifies the fluorescent signal.

I used this system to test whether β1-null acini were prone to basolateral secretion and if this was contributing to the exacerbated acute phenotype of cerulein-injected β1 integrin^flox/flox;Ptf1a-cre mice. Isolated acini were loaded with FM1-43 and after stable fluorescence was achieved, 1 nM cerulein was added to the cells. The signal increased over time, as expected, in both wild type and β1 integrin null acini. Over 45 minutes *wild*

type cells displayed a prevalently apical signal increase. β1 integrin null acini, however, showed a sharper increase in fluorescence over time and it was localized indistinctly on all membrane surfaces (Figure 17 A, C). Most notably, in β1 integrin null acini there was a considerable discharge of membrane bodies (Figure 17 B, D; arrows) and loss of cell integrity, with consequent release of intracellular content (Figure 17 D, arrowhead)
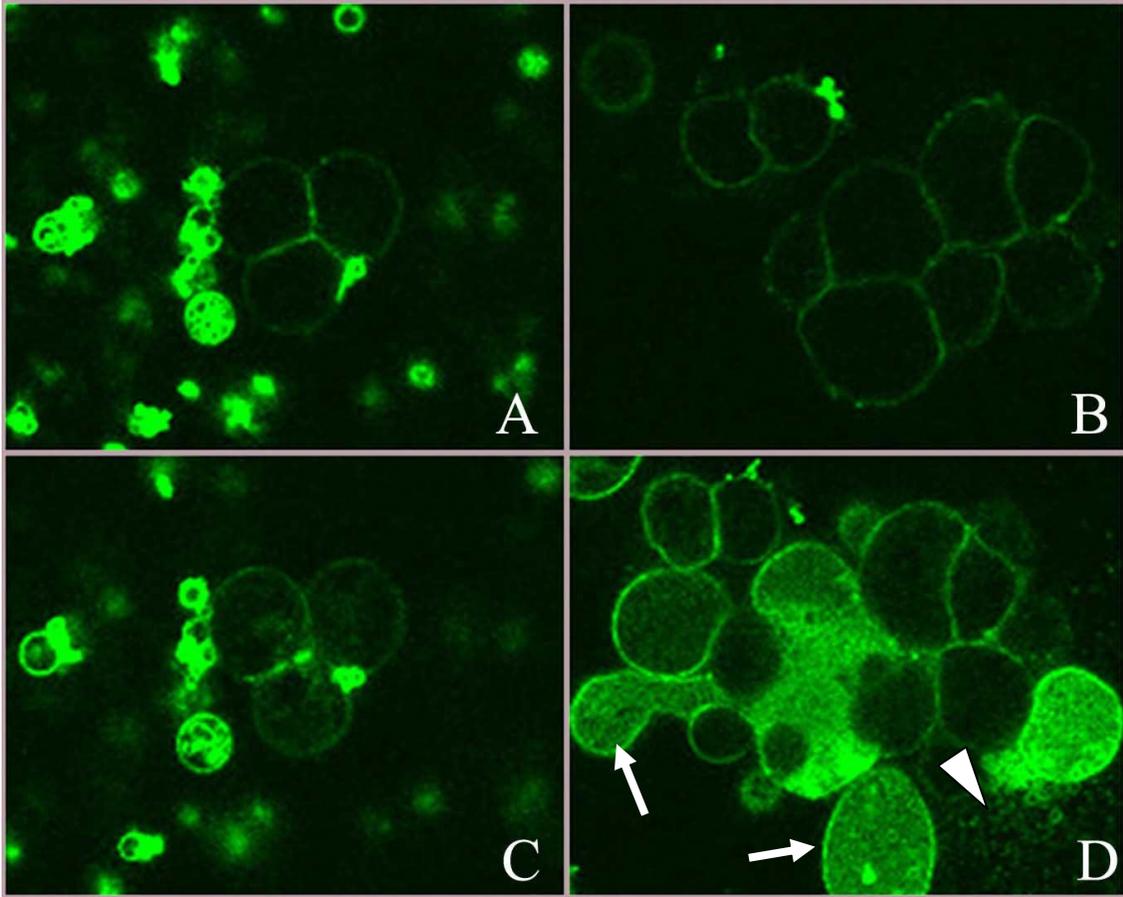
Figure 17. Live cell imaging of basolateral secretion in β1 integrin-null isolated acini Live cell imaging of *wild type* (**A, C**) and β1 integrin null acini (**B, D**) loaded with FM1-43 and stimulated with 1nM cerulein. Initially a comparable fluorescent signal was achieved (**A, B**), but after 45 min (**C, D**) only β1 integrin null acini displayed a considerable discharge of membrane bodies (**D**, arrows) and loss of cell integrity, with consequent release of intracellular content (**D**, arrowhead).

Chapter 4:

Discussion

Discussion.

The pancreatic exocrine tissue is mostly comprised of acini, structures made of a polarized layer of epithelial cells surrouded by a basement membrane (BM) and organized around an extracellular space, the lumen. Secreted digestive enzymes are directed from the lumen into the ductal network and finally into the duodenum. Like all glandular tissue, the exocrine pancreas requires appropriate epithelial cell polarity to carry out its function. Given the destructive capacity of the secreted digestive enzymes, a loss of polarity in acini has potentially dire consequences. Any event leading to inappropriate secretion or activity of digestive enzymes, or structural changes in the acinar cell cause a pancreatic injury that can lead to acute or chronic pancreatitis. For example, in humans, mutations in the cationic trypsinogen gene [54] perturb the stability and the activity of trypsinogen withing zymogen granules and cause hereditary chronic pancreatitis. Ductal obstruction by gallstones [55], can also cause pancreatitisvby blocking the pancretic juice flow and exposing acinar cell to active enzymes.

In general, the polarity of the glandular epithelial cells is a key element in the functionality of an exocrine gland with acinar structure. Several model systems have shown that establishment and maintenance of polarity are regulated mainly by integrins, the largest class of BM receptors expressed by epithelial cells [28].

To date, little is known about how the BM contact mediated by integrins affects pancreatic acinar cell polarity and function *in vivo*. To address this question, I chose to develop a "loss of function" model, where acinar cells were deprived of BM contact. Pancreatic acinar cells, unlike most glandular tissues, express the β1 but not the β4 integrin subunit, indicating that by knocking out the β1 integrin gene in acinar cells, I could also ablate their main source of contact with laminin and non-fibrillar collagen, the principal components of the pancreatic BM. I thus developed a pancreas-specific knockout of β1 integrin, which is characterized by a normal acinar development and function until 1 week of age and followed by a progressive degeneration of the parenchyma, due to the onset of acute pancreatitis.

β1 integrin ablation resulted in a normal development of the pancreas, characterized by correctly polarized, functional acini up to day P7. Starting at day P21, however, approximately 5 % of the acini had become enlarged and their normal architecture disorganized; many cells were detached from the BM and were found instead in the center of the acinus, a phenotype that essentially coincided with the misplacement of the acinar lumen. By one year of age this kind of acinar structures had become the predominant type. Interestingly, this pancreatic phenotype shared similarity with the β1integrin knockout in the luminal cells of the mammary gland [56], which is characterized by an initial normal polarization of the alveolar cells, but lack of full alveolar formation due to progressive architectural disorder and induces defective lactation *in vivo*.

I found that at day P7 both β1integrin$^{\text{flox/flox}}$;Ptf1a-cre and wild type acini were surrounded by a laminin-rich BM and expressed cell-cell adhesion molecules, such as E-cadherin, and the alternative laminin receptors α-dystroglycan [57] (Figure 8). These two

molecules, in particular E-cadherin, are well known to have an important role in initiation of epithelial polarity [58-62] suggesting that they could be part of the initial cohesion forces that establish the acinar structure and that β1 integrin function is not needed at this stage.

The normal phenotype of β1 integrin-null acini up to P7 also raised the question whether the combination of a laminin-rich BM and expression of E-cadherin and α-dystroglycan were compensating for the lack of β1 integrin and thus making epithelial polarization possible. In this regard, studies on embryonic bodies (EB), a model of a polarized structure assembling on a BM, show that an obligate step in establishment of epithelial polarity is the contact with laminin (laminin-1 in EB), whose deposition in turn requires β1integrin [62, 63]. β1integrin-null EB phenocopy the ablation of laminin γ1 and die by day E5.5, but this can be partially rescued by treatment with exogenous laminin-1, suggesting that in this system, β1 integrin is indeed necessary for laminin expression, but not for the initial cell anchorage to the BM.

I propose a similar mechanism applies to our system, the initial assembly of pancreatic acini up to day P7 was sustained by the laminin-rich BM secreted most likely by β1integrin-proficient interstitial cells, like stellate cells and fibroblast, rather than β1integrin-null acinar cells. This could also provide an explanation for the large, collapsed β1integrin-null acini. It is possible that because of the lack of β1integrin, acinar cells that cannot synthesize or secrete laminin also do not "sense" the surrounding laminin either, consequently remaining "trapped" inside the acinus and with no reference for polarity establishment.

An alternative hypothesis is that β1integrin-null acinar cells cannot utilize laminin for orientation, because they are not capable of properly binding it, regardless of its source. In fact, studies on cell lines, derived myotubes and ES [64] showed that even in the absence of β1 integrin partial expression of laminin-1 is possible, but β1integrin is necessary for the correct BM assembly and localization on the epithelial cell surface.

My *in vitro* experiments on isolated acini suggest in fact that β1integrin-null acini have an impaired laminin binding. Immunofluorescent staining for laminin α2 on w*ild type* acini (freshly isolated by collagenase digestion, see materials and methods) are surrounded by a layer of BM positive for immunostaining (Figure 18 A), while β1integrin-null acini seemed to retain only fragments of α2 laminin, if any. (Figure 18 B)

According to these results, it is possible that up to day P7, β1 integrin-null acinar cell polarity and acinar structure were not dependent on the contact with laminin in the BM, but on other cell-cell adhesion molecules.
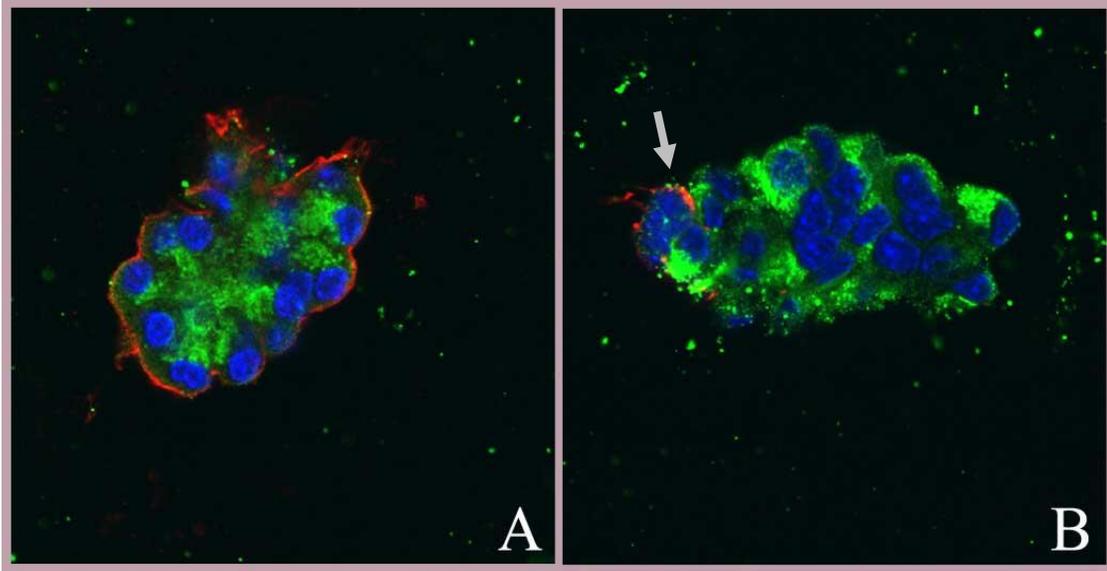
Figure 18. $\alpha 2$ laminin surrounds *wild type* isolated acini, but not $\beta 1$ integrin[flox/flox];Ptf1a-cre acini. Acini were isolated from wild type and $\beta 1$ integrin[flox/flox];Ptf1a-cre animals, placed in a collagen matrix and immediately fixed and stained for $\alpha 2$ laminin (in red) and amylase (in green). $\alpha 2$ laminin surrounds completely *wild type* acini (**A**) but only marginally (arrow) $\beta 1$ integrin [flox/flox];Ptf1a-cre (**B**) acini (100x magnification; Nuclei (blue) were stained with DAPI)

Deletion of laminin $\alpha 5$ chain [65] in the submandibulary salivary gland (SMG), an exocrine gland structurally analogous to the pancreas, provides further evidence for the requirement for laminin binding. This knockout model resulted in delayed SMG development at day E13 and disrupted epithelial organization and lumen formation at day E17, suggesting clearly an essential role for laminin in the early polarization of acinar cells.

Taken together, these experiments suggest that although other adhesion molecules can mintain the pancreatic acinar structure together, laminin and the BM supplied by interstitial cells likely "rescue" the $\beta 1$ integrin-null phenotype and allow acinar cell to establish polarity and form normal acini up to day P7.

I hypothesized that this partial rescue was not sufficient for the long-term maintenance of acinar structure and function and as a consequence, $\beta 1$ integrin-null acini undergo a gradual loss of architecture, lumen mislocalization, misdirected enzyme secretion and ultimately an acute pancreatitis-like phenotype.

In fact, the most dramatic phenotype in the β1integrin [Flox/Flox];p48-Cre mice was the progressive degeneration of the pancreatic tissue to approximately 25% the size of control by 1 year of age. In one sense, this phenotype was not surprising since cell/BM contact has long been associated with cell viability in a number of studies, and it was shown to induce anoikis [30, 31], a type of apoptosis induced by loss of ECM contact. However, given the clear loss of BM contact in the cells filling the acinar structures, it was surprising to find no signs of apoptosis, although a similar finding was also reported in the characterization of the β1integrin knockout in the mammary gland [56]. Instead, what I could detect in older β1 integrin[flox/flox];Ptf1a-cre mice was induction of necrosis, a form of cell death associated with injury and, in the pancreas, a hallmark of acute pancreatitis.

I hypothesized that focal necrosis in the β1integrin [flox/flox];Ptf1a-cre mice was not due to the loss of an intrinsic function of β1integrin, but was instead initiated in the same way AP is initiated : by the uncontrolled exposure of the parenchyma to digestive enzymes. Both the dysfunctional architecture and the basolateral secretion of β1 integrin-null acini were compatible with a diverted secretion, causing damage and inducing a chronic condition.

Furthermore, the loss of acinar architecture in the β1integrin [flox/flox];Ptf1a-cre acini could have progressively worsened this stress condition and ultimately caused a type of parenchymal damage that could not be compensated by the normal tissue regeneration. This would explain how the reduction of the pancreatic weight, the necrotic foci and the inflammatory response were all exacerbated aspects in older β1integrin [flox/flox];Ptf1a-cre mice. In addition, although it is difficult to estimate the extent of damage caused by basolateral secretion, cerulein experiments strongly suggest that β1integrin [flox/flox];Ptf1a-cre have an impaired healing capability.

Basolateral secretion of digestive enzymes may have however the most important role in the extreme phenotype of older β1 integrin [flox/flox];Ptf1a-cre mice. According to my *in vitro* experiments, after secretagogue stimulation I was able to visualize in living β1 integrin-null cells the loss of cellular integrity and consequent leak of intracellular content. While these experiments clearly linked basolateral secretion to loss of cell integrity, I cannot rule out that the protease or the mechanical force of the isolation procedure rendered acini too sensitive to cerulein or to the effects of their own secreted enzymes.

In vivo, however, I observed a phenotype entirely compatible with the basolateral secretion seen *in vitro*. When I exacerbated secretion by cerulein injections, β1 integrin-null acinar cells displayed massive cytoplasm vacuolization and discharge of membrane-contained bodies (a typical effect of cerulein-induced acute damage) and widespread necrosis compared to wild type.

I believe the main cause of this damage were the additive effects basolateral redirection of secretion and the poor acinar architecture, rather than the amount of accumulated or misregulated release of enzymes triggered by cerulein injections. In fact, tissue lysates and *in vitro* secretion assays indicated that β1integrin-null acini, not only

contain 3-fold less amylase than wild type acini, but secrete a disproportionately low amount of their enzyme content and require a higher concentration of cerulein to yield the maximum secretory response.

There are a number of explanations for the lower amylase output displayed by β1 integrin-null acini *in vitro* and they may give interesting insights about the role of β1 integrin in the pancreas. First, a structural change of the cortical actin cytoskeleton, which is physically connected to β1integrin through talin [66] and critical for exocytosis [67], could account for the reduced amylase secretion of β1integrin-null acinar cells. Alternatively, it could be the shutdown of the pathway downstream of protein kinase C (PKC) isoforms, whose signaling is known to depend on β1integrin and to control exocrine pancreatic secretion by calcium mobilization [68-70].

Other molecules involved in a secretory pathway could be regulated by β1integrin. For example, β1 integrin ablation in *ex vivo* cultured mammary gland acini caused a significant reduction in the phosphorylation levels of both p125-focal adhesion kinase (FAK) and paxillin, two β1 integrin-binding proteins, and impaired casein secretion in response to the hormone prolactin [56]. In the pancreas, FAK and paxillin mediate the CCK-induced signal transduction [71-73] and depending on the concentration of CCK, they can induce either secretion or provoke acute damage. So, in a similar way, the reduction of phosphorylated FAK and paxillin could be responsible for the higher concentration of cerulein (a CCK analog) reuqired to yoield maximal amylase secretion.

FAK is a multifunctional tyrosine kinase that binds a number of different adhesion and signaling molecules [74, 75]; several signaling pathways trigger phosphorylation of FAK and paxillin and can have very different outcomes. Most notably, transient activation of the protein kinase Src can sequentially induce FAK phosphorylation, rupture of focal adhesion, cell detachment from substratum and destruction of the actin cytoskeleton, degradation of FAK and paxillin. A strikingly similar sequence of events was described in supramaximal cerulein stimulation of isolated acini [71].

In this regard, although supramaximal and physiological levels of secretagogue may be activating different signaling pathways, β1 integrin could be critical in preventing this deleterious cascade of events, by providing both a scaffold to maintain FAK localized at the cell membrane and by regulating v-Src activity [76]. Consequently, failure to maintain control over FAK and Src signaling could provide an explanation for the extreme acute phenotype seen in cerulein-injected β1 integrin [flox/flox];Ptf1a-cre mice.

A formal possibility was that the reduced secretion of β1 integrin-null acini could be due to the indirect effect of reduced insulin production, which normally has a stimulatory effect on exocrine secretion of acinar cells [77]. In our model, Ptf1a-cre expression eliminates β1 integrin floxed alleles in the exocrine and in the endocrine compartment. Blood glucose levels of β1integrin[flox/flox];Ptf1a-cre mice however, were not significantly different than *wild type* age-matched controls, suggesting that insulin levels

may be, if at all, only moderately reduced and thus minimally affecting acinar cells secretion.

Finally, an important aspect of β1 integrin ablation in the pancreas was the delayed recover from cerulein-induced AP. My data showed that β1 integrin-null acinar cells failed to initiate a proliferative response shortly (24 hours) after induction of AP, but in the course of 7 days the overall tissue architecture could recover in a way similar to *wild type* controls.

On one hand, this might simply be a consequence of the greater extent of cell loss caused by cerulein in β1integrin[flox/flox];Ptf1a-cre pancreata: a small number of surviving acinar cells need probably a longer time to regenerate the whole tissue. On the other hand, it is possible that the lack of β1 integrin, rather than impairing the proliferation of acinar cells *per se*, was instead limiting the propagation of necessary growth factor signals mediated by factors such as EGF, VEGF and PDGF. In fact, a similar mechanism links the lack of β1 integrin and defective acinar proliferation in the mammary gland [78, 79].

Depletion of the stem cells compartment is also a possible explanation for the longer recovery of β1integrin[flox/flox];Ptf1a-cre pancreata from cerulein-induced pancreatitis. If progenitors cells are reduced in number, it would take longer for them to re-differentiate and proliferate to heal the tissue. The role and the identity of progenitor cells however, is not unequivocal and almost every pancreatic cell type has been proposed as the origin of the pancreatic stem cell. Furthermore, recently published work [80] showed that in the recovery from of AP new acinar cells are generated from preexisting acinar cells rather than other lineages, making the hypothesis of a selective depletion of progenitor cells by β1 integrin less important in this setting.

All these alternative explanations for the slower recovery of β1integrin[flox/flox];Ptf1a-cre pancreata after cerulein-induced AP are of course not mutually exclusive and a more detailed analysis of acinar cell proliferation during the entire recovery phase will clarify the contribution of β1integrin to tissue regeneration.

In summary, my study provides insight into the function of β1 integrin in the establishment and the maintenance of pancreatic acinar cell function and the importance of ECM components. I suggest that a laminin-rich BM and adhesion through E-cadherin and α-dystroglycan in the developing pancreas are part of a sufficient environment to support the initial assembly of β1 null acini into polarized and functional structures, but not their long term maintenance. I showed that β1 integrin is involved in directional secretion, and this is a critical element for the maintenance of acinar cell integrity. Finally, I suggest the intriguing possibility that the contribution of β1 integrin might be related to its signaling function, rather than to the role of physical cell-cell and cell-BM link. Accordingly, identifying the signaling defect that lead β1 null mice to irreversible degeneration, could lead the way for the development of therapy of acute and chronic pancreatitis.

Chapter 5:

Matrix Metalloproteinase-7 in pancreatic cancer

Section 1.

Project description and rationale

This project is focused on the gap in the current knowledge of matrix metalloproteinase-7 (MMP-7) function in the pancreas, particularly the role of MMP-7 in the formation and progression of invasive neoplastic lesions.

Rationale.

Matrix metalloproteinases (MMPs) are a family of extracellular, zinc-dependent proteinases frequently expressed in cancer [81]. The capability of MMPs to degrade all components of the extracellular matrix suggested initially a role in tumor invasion. However, evidence derived from mouse genetics has shown that MMPs contribute to tumorigenesis and many aspects of tumor growth, often by cleaving non-ECM substrates [82]. The MMP family member MMP-7 is expressed by the tumor cells of many adenomas, adenocarcinomas, and, by associated metaplasia in the colon [83], stomach [83] and the majority of PDACs, at all PanIN stages and in 100% of tumor-associated metaplastic ducts lesions MDL [84]. Animal models have supported a role for MMP-7 in tumorigenesis and early tumor growth. For example, in Apc^{Min} mice, MMP-7 deficiency inhibits intestinal tumor formation [85]. Conversely, overexpression of MMP-7 in the mammary gland with an MMTV-Neu transgenic background accelerates tumor formation [86]. Together, these data suggest that MMP-7 acts early in adenoma progression, and perhaps in tumorigenesis itself. Though its role in PDAC has not been directly addressed, in a mouse model of CP, it was found that all aspects of disease progression are inhibited in MMP-7 deficient (MMP-7$^{-/-}$) mice. [84]

Experimental design.

RNAi was used to generate stable MMP-7 knockdown pools in 3 different MMP-7 expressing pancreatic cancer cell lines. Their biology was studied extensively in vitro and after injection into nude mice.

The LSL-K-Ras^{G12D} mouse model of pancreatic cancer was used to study the effect of the MMP-7 null background in PDAC formation. I tested how the MMP-7 null background affects tumor size, tumor number and metastatic growth in these mice and determined the basic neoplastic properties of these tumors, such as their proliferative and apoptotic index and immune reactivity.

Section 2:

Introduction to pancreatitis and pancreatic cancer

The presence of an initiating occurrence, of either a toxic or genetic nature, is clearly not sufficient per se to drive the full development of pancreatitis. This is why, despite 85% of CP patients being alcohol abusers, overall only 10% of heavy drinkers will actually develop CP. Similarly, the penetrance of hereditary pancreatitis in PRSS1 mutation carriers (in monozygotic twins) is ~80%. There are clearly unknown environmental factors, gene-environment interactions or epigenetic changes that ultimately protect (but can also accelerate) the progression of the disease. Consequently, the knowledge of how pancreatitis develops beyond its etiology is extremely relevant to another almost incurable pancreatic pathology: pancreatic cancer.

The importance of pancreatitis as a precursor of pancreatic cancer is supported by several lines of research. [87, 88] Individuals with hereditary pancreatitis have a 50 fold increased risk of developing pancreatic cancer , and the duration of repeated episodes of acute pancreatitis also seems to correlate with an increased risk of pancreatic cancer. Recently, in a promising mouse model of pancreatic cancer, it was shown that CP is essential for the induction of pancreatic ductal adenocarcinoma by oncogenic K-Ras in adult mice. [89]

Pancreatic ductal adenocarcinoma.

Pancreatic ductal adenocarcinoma (PDAC) is the most common form of pancreatic cancer and one of the most devastating cancer diseases. Although the disease accounts for only about 2% of all cancers, it is the 4th leading cause of cancer related deaths in the US. The overall 5-year survival rate is less than 5%, with most of the patients dying within 3 to 8 months after diagnosis. These numbers have improved minimally over the last decade. (NCI, 2007) PDAC, given the location of the pancreas, is a rapid, asymptomatic disease that is usually diagnosed at the most advanced stages when the tumor mass has already metastasized and invaded most of the organ.

PDAC is a complex disease ultimately caused by defined genetic mutations and environmental risk factors. Recent studies [87, 90] based on large demographic samples confirmed that the main independent risk factors for pancreatic cancer were cigarette smoking, family history of pancreatic cancer, heavy alcohol consumption (>60 mL ethanol/day), diabetes mellitus, and history of pancreatitis. 90% of all human pancreatic cancers are ductal adenocarcinomas which are believed to stem from intraductal precursors: intraductal papillary mucinous neoplasms in the main pancreatic duct, intraepithelial neoplasias (PanINs) within intralobular ducts, and mucinous cystic neoplasms (MCN). [91] PanINs are the best characterized lesions thought to be PDAC precursors. These intraepithelial formations proceed through 3 progressive stages with increasing nuclear atypia and ultimately become invasive. They are associated with key genetic mutations, which have been identified in humans. This led to the definition of the genetics of PDAC progression, summarized in Figure 19.

Animal models of pancreatic cancer.

Preclinical models based upon the human disease have led to transgenic models. In the last few years, a number of transgenic mice have been developed to elucidate two critical points: 1) the cellular compartment of origin (acinar, centroacinar, ductal or islet) and 2) the identity of the oncogenes leading and sustaining a malignant transformation in a mouse that recapitulates the human disease. The development of a transgenic model started with combinations of constitutive overexpression of oncogenes or/and homozygous ablation of tumor suppressors genes. This led to fast spreading, often lethal tumors, but the design of transgenic animals later evolved toward better models, involving conditional alleles (of oncogenes or tumor suppressors) and cell-type specific, or inducible, cre recombinase systems. Table 2 shows a list of the currently available mouse models of PDAC; each combination of oncogenes and/or tumor suppressors yields a spectrum of histological features. There are expected limits in every model imposed by the restricted choice of transgenes, promoters, and the modality of induction. [1]

The most important finding confirmed by several models, however, is the central importance of oncogenic K-Ras (carrying a G12D mutation at codon 12 that changes the encoded amino acid from glycine to aspartic acid, leading to a constitutively active product. G12V is a similar mutation) in driving and sustaining the tumor growth in murine models of PDAC.

Today, the best model of PDAC in mouse that accurately mimics the human cancer progression is represented by a LSL-K-Ras^{G12D} conditional allele activated in the entire pancreatic lineage during the first days of embryonic development by a ptf-1a (p48) or pdx-1 promoter driven cre recombinase. [92]

The exact cell compartment of origin is not yet clear, and specific models will have to be developed to address this question. A recent model of KRas^{G12V} expression restricted to adult ductal cells failed to develop PanINs or invasive tumors, and a similar result was observed when oncogenic K-Ras was directed to mature acinar cells only. [89, 93] These results suggest that the origin of PDAC might be related to oncogenes activation in stem cells, either during development or in transdifferentiated mature adult cells. This view was reinforced by the work of Korc et al., [94] which showed that K-Ras^{G12D} targeting to the nestin-positive progenitor lineage will result in formation of tumors in a comparable way to the LSL-K-Ras$^{G12D;}$ pdx-1cre where it is active in all lineages.
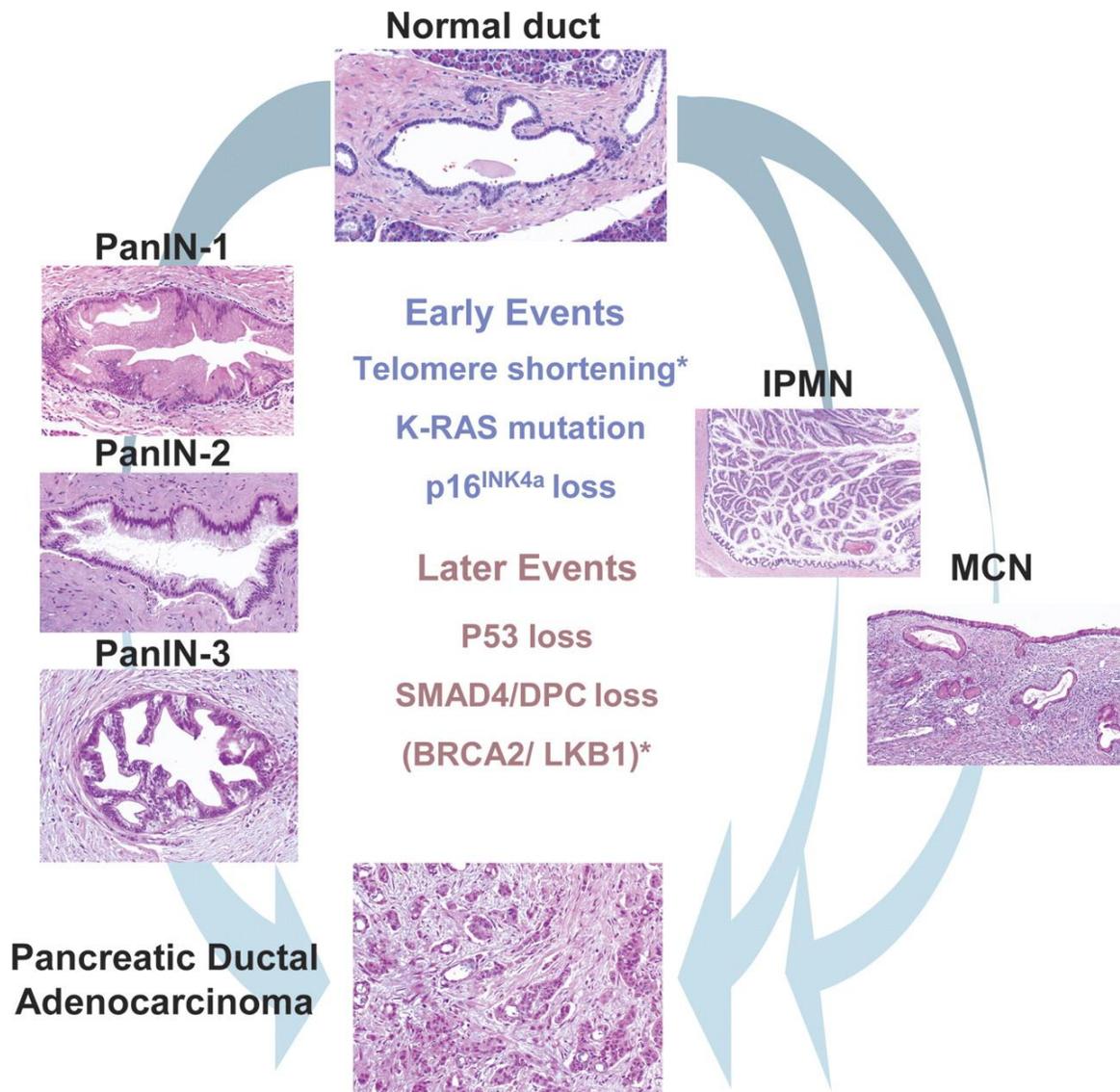
Figure 19. Pancreatic precursor lesions and genetic events involved in pancreatic adenocarcinoma progression. Pictured are three known human PDAC precursor lesions: PanIN, MCN, and IPMN. The PanIN grading scheme is shown on the *left*; increasing grade (1–3) reflects increasing atypia, eventually leading to frank adenocarcinoma. The *right* side illustrates the potential progression of MCNs and IPMNs to PDAC. The genetic alterations documented in adenocarcinomas also occur in PanIN, and to a lesser extent MCNs and IPMNs, in an apparent temporal sequence, although these alterations have not been correlated with the acquisition of specific histopathologic features. The various genetic events are listed and divided into those that predominantly occur early or late in PDAC progression. Asterisks indicate events that are not known to be common to all precursors (telomere shortening and BRCA2 loss are documented in PanIN and LKB1 loss is documented in a subset of PDACs and IPMNs). From: Genetics and biology of pancreatic ductal adenocarcinoma. Genes Dev. 2006 May 15;20(10):1218-49.

Transgene	Tumor phenotype
T-Ag/elastase	Acinar cell carcinoma
Hras/elastase	Acinar cell carcinoma
TGF-_/elastase	Acinar cell carcinoma. Develops mixed acinar-ductal tumors on a p53+/− background
metallothionein (MT)-TGF-α	Tubular metaplasia. Develops lesions resembling serous cystadenomas on Ink4a/Arf- or p53-null background.
c-myc/elastase	Mixed acinar-ductal tumors
KrasG12D/Mist1	Acinar cell carcinoma
c-myc/elastase	Islet cell tumors in Ink4a/Arf-null mice
PyMT/elastase	Mixed acinar-ductal tumors in Ink4a/Arf-null mice.
KrasG12D Pdx1-Cre	Spectrum of PanINs and some mice develop PDAC with long latency
KrasG12D Pdx1-Cre Ink4a−/−	Develop PDAC with shorter latency than KrasG12D alone.
KrasG12D Pdx1-Cre Ink4a/Arf−/−	Develop PDAC with high penetrance and short latency. Micrometastatic disease.
KrasG12D Pdx1-Cre p53 R273H or p53+/−	Develop PDAC with high penetrance. Gross metastatic disease. LOH of wild-type p53 allele.
KrasG12D Pdx1-Cre Ink4a/Arf +/−	Develop PDAC with longer latency than Ink/Arf-null mice. Gross metastatic disease. LOH of wild-type Ink4a/Arf allele.
KrasG12D Pdx1-Cre p53+/− Ink4a +/−	Develop PDAC with high penetrance and shorter latency than p53+/−. LOH of wild-type p53 allele and loss of Ink4a expression.
Pten−/− Pdx1-Cre	Ductal metaplasia with a fraction of the mice developing PDAC.
Pdx-1-Shh	Ductal-intestinal metaplasia.

Table 2. Mouse models of pancreatic cancer and their phenotypes. From: Genetics and biology of pancreatic ductal adenocarcinoma. Genes Dev. 2006 May 15;20(10):1218-49.

Role of acinar to ductal metaplasia.

The possible transdifferentiation of adult, terminally differentiated cells is also an important aspect of the PDAC biology. Pancreatic acinar cells, in particular, can exhibit a remarkable plasticity during tissue regeneration and can undergo a process called acinar to ductal metaplasia. [92, 93] (Metaplasia is the replacement of one adult cell type with another and is often associated with tumorigenesis)

In the pancreas, when this process occurs in response to an injury, it involves acinar cells transiently switching to a ductal, proliferative intermediate and then re-differentiating into an acinar type. Metaplastic ducts, however, are also a hallmark of CP and human PDAC and they been shown to develop in several mouse models of PDAC. The role of these ductal structures is not yet completely clear, but given their proliferative potential and their responsiveness to growth factors, like TGF-α and EGF, the most likely hypothesis is that they can turn into PanINs and eventually develop into invasive cancer. [84, 94]

Section 3:

Matrix metalloproteinases and MMP-7.

Matrix metalloproteinases (MMPs) are a family of 26 enzymes, characterized by their collective ability to degrade all components of the ECM and their dependence on zinc and calcium for proteolytic activity (Figure 20). MMPs were initially thought to facilitate tumor cell invasion and metastasis by proteolytic digestion of the surrounding ECM. More recent work has shown that MMPs actually have a much wider spectrum of action, and their interaction with specific substrates can contribute to cell proliferation, survival, and angiogenesis in normal and neoplastic tissue.

For example, the angiogenesis blocker endostatin is generated from type XVIII collagen by MMP3, MMP9, MMP12, MMP13 and MMP20 processing in vitro [95, 96] . Through disruption of cell–cell contacts, MMPs also initiate epithelial–mesenchymal transition and genomic instability. [97] In addition, MMPs mediate chemokine and Fas-ligand shedding. [98] Generally, MMP-mediated proteolysis regulates cell signaling that controls homeostasis of the extracellular environment, including mechanisms of host-resistance to tumors [99] and should be considered signaling molecules themselves.

MMP-7 and its application in pancreatic cancer is the focus of my research. MMP-7 is a secreted MMP detectable in abnormal epithelia and is highly restricted in normal tissues. One particular interest in our research is MMP-7's role in cancer, given its high level and frequent expression in adenocarcinomas of breast, stomach, colon, prostate, upper aerodigestive tract, lung, and pancreas. Based mainly on evidence from models of colon and breast cancers [85, 86] we know that MMP-7 can play a pivotal role in several aspects of carcinogenesis, especially in the early neoplastic events. MMP-7 is expressed in 99% of PDAC patient samples, significantly exceeding the frequency of

expression in tumors of other tissues, which can be up to ~80%. Expression ranges from the earliest stages of tumor formation through to invasive carcinoma, as well as metaplastic duct epithelium in 100% of PDAC and 93% of CP samples examined. Inducing chronic pancreatitis in mice that have had the MMP-7 locus inactivated by homologous recombination (MMP-7$^{-/-}$) shows that all aspects of CP are severely inhibited, including the formation of metaplastic duct epithelium and the desmoplastic response. Thus, we surmise that MMP-7 is involved in pancreatic tumor formation at least in part through its ability to promote the formation of metaplastic duct epithelium. [84]

MMP-7 Substrates.

MMP-7's ability to release the proapoptotic molecule Fas ligand (FasL) from the cell surface has been shown to enhance apoptosis in susceptible cells. Chronic exposure of FasL expressing cells to MMP-7 selects for cell populations that are resistant to apoptotic stimuli. [84, 98, 100] In a model of herniated disc resorption, MMP-7 cleavage can release soluble TNF–α and indirectly promote macrophage infiltration, a relevant process in cancer as well [101]. MMP-7 cleaved TNF–α induces MMP-3, which in turn is required for the generation of a macrophage chemoattractant. MMP-7 has also been shown to activate cellular proliferation and invasion by releasing cell surface molecules. For instance, MMP-7 releases heparin-binding epidermal growth factor (HB-EGF), enhancing tyrosine phosphorylation of the EGF receptor family member ErbB4. [102] This has been shown to enhance cellular proliferation and to contribute to apoptotic resistance.

MMP-7 also can degrade all insulin-like growth factor binding proteins (IGFBPs) and facilitates insulin-like growth factor (IGF) bioavailability, causative of fibrosis and possibly favoring cancer cell growth and survival during the processes of invasion and metastasis [103]. MMP-7 has been shown to cleave the cell-cell adhesion molecule E-cadherin from the cell surface, releasing a soluble fragment capable of interacting with intact E-cadherin molecules and thus breaking apart cell-cell junctions to induce invasion [104-106]. Similarly, β4 integrin, which promotes interaction with laminin-containing ECM, is a substrate for MMP-7 ; [107] its disruption promotes migration and invasion. MMP-7 can also cleave the serum/ECM molecule osteopontin, [108] creating a bioactive epitope that can disrupt cellular interactions with fibronectin, thus enhancing invasion. RANKL (receptor activator of NF-κB ligand), is released as a soluble molecule by MMP-7 [109] and regulates osteolysis in prostate cancer bone metastases. In lung injury, neutrophil migration is regulated by MMP-7 shedding of Syndecan-1 which results in cytokine mobilization. [110, 111]
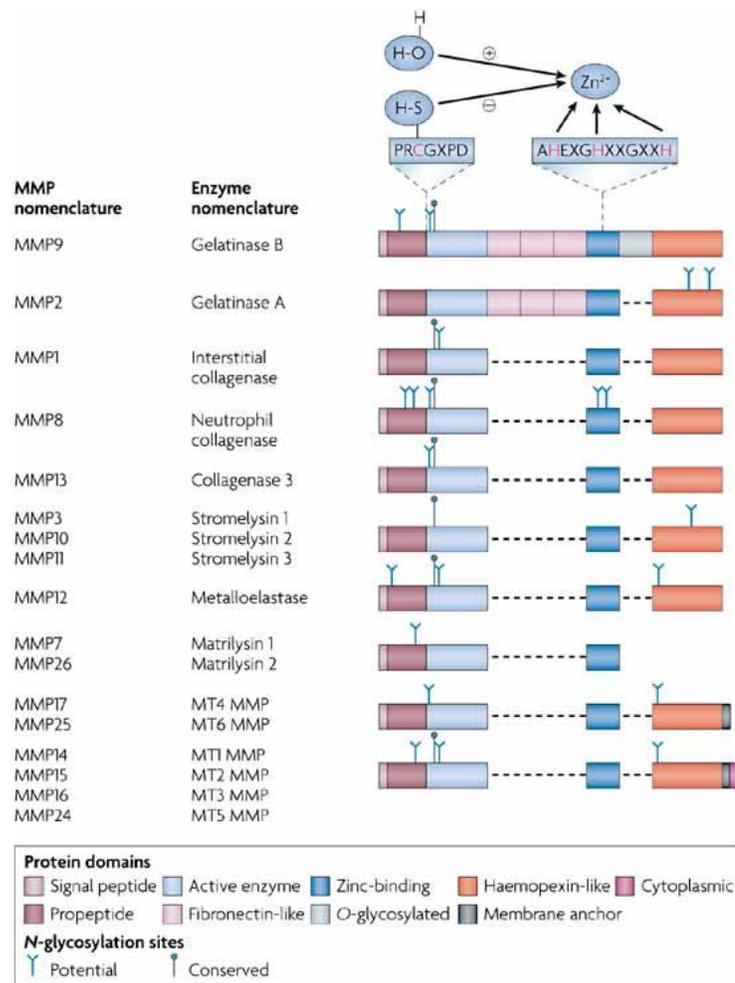
Figure 20: Matrix metalloproteinases (MMPs) are multidomain enzymes that have a pro-domain, an active domain, a zinc-binding domain and a haemopexin domain (except MMP7 and MMP26). Additionally, membrane-type MMPs (MT-MMPs) contain a membrane anchor with certain MT-MMPs also possessing a cytoplasmic domain at the carboxyl terminus. Gelatinases contain a gelatin-binding domain with three fibronectin-like repeats. In particular, MMP9 also contains a serine-, threonine- and proline-rich O-glycosylated domain. N-glycosylation sites, one of which is conserved among most MMPs, are indicated with a Y symbol. Part of the pro-peptide, which contains the chelating cysteine, and part of the zinc-binding domain with three histidines are indicated in one-letter code for the amino acids at the top of the figure. From: Matrix metalloproteinase inhibitors as therapy for inflammatory and vascular diseases. Nature Reviews Drug Discovery 6, 480-498 (June 2007)

61

In vitro studies.

MMP-7 has been shown to have many biological activities potentially relevant to tumor progression: in cell lines, MMP-7 selects for apoptotic resistant cells [84, 98, 100, 112] and confers cancer-specific features in cell lines derived from various tissues. These involve growth advantage, [100, 113] increased tumorigenicity in nude mice, [114] and invasion in vitro. [103, 115-117]

In vivo studies.

Recently it has been shown that MMP-7 can significantly increase tumor formation in a mouse model of breast cancer. [86] The presence of pre-malignant nodules and the accelerated development of oncogene-induced mammary tumors are enhanced in transgenic animals overexpressing MMP-7. [118] In athymic mice, injection of MDA-MB-231 cells where MMP-7 expression has been suppressed by RNai, results ins maller tumors and displayed less invasive potential in vitro compared to the MMP-7 expressing control line [117]. Wilson et al. [85] showed that MMP-7 contributes to the reduction of tumor size and number (60% less) in Min mice (a model for familial adenomatous polyposis) when in the MMP-7 null background.

Clinical studies.

Perhaps the most relevant support for the relevance of MMP-7 in cancer biology comes from a large number of clinical studies [119-123] which in general point out a strong correlation between MMP-7 expression and poor prognosis in several types of cancer, particularly endometrial [124], lung [125], colon and pancreatic cancer. Of particular interest is MMP-7 expression in PDAC; recent studies [126, 127] suggest that MMP-7 is an independent prognostic indicator and potentially of considerable clinical value in the pancreas. MMP-7 expression often seems to be localized at the invasive front of tumors [119, 121, 122] supporting the idea that MMP-7 could confer an enhanced invasive potential to a subpopulation of cancer cells ultimately resulting in an overall poor prognosis.

Chapter 6

Matrix metalloproteinase-7 in pancreatic cancer: Results

Results.

Phenotype of MMP-7 RNAi knockdown in pancreatic cancer cell lines

I chose to investigate MMP-7 contribution to pancreatic cancer using *in vitro* and *in vivo* experimentation. My goal was to establish an appropriate cell culture system to study MMP-7 contribution to the biology of PDAC and PDAC precursors, such as or PanINs. I first considered both MMP-7 overexpression and a loss of function approach in pancreatic cell lines and primary cultures. Overexpression-based experimental approaches of MMP-7 function are well-reported in other cell types, and would have been suitable to determine what MMP-7 *can* do.

The available pancreatic cell lines that do not express MMP-7 however, have in general poor epithelial differentiation, suggesting that they may rather represent advanced tumors and are not suitable as a model of pre-cancerous formations or PanINs. In addition, primary acinar or ductal cultures, although appropriate for MMP-7 overexpression, last only a few days in culture and the only effective transgene delivery requires adenoviral infection, which precludes the study of long term-effects.

In addition, since MMP-7 is highly expressed in pancreatic tumors, it was important to look at the effects of its depletion. RNAi was used to knock down MMP-7 expression in pancreatic cancer cell lines to generate a loss of function model system; I chose cell lines displaying high MMP-7 expression and epithelial differentiation.(defined by their E-cadherin expression and membrane localization).

I generated two stable MMP-7 RNAi pools and one scrambled, non-silencing control RNAi in three cell lines, CFPAC-1, S2-013 and HPAF-II by retroviral gene delivery.

Figure 21 shows MMP-7 expression of puromycin-selected pools; based only on MMP-7 protein levels RNAi silencing construct n.2 was discarded because it was not efficient.
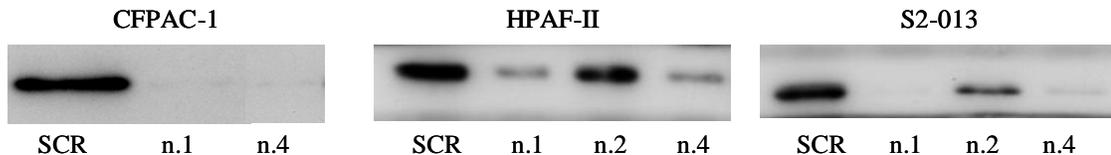

Figure 21: MMP-7 Western Blot of conditioned media of cell pools infected with RNAi constructs in three different cell lines: CFPAC-1, HPAF-II and S2-013. SCR, non silencing RNAi; n.1 to n.4, silencing vectors targeting different sequences in the mRNA.

In order to determine the basic properties of S2-013 and CFPAC-1 RNAi and control pools I first evaluated the proliferative potential in confluent or semi-confluent monolayer, in the presence and absence of FBS. No proliferation effect was found.

I hypothesized that in a confluent or semi-confluent monolayer, a network of cell-cell contacts mediated by E-cadherin may be already established and the effects of further E-cadherin ectodomain shedding by MMP-7 might be minimal or harder to detect. Alternatively, a confluent or semi-confluent monolayer may not respond as dispersed cells do to known soluble ligands released by MMP-7, like FasL and HB-EGF. To test the possible effects of soluble ligands generated by MMP-7 in coltured cells, I consequently devised the following condition: (Figure 22-25)

1) Cells at both high and low density, to maximize the possible effects of soluble factors or shedding of adhesion molecules like E-cadherin, a known substrate for MMP-7.

2) Cells in a small amount of media that was never replaced versus a larger, frequently replaced amount of media to allow accumulation of soluble factors. The reason is that the more concentrated conditioned media could provide the effective concentration of soluble molecules like cytokines, growth or death factors released by MMP-7 activity

3) Serum free and serum rich cultures. Knowing that serum contains inhibitors of MMPs (for example $\alpha 2$ macroglobulin), I cultured cells in both serum rich (10%FBS) and serum free media.

On the other hand, it is also possible that in a context of poor contact inhibition, typical of CFPAC-1 and S2-013, extensive cell-cell contact may be regulating the availability MMP-7 substrates and consequently cell growth. I thus analyzed the "overgrowth" curve of already confluent RNAi and control pools.

Cells cultured at sub-confluent or at confluent densities did not highlight any difference between RNAi and controls, in either cell line. (Figure 22-25) This might be due the limitations of the cell lines used and of the 2D cultures system. It also emphasizes the necessity of mouse models. Other reasons are discussed in the concluding remarks chapter.
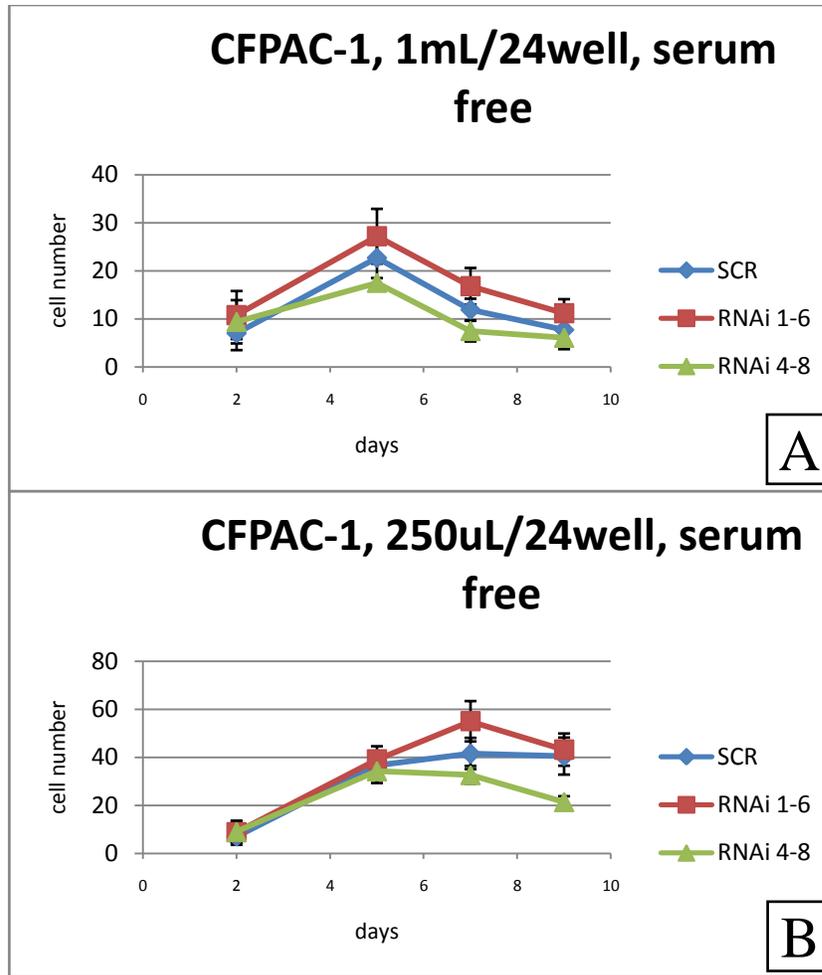
Figure 22: Growth curves of CFPAC-1 cells in serum-free media. (**A**) 40,000 CFPAC-1 cells were plated (24wells-plate; sub-confluent density) at day 0 and cultured in 1 ml serum free DMEM, replaced every day or (**B**) plated 250 μL serum free DMEM (not replaced, but supplemented with an additional 50μL serum free DMEM every 2 days). Cells were counted by Trypan Blue exclusion and the normalized number of cells/well was computed and plotted as average of 3 counts**. "RNAi 1-6"** and "**RNAi 4-8**" are MMP-7 silencing constructs; "**scr**" non silencing, scrambled sequence RNAi. Error bar: +/- SEM.
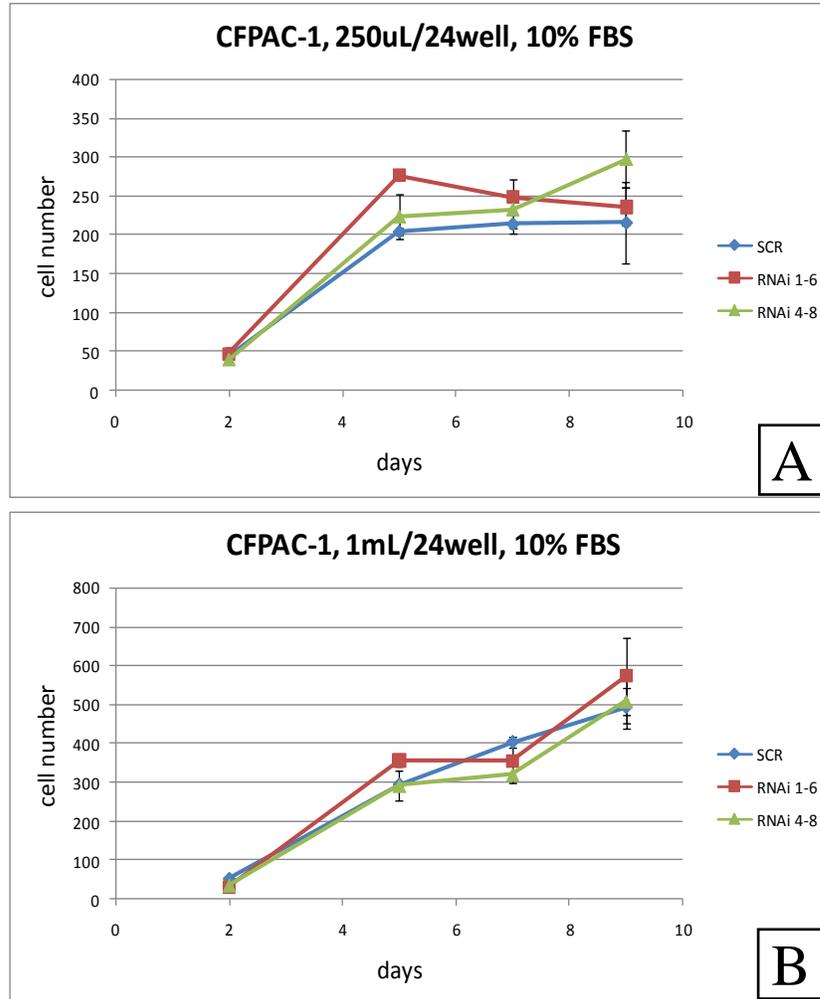
Figure 23: Growth curves of CFPAC-1 cells in serum-rich media. (**A**) 20,000 CFPAC-1 cells were plated (24wells-plate; sub-confluent density) at day 0 and cultured in 1 ml DMEM+10% FBS, replaced every day (left) or (**B**) plated 250uL DMEM+10%FBS (not replaced, but supplemented with an additional 50mL DMEM+FBS every 2 days). Cells were counted by Trypan Blue exclusion and the normalized number of cells/well was computed and plotted as average of 3 counts. **"RNAi 1-6"** and "**RNAi 4-8**" are MMP-7 silencing constructs; "**scr**" non silencing, scrambled sequence RNAi. Error bar: +/- SEM.
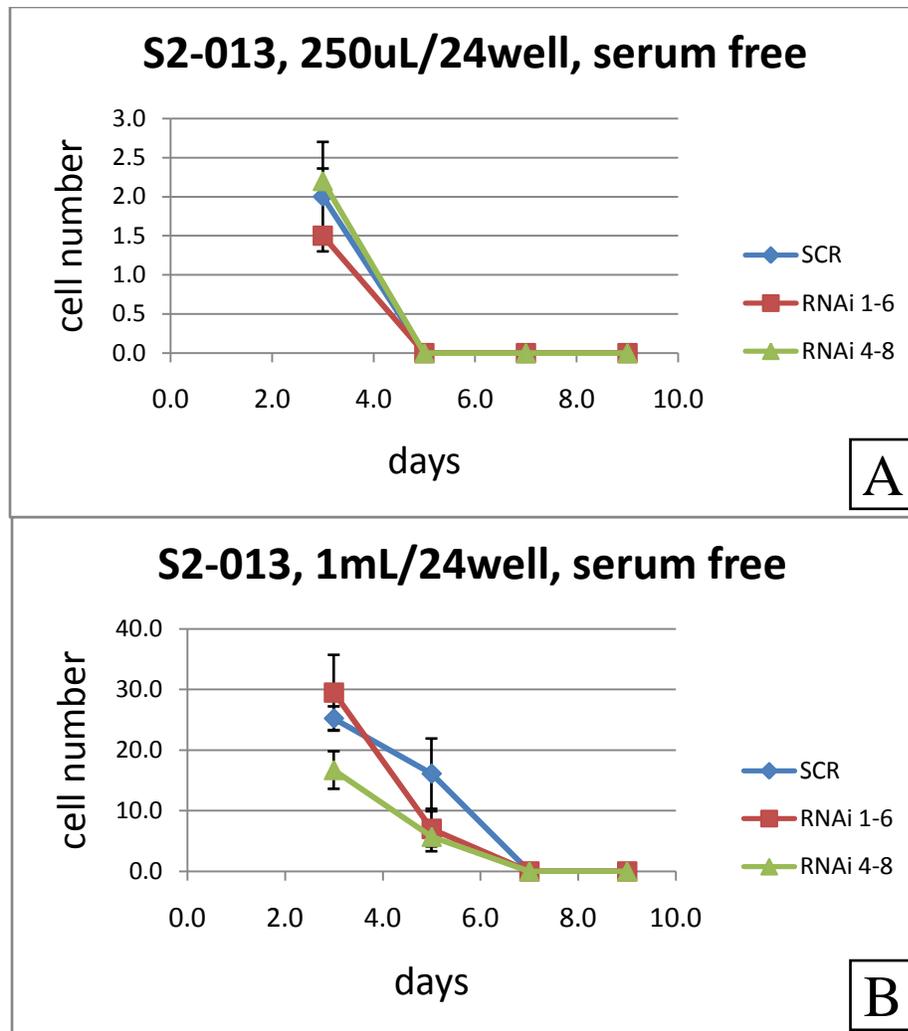
Figure 24: Growth curves of S2-013 cells in serum-free media.(**A**) 40,000 S2-013 cells were plated (24wells-plate; sub-confluent density) at day 0 and cultured in serum free DMEM, replaced every day.(left) or (**B**) plated 250uL serum free DMEM (not replaced, but supplemented with an additional 50uL serum free DMEM every 2 days). Cells were counted by Trypan Blue exclusion and the normalized number of cells/well was computed and plotted as average of 3 counts. **"RNAi 1-6"** and "**RNAi 4-8**" are MMP-7 silencing constructs; "**scr**" non silencing, scrambled sequence RNAi. Error bar: +/- SEM.
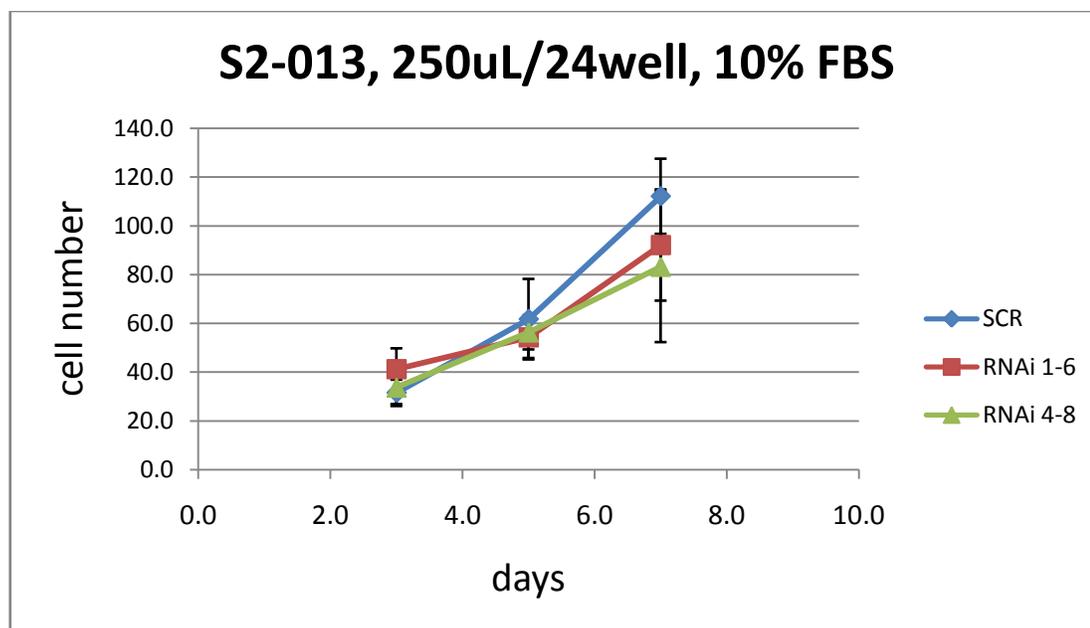
Figure 25: Growth curve of S2-013 cells in serum-rich media. 20,000 S2-013 cells were plated (24wells-plate; sub-confluent density) at day 0 and cultured in 250uL DMEM+10%FBS (not replaced, but supplemented with an additional 50uL DMEM+FBS every 2 days.) Cells were counted by Trypan Blue exclusion and the normalized number of cells/well was computed and plotted as average of 3 counts. **"RNAi 1-6"** and "**RNAi 4-8**" are MMP-7 silencing constructs; "**scr**" non silencing, scrambled sequence RNAi. . Error bar: +/- SEM

Methionine dependency in the S2-013 cell line.

A serendipitous discovery was the methionine dependence in the MMP-7 RNAi pools in the S2-013 cell line. In fact, this dependence is a known phenomenon and has been exploited as a chemotherapeutic strategy: [128] many human cancer cell lines and primary tumors have an absolute need of the essential amino acid methionine, while normal cells are quite resistant to methionine restriction. [129] The mechanism is not completely clear, but it seems related to the incapacity of cancer cell to utilize homocysteine in place of methionine.

I proceeded to look at the proliferation of S2-013 cell pools in DMEM lacking cysteine and methionine, supplemented with 10% FBS. At day 3, a statistically significant higher number of MMP-7 expressing control cells survive compared to both the two RNAi pools (silencing vectors 1-6 and 4-8; T test, p<0.005) (Figure 26)

I observed a marked decrease in cell survival in one of the two pools, although they both suppress MMP-7 in a similar way. In order to test whether this was determined

by the lack of MMP-7 or was an off-target effect, I attempted to rescue the phenotype by re-expressing a flag-tagged human MMP-7 via retroviral gene delivery.

The only suitable RNAi silenced pool 4-8 (silencing construct 4-8 is targeting the 3' UTR of the endogenous MMP-7 gene and should not affect a rescue mRNA expression) however effectively suppressed the rescue MMP-7 retroviral vector. Another possibility was an ineffective rescue gene delivery, but due to these limitations, I could not conclusively rule out an RNAi artifact and accept this phenotype.
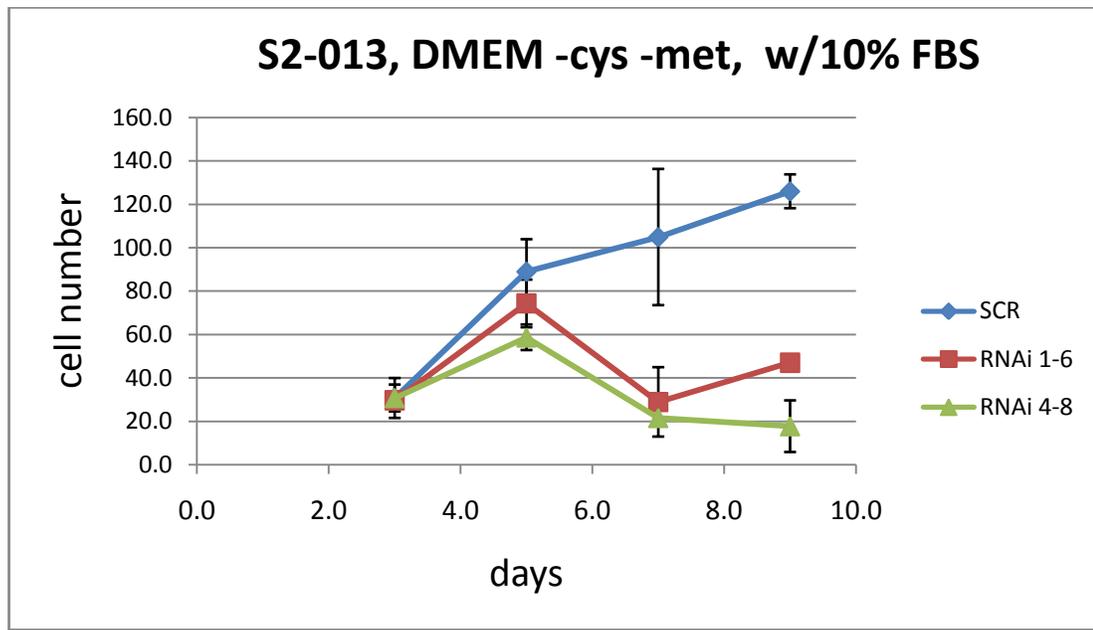
**Figure 26:** Growth curve of S2-013 cells in methionine-depleted media. S2-013 cell pools were cultured in 1ml DMEM +10% FBS lacking cysteine and methionine, changed every 48hrs. Cells were counted by Trypan Blue exclusion and the number of cells/well was computed and plotted as average of 3 counts. **"RNAi 1-6"** and "**RNAi 4-8**" are MMP-7 silencing constructs; "**scr**" non silencing, scrambled sequence RNAi. Error bar: +/- SEM

Invasion and migration assays.

According to different published experimental results, MMP-7 affects the invasive potential of cancer cell lines. [104, 105, 115, 117, 130, 131] To test this possibility, I performed invasion and migration assays in transwell chambers for both CFPAC-1 and S2-013 cell line as described in materials and methods. In this system, cells were seeded on a transwell filter with pore sizes large enough for cells to cross with minimal media in the upper chamber. In the invasion assay, transwell filters were coated with Matrigel, a basement membrane-like mixture of extracellular matrix proteins. In the lower chamber, 150 μL of a gel composed of polymerized Type I collagen and 25%FBS was placed in the media to serve as a chemoattractant to maximize directional migration/invasion. After 10-12 hrs, the upper surface of the chamber was cleared of cells by scraping and the cells on the lower surface were hematoxylin stained and counted.

To this end, I found no significant difference between the migration potential of MMP-7 expressing and RNAi silenced pools, both for CFPAC-1 line (Figure 27) and S2-013 (not shown). Matrigel invasion experiments (not shown) yieled similar results.
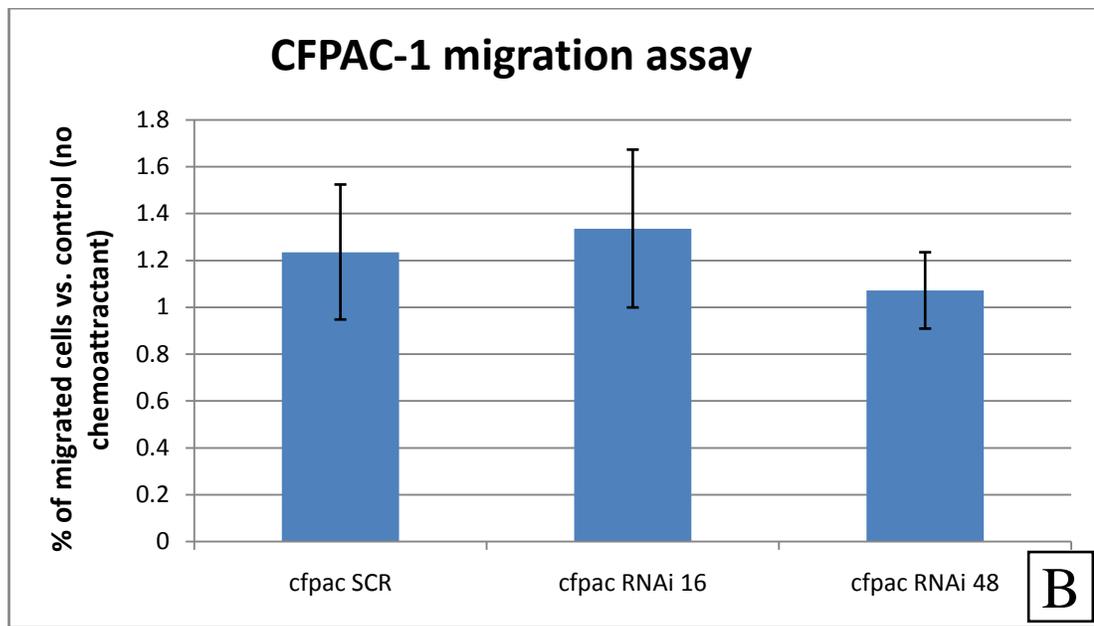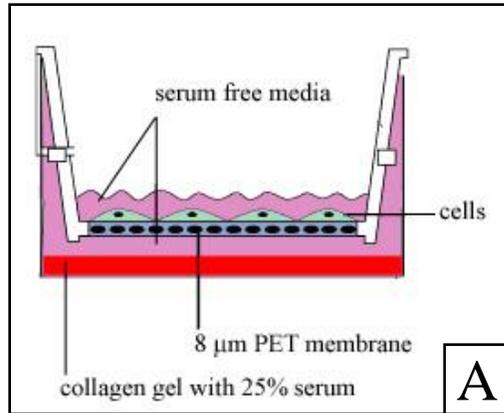
Figure 27: MMP-7 RNAi pools migration assay. 15,000 CFPAC-1 cells were placed in a BD Biosciences cell Culture Inserts containing an 8 μm pore-size PET membrane, allowed to migrate to the filter for 6-8 hours.(**A**, schematics) Inserts were then washed, hematoxylin stained and the cells on the filter counted. (**B**) The average of 15 counts was plotted as percentage of migrating cell relative to the control lacking the chemoattractant gel. **"RNAi 1-6"** and "**RNAi 4-8**" are MMP-7 silencing constructs; "**scr**" non silencing, scrambled sequence RNAi. Error bar: +/- SEM

MMP-7$^{-/-}$ cell lines tumorigenicity in nude mice.

The 2D cultures did not reveal differences between MMP-7 RNAi pools and controls. However, this could be due to the limitations of in vitro assays. To better investigate the contribution of MMP-7 in tumor formation and progression in vivo I injected RNAi and control pools in athymic nude mice, which do not reject implants of human cancer cells or tumor grafts.

I was able to measure tumor numbers, size and cell density within tumor masses, utilizing the GFP signal intensity of cells injected subcutaneously into nude mice. Tumor formation and progression was monitored by fluorescent in vivo imaging over a period of 3 weeks. Afterwards, the acquired images were used to compute the volumes and the average GFP signal intensity of each tumor mass. One mouse per cell pool (RNAi or SCR)was used. Each mouse received 2 subcutaneous injection. Consequently, each time point of the curves in figure 29 represents the average of 2 individual tumors on the same mouse.

As suggested in Figures 29, the tumor masses formed by the CFPAC-1 control and RNAi pools, were present in each mouse and at each site of injection, consisting of one or more tumor GFP positive masses. S2-013 GFP-positive cells injection resulted in an overall similar, but more variable pattern of tumor formation.

There was a consistent and expected correlation between tumor size and average GFP signal; but it was not possible to discern any significant difference between the average or the cumulative sizes of tumors (considered as the total tumor burden) per mouse formed by MMP-7 RNAi or control injected cell pools. (Figure 29 - 30)
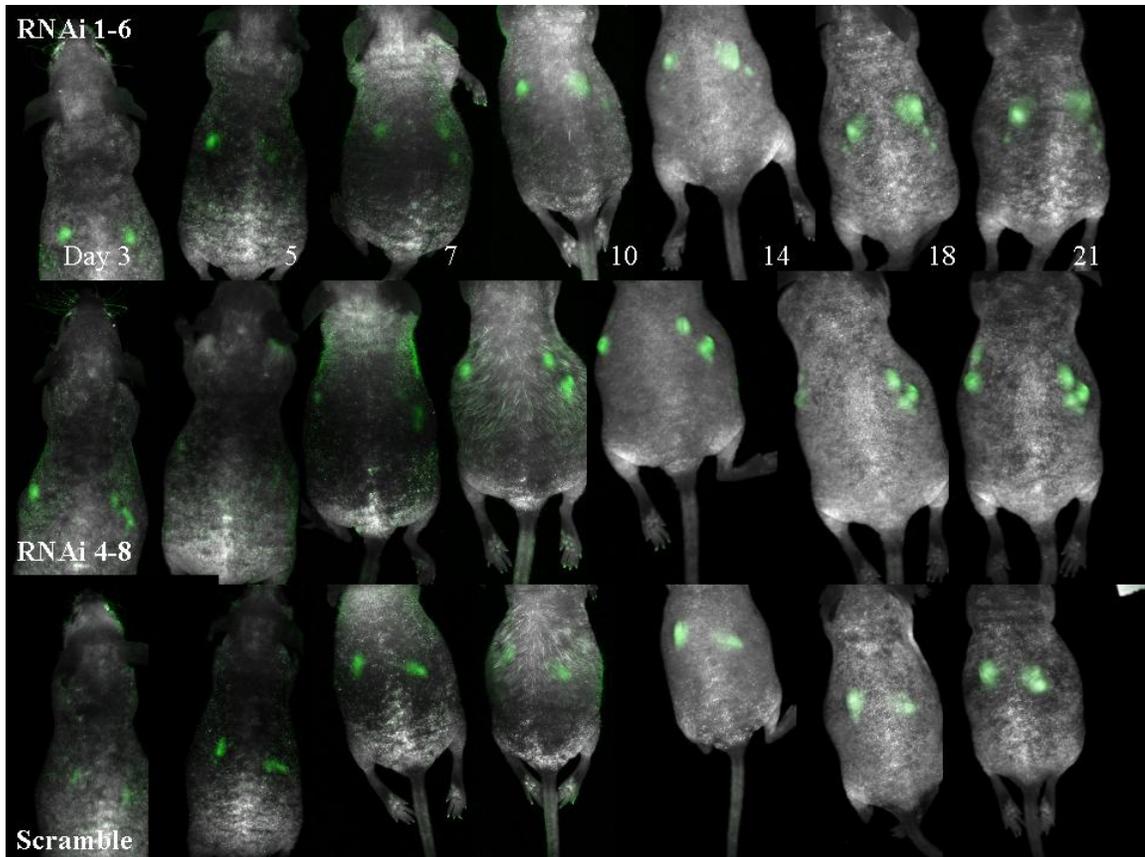
Figure 28: Tumor growth in nude mice over 3 weeks. 700,000 CFPAC-1 GFP-positive pools were injected at day 1 into nude mice. **Scramble**=scrambled sequence non silencing vector, **RNAi 1-6** = silencing vector, **RNAi 4-8** = silencing vector. S2-013 line gave comparable results.
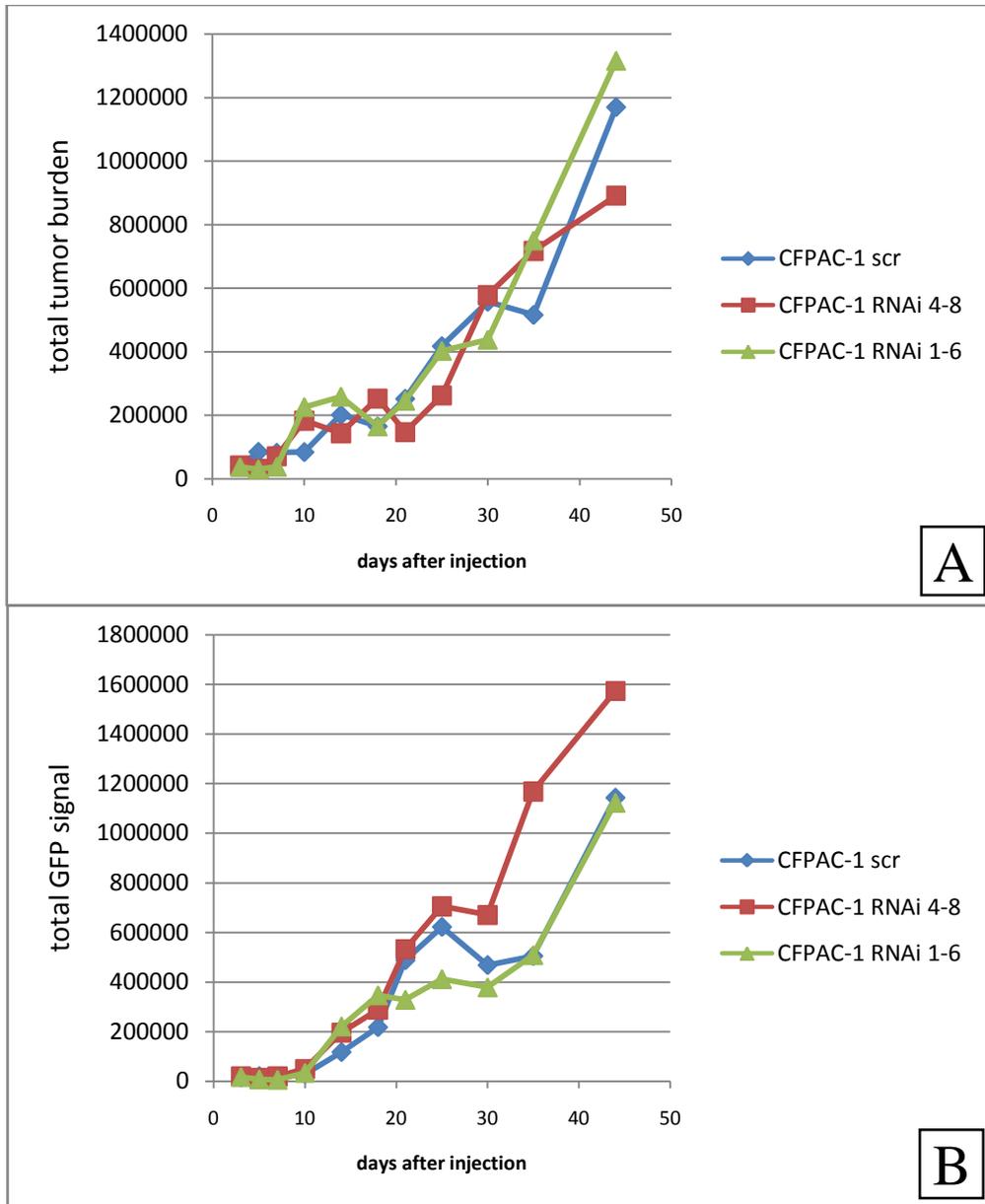
Figure 29: Total tumor burden per animal (**A**) and GFP signal (**B**). Each curve represents the sum of the tumor volumes, (or the sum of the GFP signals) in arbitrary units, on one mouse. 700,000 CFPAC-1 GFP-positive pools were injected at day 1 into nude mice. **"RNAi 1-6"** and "**RNAi 4-8**" are MMP-7 silencing constructs; "**scr**" non silencing, scrambled sequence RNAi.
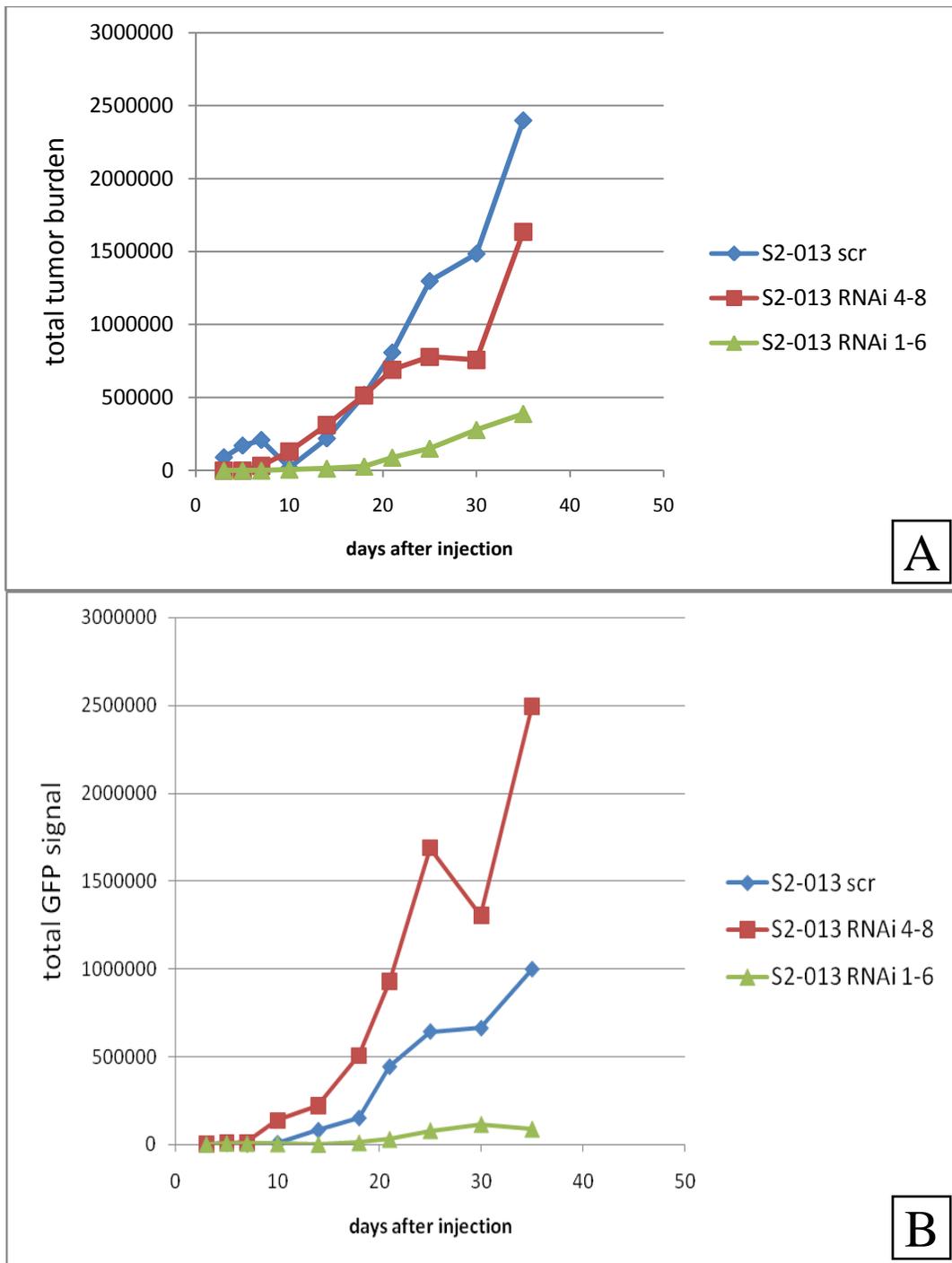
**Figure 30**: Total tumor burden per animal (**A**) and GFP signal (**B**). Each curve represents the sum of the tumor volumes, (or the sum of the GFP signals) in arbitrary units, on one mouse. 700,000 S2-013 GFP-positive pools were injected at day 1 into nude mice. **"RNAi 1-6"** and "**RNAi 4-8**" are MMP-7 silencing constructs; "**scr**" non silencing, scrambled sequence RNAi.

Pancreatic tumorigenesis and progression MMP-7$^{-/-}$ mice.

As described previously, the LSL-Kras^{G12D} mouse, when mated to transgenic mice carrying the Cre transgene under the control of a pancreas specific promoter (Pdx-1 or p48), form pancreatic tumors that accurately mimic human PanIN and PDAC. Having access to the MMP-7$^{-/-}$ mouse, I chose to examine the effects of MMP-7 loss in pancreatic tumorigenesis and progression.

First I crossed both the LSL-Kras^{G12D} mouse and the p48-Cre mouse with MMP-7$^{-/-}$ mice, all three of which were maintained in the C57Bl/6J genetic background, to generate LSL-Kras^{G12D};MMP7$^{-/-}$ and Ptf1a-cre;MMP7$^{-/-}$ animals. LSL-Kras^{G12D};Ptf1a-cre;MMP-7$^{-/-}$ were generated by crossing these animals with each other. Separately, C57Bl/6J LSL-Kras and Ptf1a-cre animals were mated to generate wild type control versions of the LSL-Kras^{G12D};Ptf1a-cre model system. In these mice, the K-Ras^{G12D} mutant allele is expressed in exocrine, endocrine and centroacinar cells after a Ptf1a-cre promoter-driven, recombinase-mediated removal of the lox-stop-lox (LSL) element early in development.

Mice were sacrificed at the time points indicated in table 3 and mouse weight and pancreatic wet weight were determined. Pancreata were then fixed, dehydrated, paraffin embedded and sectioned for histological analysis. A total of forty consecutive sections were prepared from each paraffin embedded sample. In order to obtain representative samples for morphological analysis, twenty consecutive sections were cut at approximately 1/3 of depth into the paraffin block embedding the tissue and twenty more at 2/3 of the total block depth.

Every quantitative analysis was considered valid only if consistent between sections taken at different spots in the embedded sample. Two sections were placed on each slide such that the second section was approximately 200 μm from the first section. Thus, each stained slide represented data progressively from regions 200 μm apart in the pancreatic tissue.

Mouse and pancreatic mass were determined upon sacrifice and the following parameters were obtained by light microscopy or from scanned digital images of histological sections:

1. ***Number of tumor foci/area*** analyzed

2. ***Dimensions*** (approximated to an elliptical shape, length and width were measured) of every tumor lesion; used to estimate volume

3. ***Histological features of lesions*** (presence of ductal or undifferentiated component)

4. ***Properties of tumor lesions*** (number of ducts, cells per duct, proliferative/apoptotic cells per duct)

5. ***Proliferation*** (BrdU was IP injected twice 2 and 20 hrs before sacrifice followed by was anti-BrdU immunostain)

Age	LSL-Kras,Ptf1a-cre	LSL-Kras,Ptf1a-cre, MMP-7 $^{-/-}$
6 weeks	7	6
6.5 weeks	5	8
7 weeks	1	1
2 months	5	5
8-9 months	3	3

Table 3. Numbers of analyzed mice, sorted by age and genotype.

The analysis of age-matched animals showed consistently that the pancreas/body mass ratio was 15% higher (2.16% vs 1.81%) in the wild type compared to the MMP-7 null background. In general, I have found that wet weight reflects the tumor mass in an animal. However, while significant at certain ages, this small difference could reflect something other than tumor cell number and may be instead the degree of fibrosis or edema, related to the degree of inflammation. The hypothesis of organ swelling because of fluid accumulation could not be confirmed by histology, mainly because of the tissue dehydration necessary for paraffin embedding. The measurement of the volume/dry weight ratio would be a more suitable technique.

Tumor formation occurred both in the wild type and MMP-7 null background in a similar time frame. As early as 5 weeks of age tumor foci could be observed on histological sections. At two months of age the variability mice in both genetic background displayed tumor formation that could range from minimal (5-10 microscopic foci) to extensive (50% of the pancreas replace completely by a tumor). I choose to narrow my analysis on the age groups where lesions occurred almost uniquely in discrete foci, which can be counted and individually characterized with respect to the above enumerated parameters (1-5).

6 and 6.5 weeks old mice were grouped (wild type: N=12; MMP$^{-/-}$ N=12) and the T test (2 tailed, unpaired) was performed to calculate the statistical significance of the data. Results are displayed in Figure 31.

Given the relatively small size of the population observed and the high variability of the pattern of tumor growth it was not possible to detect any statistically significant difference between LSL-Kras^{G12D};Ptf1a-cre, wild type and LSL-Kras^{G12D}; Ptf1a-cre; MMP-7$^{-/-}$ tumors, with respect to the listed features; a larger number of mice is required.

To assess cancer spreading to distant sites. I analyzed five serial sections at intervals of 250 μm for all lungs and livers in older mice (aged 8-9 months). I did not detect any significant difference in overall survival or presence of metastatic spreading to lungs and liver in older mice of either *wild type* and the MMP-7 null background. Given the relative large size and position of the tumors in mice of 8-9 months of age, local invasion to the intestine was seen in all animals.

The absence of metastases in mice of 8-9 months of ages was unexpected, given the relative large size of the primary mass at 2 months. Combining the K-Ras mutation with p53 or p16 mutations would be a better model to study metastatic spreading. These studies would appear to be very important given the association of MMP-7 expression and invasive cancer and poor prognosis found in human patient. However, my lack of results may have been affected by the limited amount of mice analyzed per group (n=3).
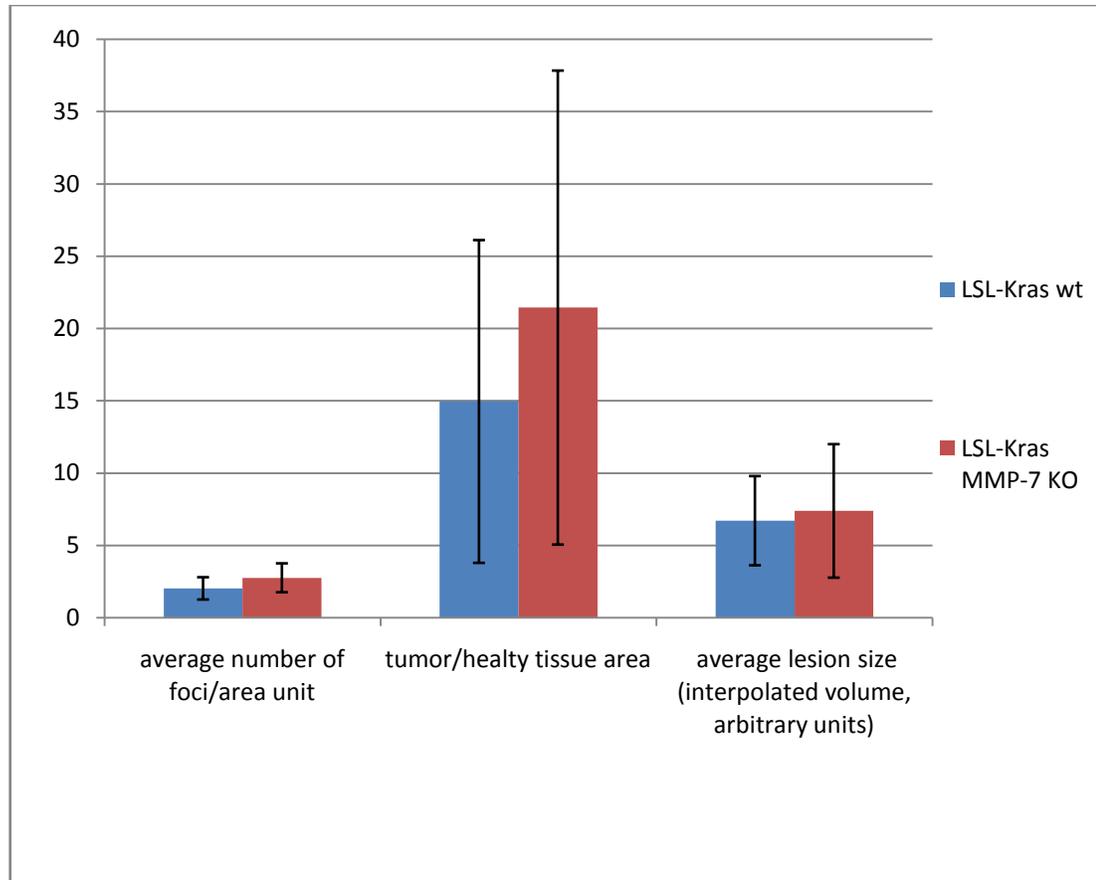
Figure 31: Tumor formation in the *wild type* and MMP-7 [-/-] background occurs in a similar pattern; as early as 5 weeks of age individual tumor foci can be observed. Mice 6 and 6.5 weeks old were grouped (wild type: N=12; MMP^{-/-} N=12) and the individual tumor foci were counted and normalized to the analyzed area on the histological section. The ratio tumor/health tissue area was computed on a scanned image of the histological sections. The average lesion size, was computed as the sum of the volumes of all tumor lesions. The shape of individual tumor foci was approximated to an ellipsoid and the volume computed based on its width and length. (Error bars: SD)
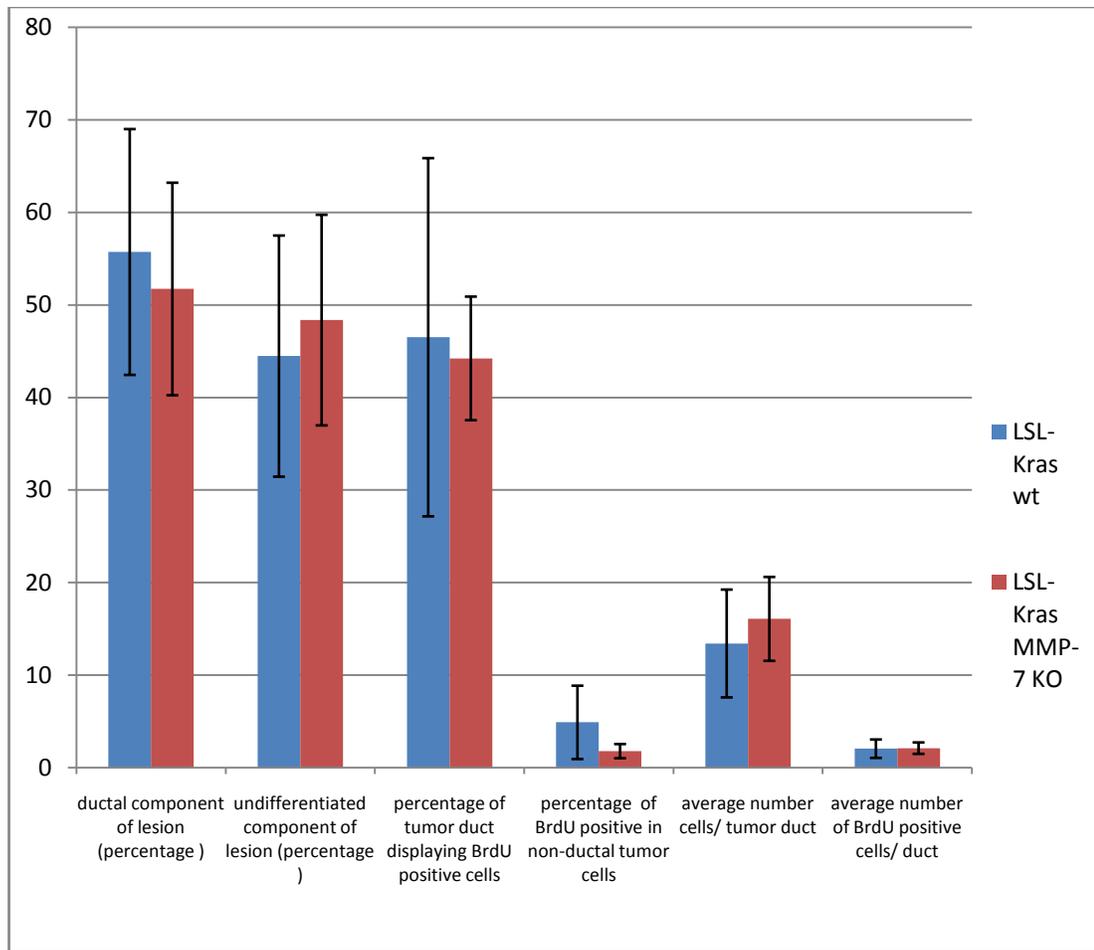
Figure 32: Characteristics of individual LSL-KRas induced tumor s in the *wild type* and MMP-7 $^{-/-}$ background. 6 and 6.5 weeks old mice were grouped (wild type: N=12; MMP$^{-/-}$ N=12). On average, 12-20 tumor foci per mouse were analyzed with respect to the features shown. (Error bars: SD)

Chapter 7

Matrix metalloproteinase-7 in pancreatic cancer: Discussion

Discussion of results.

I used a systematic approach to analyze the role of MMP-7 in pancreatic cancer, taking advantage of the most common available tools for this kind of research: cell lines in culture, xenografts and transgenic models. The general picture suggested however that in these models, MMP-7 contribution to tumor formation and growth in vivo and in vitro is marginal, or masked by other processes. This was a known potential pitfall with respect to the experiments in cell lines and nude mice.

The choice of cell lines, for example was one of the limitations of this system. I choose to use only cell lines expressing the epithelial marker E-cadherin and high levels of MMP-7. In the CFPAC-1 cell line, for example, MMP-7 mRNA is comparable to GAPDH mRNA and MMP-7 is among the 10 major secreted proteins. While it was desirable to have at least one such cell line, it would have been wiser to use at least another line expressing lower levels of MMP-7, because long-term expression of MMP-7 can lead to desensitization to apoptosis due to continuous shedding and exposure to FasL. This would have probably helped in the athymic nude mice, where the fast growth of solid tumors is often associated with extensive apoptosis and a necrotic core.

The xenograft experiment also pointed out the necessity of a higher number of mice, given the variability of tumor formation. I believe that minimal changes in the depth of the subcutaneous injections were sufficient to affect tumor take more than tumor growth. In fact, some tumor did not grow at all, despite a comparable and clearly detectable GFP signal 24 hours post injection in all mice.

Analysis of the literature points out numerous associations between MMP-7 and late cancer stages, poor prognosis, and an overall more aggressive cancer phenotype in humans. Also, mouse studies have confirmed similar results in intestinal and mammary gland tumorigenesis; consequently, the lack of statistically significant differences between the analyzed features of LSL-Kras^{G12D};Ptf1a-cre and LSL-Kras^{G12D}; Ptf1a-cre; MMP-7$^{-/-}$ tumors was an unexpected result.

A difference between the volumes or the distribution of LSL-Kras^{G12D};Ptf1a-cre and LSL-Kras^{G12D};Ptf1a-cre;MMP-7$^{-/-}$ tumors in the pancreas is not excluded, however the statistical significance is not reached at the time points considered because of the high variability of pattern of growth of these tumors. (Figure 32)

There are however a few important observations about the employed K-Ras^{G12D} model. The first is relative to the genetic background. While backcrossing LSL-Kras mice for 10 generations with C57BL/6J Ptf1a-cre, I noticed a progressive earlier onset of tumors, compared to the initial published report of this mouse model. I worked with mice that on average displayed 50% or more of the pancreatic tissue replaced by an invasive tumor at 2-3 months of age. It is thus conceivable that the effects of the K-Ras^{G12D} oncogene were actually amplified by the C57Bl6/J background, making it difficult to assess the role of MMP-7.

The second possible explanation of my results is related to the early events in PDAC progression. Recent research employing a mouse model of inducible K-Ras^{G12D}

83

oncogene demonstrated how the early occurrence of chronic pancreatitis is critical to begin and maintain the growth of invasive tumors subsequently induced by K-Ras^{G12D} oncogene expression.

In my opinion, this is a good and relevant model, because it can mimic what probably occurs in humans: an early chemical injury or a chronic condition like CP (caused by smoking or alcohol abuse) that make the pancreas more prone to PDAC development when later hit by a mutation in the K-Ras gene, or in a tumor suppressor gene, like p53. This is in accord with most epidemiological studies that clearly indicate chemical damage induced by cigarette smoking and alcohol abuse as risk factors for both pancreatitis and pancreatic cancer I believe that it would be very informative and relevant to bring the pancreatitis/inducible K-Ras^{G12D} mouse model to the MMP-7 null background, because MMP-7 has the capacity *in vitro* to activate Notch (Eric Sawey, article in press) and lead to the differentiation of acinar cells through a nestin-positive intermediate. These intermediates, if subsequently hit by a K-Ras mutation, are thought to be the cellular compartment that originates PDAC. [132]

References.

1.	Hezel, A.F., et al., *Genetics and biology of pancreatic ductal adenocarcinoma.* Genes Dev, 2006. **20**(10): p. 1218-49.
2.	Leach, S.D., *Epithelial differentiation in pancreatic development and neoplasia: new niches for nestin and Notch.* J Clin Gastroenterol, 2005. **39**(4 Suppl 2): p. S78-82.
3.	Singer, M.V., K. Gyr, and H. Sarles, *Revised classification of pancreatitis. Report of the Second International Symposium on the Classification of Pancreatitis in Marseille, France, March 28-30, 1984.* Gastroenterology, 1985. **89**(3): p. 683-5.
4.	Chari, S.T. and M.V. Singer, *The problem of classification and staging of chronic pancreatitis. Proposals based on current knowledge of its natural history.* Scand J Gastroenterol, 1994. **29**(10): p. 949-60.
5.	Sarles, H., et al., *Observations on 205 confirmed cases of acute pancreatitis, recurring pancreatitis, and chronic pancreatitis.* Gut, 1965. **6**(6): p. 545-59.
6.	Etemad, B. and D.C. Whitcomb, *Chronic pancreatitis: diagnosis, classification, and new genetic developments.* Gastroenterology, 2001. **120**(3): p. 682-707.
7.	Draganov, P. and P.P. Toskes, *Chronic pancreatitis.* Curr Opin Gastroenterol, 2002. **18**(5): p. 558-62.
8.	Stevens, T., D.L. Conwell, and G. Zuccaro, *Pathogenesis of chronic pancreatitis: an evidence-based review of past theories and recent developments.* Am J Gastroenterol, 2004. **99**(11): p. 2256-70.
9.	Kloppel, G., et al., *Human acute pancreatitis: its pathogenesis in the light of immunocytochemical and ultrastructural findings in acinar cells.* Virchows Arch A Pathol Anat Histopathol, 1986. **409**(6): p. 791-803.
10.	Geokas, M.C., R. Murphy, and R.D. McKenna, *The role of elastase in acute pancreatitis. I. Intrapancreatic elastolytic activity in bile-induced acute pancreatitis in dogs.* Arch Pathol, 1968. **86**(2): p. 117-26.
11.	Ohlsson, K. and A. Eddeland, *Release of proteolytic enzymes in bile-induced pancreatitis in dogs.* Gastroenterology, 1975. **69**(3): p. 668-75.
12.	Schiller, W.R., C. Suriyapa, and M.C. Anderson, *A review of experimental pancreatitis.* J Surg Res, 1974. **16**(1): p. 69-90.
13.	Pandol, S.J., et al., *Acute pancreatitis: bench to the bedside.* Gastroenterology, 2007. **132**(3): p. 1127-51.
14.	Gorelick, F.S., Kern, H. F. Adler, G., *Cerulein induced pancreatitis*, in *The Pancreas: Biology, Pathobiology, and Disease.* . 1993. p. 501-526
15.	Lerch, M.M. and G. Adler, *Experimental animal models of acute pancreatitis.* Int J Pancreatol, 1994. **15**(3): p. 159-70.
16.	Sakaguchi, Y., et al., *Establishment of animal models for three types of pancreatitis and analyses of regeneration mechanisms.* Pancreas, 2006. **33**(4): p. 371-81.
17.	Gilliland, L. and M.L. Steer, *Effects of ethionine on digestive enzyme synthesis and discharge by mouse pancreas.* Am J Physiol, 1980. **239**(5): p. G418-26.

18. Ji, B., et al., *Human pancreatic acinar cells do not respond to cholecystokinin.* Pharmacol Toxicol, 2002. **91**(6): p. 327-32.

19. Whitcomb, D.C., et al., *Hereditary pancreatitis is caused by a mutation in the cationic trypsinogen gene.* Nat Genet, 1996. **14**(2): p. 141-5.

20. Leach, S.D., et al., *Intracellular activation of digestive zymogens in rat pancreatic acini. Stimulation by high doses of cholecystokinin.* J Clin Invest, 1991. **87**(1): p. 362-6.

21. Halangk, W., et al., *Role of cathepsin B in intracellular trypsinogen activation and the onset of acute pancreatitis.* J Clin Invest, 2000. **106**(6): p. 773-81.

22. Weber, H., et al., *Dysregulation of the calpain-calpastatin system plays a role in the development of cerulein-induced acute pancreatitis in the rat.* Am J Physiol Gastrointest Liver Physiol, 2004. **286**(6): p. G932-41.

23. Chen, J.M., T. Montier, and C. Ferec, *Molecular pathology and evolutionary and physiological implications of pancreatitis-associated cationic trypsinogen mutations.* Hum Genet, 2001. **109**(3): p. 245-52.

24. Archer, H., et al., *A mouse model of hereditary pancreatitis generated by transgenic expression of R122H trypsinogen.* Gastroenterology, 2006. **131**(6): p. 1844-55.

25. Selig, L., et al., *Characterisation of a transgenic mouse expressing R122H human cationic trypsinogen.* BMC Gastroenterol, 2006. **6**: p. 30.

26. Frossard, J.L., *Trypsinogen activation peptide in acute pancreatitis.* Lancet, 2000. **356**(9231): p. 766-7.

27. Bergelson, J.M. and R.W. Finberg, *Integrins as receptors for virus attachment and cell entry.* Trends Microbiol, 1993. **1**(8): p. 287-8.

28. Hynes, R.O., *Integrins: bidirectional, allosteric signaling machines.* Cell, 2002. **110**(6): p. 673-87.

29. Frisch, S.M. and R.A. Screaton, *Anoikis mechanisms.* Curr Opin Cell Biol, 2001. **13**(5): p. 555-62.

30. Gilmore, A.P., *Anoikis.* Cell Death Differ, 2005. **12 Suppl 2**: p. 1473-7.

31. Frisch, S.M. and E. Ruoslahti, *Integrins and anoikis.* Curr Opin Cell Biol, 1997. **9**(5): p. 701-6.

32. Jiang, H. and F. Grinnell, *Cell-matrix entanglement and mechanical anchorage of fibroblasts in three-dimensional collagen matrices.* Mol Biol Cell, 2005. **16**(11): p. 5070-6.

33. O'Toole, T.E., et al., *Integrin cytoplasmic domains mediate inside-out signal transduction.* J Cell Biol, 1994. **124**(6): p. 1047-59.

34. Takagi, J. and T.A. Springer, *Integrin activation and structural rearrangement.* Immunol Rev, 2002. **186**: p. 141-63.

35. Mitra, S.K. and D.D. Schlaepfer, *Integrin-regulated FAK-Src signaling in normal and cancer cells.* Curr Opin Cell Biol, 2006. **18**(5): p. 516-23.

36. Ischenko, I., et al., *Effect of Src kinase inhibition on metastasis and tumor angiogenesis in human pancreatic cancer.* Angiogenesis, 2007. **10**(3): p. 167-82.

37. Duxbury, M.S., et al., *RNA interference targeting focal adhesion kinase enhances pancreatic adenocarcinoma gemcitabine chemosensitivity.* Biochem Biophys Res Commun, 2003. **311**(3): p. 786-92.

38.   Trevino, J.G., et al., *Inhibition of SRC expression and activity inhibits tumor progression and metastasis of human pancreatic adenocarcinoma cells in an orthotopic nude mouse model.* Am J Pathol, 2006. **168**(3): p. 962-72.

39.   Dehm, S.M. and K. Bonham, *SRC gene expression in human cancer: the role of transcriptional activation.* Biochem Cell Biol, 2004. **82**(2): p. 263-74.

40.   Fitzgerald, P.J., B.M. Carol, and L. Rosenstock, *Pancreatic acinar cell regeneration.* Nature, 1966. **212**(5062): p. 594-6.

41.   Fitzgerald, P.J., et al., *Pancreatic acinar cell regeneration.* Am J Pathol, 1968. **52**(5): p. 983-1011.

42.   Jiang, F.X., G. Naselli, and L.C. Harrison, *Distinct distribution of laminin and its integrin receptors in the pancreas.* J Histochem Cytochem, 2002. **50**(12): p. 1625-32.

43.   Campos, L.S., et al., *Beta1 integrins activate a MAPK signalling pathway in neural stem cells that contributes to their maintenance.* Development, 2004. **131**(14): p. 3433-44.

44.   Zhu, A.J., I. Haase, and F.M. Watt, *Signaling via beta1 integrins and mitogen-activated protein kinase determines human epidermal stem cell fate in vitro.* Proc Natl Acad Sci U S A, 1999. **96**(12): p. 6728-33.

45.   Brakebusch, C., et al., *Skin and hair follicle integrity is crucially dependent on beta 1 integrin expression on keratinocytes.* EMBO J, 2000. **19**(15): p. 3990-4003.

46.   Kawaguchi, Y., et al., *The role of the transcriptional regulator Ptf1a in converting intestinal to pancreatic progenitors.* Nat Genet, 2002. **32**(1): p. 128-34.

47.   Gaisano, H.Y., et al., *Supramaximal cholecystokinin displaces Munc18c from the pancreatic acinar basal surface, redirecting apical exocytosis to the basal membrane.* J Clin Invest, 2001. **108**(11): p. 1597-611.

48.   Parrish, W. and L. Ulloa, *High-mobility group box-1 isoforms as potential therapeutic targets in sepsis.* Methods Mol Biol, 2007. **361**: p. 145-62.

49.   Kren, A., et al., *Increased tumor cell dissemination and cellular senescence in the absence of beta1-integrin function.* EMBO J, 2007. **26**(12): p. 2832-42.

50.   Dimri, G.P., et al., *A biomarker that identifies senescent human cells in culture and in aging skin in vivo.* Proc Natl Acad Sci U S A, 1995. **92**(20): p. 9363-7.

51.   Lampel, M. and H.F. Kern, *Acute interstitial pancreatitis in the rat induced by excessive doses of a pancreatic secretagogue.* Virchows Arch A Pathol Anat Histol, 1977. **373**(2): p. 97-117.

52.   Adler, G., T. Hupp, and H.F. Kern, *Course and spontaneous regression of acute pancreatitis in the rat.* Virchows Arch A Pathol Anat Histol, 1979. **382**(1): p. 31-47.

53.   Cochilla, A.J., J.K. Angleson, and W.J. Betz, *Monitoring secretory membrane with FM1-43 fluorescence.* Annu Rev Neurosci, 1999. **22**: p. 1-10.

54.   Teich, N., et al., *Mutations of human cationic trypsinogen (PRSS1) and chronic pancreatitis.* Hum Mutat, 2006. **27**(8): p. 721-30.

55.   Cano, D.A., S. Sekine, and M. Hebrok, *Primary cilia deletion in pancreatic epithelial cells results in cyst formation and pancreatitis.* Gastroenterology, 2006. **131**(6): p. 1856-69.

56. Naylor, M.J., et al., *Ablation of beta1 integrin in mammary epithelium reveals a key role for integrin in glandular morphogenesis and differentiation.* J Cell Biol, 2005. **171**(4): p. 717-28.

57. Durbeej, M. and P. Ekblom, *Dystroglycan and laminins: glycoconjugates involved in branching epithelial morphogenesis.* Exp Lung Res, 1997. **23**(2): p. 109-18.

58. Deng, W.M., et al., *Dystroglycan is required for polarizing the epithelial cells and the oocyte in Drosophila.* Development, 2003. **130**(1): p. 173-84.

59. Cavallaro, U. and G. Christofori, *Cell adhesion and signalling by cadherins and Ig-CAMs in cancer.* Nat Rev Cancer, 2004. **4**(2): p. 118-32.

60. Hermiston, M.L. and J.I. Gordon, *In vivo analysis of cadherin function in the mouse intestinal epithelium: essential roles in adhesion, maintenance of differentiation, and regulation of programmed cell death.* J Cell Biol, 1995. **129**(2): p. 489-506.

61. Knust, E. and O. Bossinger, *Composition and formation of intercellular junctions in epithelial cells.* Science, 2002. **298**(5600): p. 1955-9.

62. Li, S., et al., *The role of laminin in embryonic cell polarization and tissue organization.* Dev Cell, 2003. **4**(5): p. 613-24.

63. Yu, W., et al., *Beta1-integrin orients epithelial polarity via Rac1 and laminin.* Mol Biol Cell, 2005. **16**(2): p. 433-45.

64. Lohikangas, L., D. Gullberg, and S. Johansson, *Assembly of laminin polymers is dependent on beta1-integrins.* Exp Cell Res, 2001. **265**(1): p. 135-44.

65. Rebustini, I.T., et al., *Laminin alpha5 is necessary for submandibular gland epithelial morphogenesis and influences FGFR expression through beta1 integrin signaling.* Dev Biol, 2007. **308**(1): p. 15-29.

66. Brakebusch, C. and R. Fassler, *The integrin-actin connection, an eternal love affair.* EMBO J, 2003. **22**(10): p. 2324-33.

67. Lanzetti, L., *Actin in membrane trafficking.* Curr Opin Cell Biol, 2007. **19**(4): p. 453-8.

68. Wrenn, R.W. and L.E. Herman, *Integrin-linked tyrosine phosphorylation increases membrane association of protein kinase C alpha in pancreatic acinar cells.* Biochem Biophys Res Commun, 1995. **208**(3): p. 978-84.

69. Tapia, J.A., et al., *Cholecystokinin-stimulated tyrosine phosphorylation of PKC-delta in pancreatic acinar cells is regulated bidirectionally by PKC activation.* Biochim Biophys Acta, 2002. **1593**(1): p. 99-113.

70. Li, C., X. Chen, and J.A. Williams, *Regulation of CCK-induced amylase release by PKC-delta in rat pancreatic acinar cells.* Am J Physiol Gastrointest Liver Physiol, 2004. **287**(4): p. G764-71.

71. Leser, J., et al., *Cholecystokinin-induced redistribution of paxillin in rat pancreatic acinar cells.* Biochem Biophys Res Commun, 1999. **254**(2): p. 400-5.

72. Garcia, L.J., et al., *CCK causes rapid tyrosine phosphorylation of p125FAK focal adhesion kinase and paxillin in rat pancreatic acini.* Biochim Biophys Acta, 1997. **1358**(2): p. 189-99.

73. Lutz, M.P., et al., *Protein tyrosine phosphorylation in pancreatic acini: differential effects of VIP and CCK.* Am J Physiol, 1997. **273**(6 Pt 1): p. G1226-32.

74. Giancotti, F.G., *Integrin signaling: specificity and control of cell survival and cell cycle progression.* Curr Opin Cell Biol, 1997. **9**(5): p. 691-700.

75. Geiger, B., et al., *Transmembrane crosstalk between the extracellular matrix--cytoskeleton crosstalk.* Nat Rev Mol Cell Biol, 2001. **2**(11): p. 793-805.

76. Fincham, V.J., J.A. Wyke, and M.C. Frame, *v-Src-induced degradation of focal adhesion kinase during morphological transformation of chicken embryo fibroblasts.* Oncogene, 1995. **10**(11): p. 2247-52.

77. Saito, A., J.A. Williams, and T. Kanno, *Potentiation of cholecystokinin-induced exocrine secretion by both exogenous and endogenous insulin in isolated and perfused rat pancreata.* J Clin Invest, 1980. **65**(4): p. 777-82.

78. Li, N., et al., *Beta1 integrins regulate mammary gland proliferation and maintain the integrity of mammary alveoli.* EMBO J, 2005. **24**(11): p. 1942-53.

79. Wang, F., et al., *Reciprocal interactions between beta1-integrin and epidermal growth factor receptor in three-dimensional basement membrane breast cultures: a different perspective in epithelial biology.* Proc Natl Acad Sci U S A, 1998. **95**(25): p. 14821-6.

80. Strobel, O., et al., *In vivo lineage tracing defines the role of acinar-to-ductal transdifferentiation in inflammatory ductal metaplasia.* Gastroenterology, 2007. **133**(6): p. 1999-2009.

81. Chambers AF and L. Matrisian, *Changing views of the role of matrix metalloproteinases in metastasis.* J Natl Cancer Inst, 1997. **89**(17): p. 1260-70.

82. Matrisian LM, et al., *Matrix-degrading metalloproteinases in tumor progression.* Princess Takamatsu Symp, 1994. **24**: p. 152-61.

83. McDonnell, S., et al., *Expression and localization of the matrix metalloproteinase pump-1 (MMP-7) in human gastric and colon carcinomas.* Mol Carcinog, 1991. **4**(6): p. 527-33.

84. Crawford, H.C., et al., *Matrix metalloproteinase-7 is expressed by pancreatic cancer precursors and regulates acinar-to-ductal metaplasia in exocrine pancreas.* J Clin Invest, 2002. **109**(11): p. 1437-44.

85. Wilson, C.L., et al., *Intestinal tumorigenesis is suppressed in mice lacking the metalloproteinase matrilysin.* Proc Natl Acad Sci U S A, 1997. **94**(4): p. 1402-7.

86. Rudolph-Owen, L.A., et al., *The matrix metalloproteinase matrilysin influences early-stage mammary tumorigenesis.* Cancer Res, 1998. **58**(23): p. 5500-6.

87. Hassan, M.M., et al., *Risk Factors for Pancreatic Cancer: Case-Control Study.* Am J Gastroenterol, 2007.

88. Lowenfels, A.B. and P. Maisonneuve, *Risk factors for pancreatic cancer.* J Cell Biochem, 2005. **95**(4): p. 649-56.

89. Guerra, C., et al., *Chronic pancreatitis is essential for induction of pancreatic ductal adenocarcinoma by K-Ras oncogenes in adult mice.* Cancer Cell, 2007. **11**(3): p. 291-302.

90. Lowenfels, A.B., et al., *Cigarette smoking as a risk factor for pancreatic cancer in patients with hereditary pancreatitis.* JAMA, 2001. **286**(2): p. 169-70.

91. Zhu, L., et al., *Acinar Cells Contribute to the Molecular Heterogeneity of Pancreatic Intraepithelial Neoplasia.* Am J Pathol, 2007.

92. Means, A.L., et al., *Pancreatic epithelial plasticity mediated by acinar cell transdifferentiation and generation of nestin-positive intermediates.* Development, 2005. **132**(16): p. 3767-76.

93. Miyamoto, Y., et al., *Notch mediates TGF alpha-induced changes in epithelial differentiation during pancreatic tumorigenesis.* Cancer Cell, 2003. **3**(6): p. 565-76.

94. Schmid, R.M., *Acinar-to-ductal metaplasia in pancreatic cancer development.* J Clin Invest, 2002. **109**(11): p. 1403-4.

95. Bergers, G., et al., *Effects of angiogenesis inhibitors on multistage carcinogenesis in mice.* Science, 1999. **284**(5415): p. 808-12.

96. O'Reilly, M.S., et al., *Angiostatin induces and sustains dormancy of human primary tumors in mice.* Nat Med, 1996. **2**(6): p. 689-92.

97. Radisky, D.C., et al., *Rac1b and reactive oxygen species mediate MMP-3-induced EMT and genomic instability.* Nature, 2005. **436**(7047): p. 123-7.

98. Vargo-Gogola, T., et al., *Matrilysin (matrix metalloproteinase-7) selects for apoptosis-resistant mammary cells in vivo.* Cancer Res, 2002. **62**(19): p. 5559-63.

99. Maemoto, A., et al., *Functional analysis of the alpha-defensin disulfide array in mouse cryptdin-4.* J Biol Chem, 2004. **279**(42): p. 44188-96.

100. Calvisi, D.F., et al., *Activation of beta-catenin provides proliferative and invasive advantages in c-myc/TGF-alpha hepatocarcinogenesis promoted by phenobarbital.* Carcinogenesis, 2004. **25**(6): p. 901-8.

101. Cowland, J.B., et al., *Neutrophil gelatinase-associated lipocalin is up-regulated in human epithelial cells by IL-1 beta, but not by TNF-alpha.* J Immunol, 2003. **171**(12): p. 6630-9.

102. Yu, W.H., et al., *CD44 anchors the assembly of matrilysin/MMP-7 with heparin-binding epidermal growth factor precursor and ErbB4 and regulates female reproductive organ remodeling.* Genes Dev, 2002. **16**(3): p. 307-23.

103. Nakamura, M., et al., *Matrix metalloproteinase-7 degrades all insulin-like growth factor binding proteins and facilitates insulin-like growth factor bioavailability.* Biochem Biophys Res Commun, 2005. **333**(3): p. 1011-6.

104. Noe, V., et al., *Release of an invasion promoter E-cadherin fragment by matrilysin and stromelysin-1.* J Cell Sci, 2001. **114**(Pt 1): p. 111-118.

105. Davies, G., W.G. Jiang, and M.D. Mason, *Matrilysin mediates extracellular cleavage of E-cadherin from prostate cancer cells: a key mechanism in hepatocyte growth factor/scatter factor-induced cell-cell dissociation and in vitro invasion.* Clin Cancer Res, 2001. **7**(10): p. 3289-97.

106. McGuire, J.K., Q. Li, and W.C. Parks, *Matrilysin (matrix metalloproteinase-7) mediates E-cadherin ectodomain shedding in injured lung epithelium.* Am J Pathol, 2003. **162**(6): p. 1831-43.

107. von Bredow, D.C., et al., *Cleavage of beta 4 integrin by matrilysin.* Exp Cell Res, 1997. **236**(1): p. 341-5.

108. Agnihotri, R., et al., *Osteopontin, a novel substrate for matrix metalloproteinase-3 (stromelysin-1) and matrix metalloproteinase-7 (matrilysin).* J Biol Chem, 2001. **276**(30): p. 28261-7.

109. Lynch, C.C., et al., *MMP-7 promotes prostate cancer-induced osteolysis via the solubilization of RANKL.* Cancer Cell, 2005. **7**(5): p. 485-96.

110. Parks, W.C., C.L. Wilson, and Y.S. Lopez-Boado, *Matrix metalloproteinases as modulators of inflammation and innate immunity.* Nat Rev Immunol, 2004. **4**(8): p. 617-29.

111. Li, Q., et al., *Matrilysin shedding of syndecan-1 regulates chemokine mobilization and transepithelial efflux of neutrophils in acute lung injury.* Cell, 2002. **111**(5): p. 635-46.

112. Strand, S., et al., *Cleavage of CD95 by matrix metalloproteinase-7 induces apoptosis resistance in tumour cells.* Oncogene, 2004. **23**(20): p. 3732-6.

113. Harrell, P.C., et al., *Proliferative effects of apical, but not basal, matrix metalloproteinase-7 activity in polarized MDCK cells.* Exp Cell Res, 2005. **303**(2): p. 308-20.

114. Witty, J.P., et al., *Modulation of matrilysin levels in colon carcinoma cell lines affects tumorigenicity in vivo.* Cancer Res, 1994. **54**(17): p. 4805-12.

115. Wang, F.Q., et al., *Matrilysin (MMP-7) promotes invasion of ovarian cancer cells by activation of progelatinase.* Int J Cancer, 2005. **114**(1): p. 19-31.

116. Kioi, M., et al., *Matrilysin (MMP-7) induces homotypic adhesion of human colon cancer cells and enhances their metastatic potential in nude mouse model.* Oncogene, 2003. **22**(54): p. 8662-70.

117. Jiang, W.G., et al., *Targeting matrilysin and its impact on tumor growth in vivo: the potential implications in breast cancer therapy.* Clin Cancer Res, 2005. **11**(16): p. 6012-9.

118. Fingleton, B.M., et al., *Matrilysin in early stage intestinal tumorigenesis.* APMIS, 1999. **107**(1): p. 102-10.

119. Adachi, Y., et al., *Clinicopathologic and prognostic significance of matrilysin expression at the invasive front in human colorectal cancers.* Int J Cancer, 2001. **95**(5): p. 290-4.

120. Ougolkov, A.V., et al., *Oncogenic beta-catenin and MMP-7 (matrilysin) cosegregate in late-stage clinical colon cancer.* Gastroenterology, 2002. **122**(1): p. 60-71.

121. Masaki, T., et al., *Matrix metalloproteinases may contribute compensationally to tumor invasion in T1 colorectal carcinomas.* Anticancer Res, 2003. **23**(5b): p. 4169-73.

122. Masaki, T., et al., *Matrilysin (MMP-7) as a significant determinant of malignant potential of early invasive colorectal carcinomas.* Br J Cancer, 2001. **84**(10): p. 1317-21.

123. Tanioka, Y., et al., *Matrix metalloproteinase-7 and matrix metalloproteinase-9 are associated with unfavourable prognosis in superficial oesophageal cancer.* Br J Cancer, 2003. **89**(11): p. 2116-21.

124. Obokata, A., et al., *Significance of matrix metalloproteinase-7 [correction of matrix metalloproteinase-2], -11 and tissue inhibitor of metalloproteinase-1 expression in normal, hyperplastic and neoplastic endometrium.* Anticancer Res, 2007. **27**(1A): p. 95-105.

125. Liu, D., et al., *Overexpression of matrix metalloproteinase-7 (MMP-7) correlates with tumor proliferation, and a poor prognosis in non-small cell lung cancer.* Lung Cancer, 2007. **58**(3): p. 384-91.

126. Nakamura, H., et al., *Association of matrilysin expression with progression and poor prognosis in human pancreatic adenocarcinoma.* Oncol Rep, 2002. **9**(4): p. 751-5.

127. Jones, L.E., et al., *Comprehensive analysis of matrix metalloproteinase and tissue inhibitor expression in pancreatic cancer: increased expression of matrix metalloproteinase-7 predicts poor survival.* Clin Cancer Res, 2004. **10**(8): p. 2832-45.

128. Kokkinakis, D.M., *Methionine-stress: a pleiotropic approach in enhancing the efficacy of chemotherapy.* Cancer Lett, 2006. **233**(2): p. 195-207.

129. Cellarier, E., et al., *Methionine dependency and cancer treatment.* Cancer Treat Rev, 2003. **29**(6): p. 489-99.

130. Lee, K.H., et al., *Association of extracellular cleavage of E-cadherin mediated by MMP-7 with HGF-induced in vitro invasion in human stomach cancer cells.* Eur Surg Res, 2007. **39**(4): p. 208-15.

131. Lynch, C.C. and S. McDonnell, *The role of matrilysin (MMP-7) in leukaemia cell invasion.* Clin Exp Metastasis, 2000. **18**(5): p. 401-6.

132. Carriere, C., et al., *The Nestin progenitor lineage is the compartment of origin for pancreatic intraepithelial neoplasia.* Proc Natl Acad Sci U S A, 2007. **104**(11): p. 4437-42.